INFORMATION TO USERS

This manuscript has been reproduced from the microfilm master. UMI films the text directly from the original or copy submitted. Thus, some thesis and dissertation copies are in typewriter face, while others may be from any type of computer printer.

The quality of this reproduction is dependent upon the quality of the copy submitted. Broken or indistinct print, colored or poor quality illustrations and photographs, print bleedthrough, substandard margins, and improper alignment can adversely affect reproduction.

In the unlikely event that the author did not send UMI a complete manuscript and there are missing pages, these will be noted. Also, if unauthorized copyright material had to be removed, a note will indicate the deletion.

Oversize materials (e.g., maps, drawings, charts) are reproduced by sectioning the original, beginning at the upper left-hand corner and continuing from left to right in equal sections with small overlaps.

Photographs included in the original manuscript have been reproduced xerographically in this copy. Higher quality 6" x 9" black and white photographic prints are available for any photographs or illustrations appearing in this copy for an additional charge. Contact UMI directly to order.

Bell & Howell Information and Learning
300 North Zeeb Road, Ann Arbor, MI 48106-1346 USA
800-521-0600

UMI®

DISSERTATION

HCET: A FINITE ELEMENT MODEL FOR SOLUTE TRANSPORT DRIVEN BY HYDRAULIC, CHEMICAL, ELECTRICAL, AND THERMAL GRADIENTS

Submitted by

ING-DEAN YAN

Department of Civil Engineering

(Groundwater/Environmental Hydrogeology Program)

In partial fulfillment of the requirements

For the Degree of Doctor of Philosophy

Colorado State University

Fort Collins, Colorado

Fall 2000

COLORADO STATE UNIVERSITY

October 31, 2000

WE HERE BY RECOMMEND THAT THE DISSERTATION PREPARED UNDER OUR SUPERVISION BY ING-DEAN YAN ENTITLED HCET: A FINITE ELEMENT MODEL FOR SOLUTE TRANSPORT DRIVEN BY HYDRAULIC, CHEMICAL, ELECTRICAL, AND THERMAL GRADIENTS BE ACCEPTED AS FULFILLING IN PART REQUIREMENTS FOR THE DEGREE OF DOCTOR OF PHILOSOPHY.

Committee on Graduate Work

W. W. Zachmann

T. M. Holik

Charles D. Shackelford
Adviser

James W. Warren
Co-Adviser

Larry A. Roesner
Department Head

ABSTRACT OF DISSERTATION

HCET: A FINITE ELEMENT MODEL FOR SOLUTE TRANSPORT DRIVEN BY HYDRAULIC, CHEMICAL, ELECTRICAL, AND THERMAL GRADIENTS

There are many alternatives to remediate contaminants in coarse-grained soils. However, most of these methods fail to accomplish their task in fine-grained soils. When a single driving force dominates and other cross effects are less important, direct flow conduction phenomena is main concerned in the study of contaminants transport. In the thermodynamics of irreversible processes, any driving force may give rise to any flux. For example, electrical gradient and hydraulic gradient both may cause the flow of water. Increased concerns over the environment have the need to better understand the behavior of the fine-grained soil barriers. Geotechnical engineers have been given attention on coupled transport processes on electrokinetic's remediation. The computational capability available to the geotechnical engineers has also strongly influenced the engineer's ability to address these complex problems.

This dissertation presents solute transport driven by the hydraulic, chemical, electrical, and thermal gradients including: 1) introduction, 2) literature review, 3)

mathematical development, 4) finite element formulation, 5) evaluation of the HCET model, and 6) conclusions, summary, and future studies. The study was extended by simulating experimental results on thermal effects of electrokinetic's remediation of lead removal available in the literature.

The numerical model HCET was developed to simulate the coupled transport processes as a function of time. The HCET model has a few advantages over other models and shows that: 1) The model is capable of handling very general case with one-variable to four-variable problems, 2) The model is capable of exploring heat effects in the field of electrokinetic's remediation, 3) The model uses a simultaneous algorithm to solve these multiple variables of the coupled transport processes, and 4) The HCET model can be used to perform parameter analysis for the decision making and evaluation in fined-grained soil application.

Keywords: Finite element method; Coupled transport processes; Solute transport; Electrokinetic remediation; Contaminant transport; Fine-grained soils; thermal transport

Ing-Dean YAN
Civil Engineering Department
Colorado State University
Fort Collins, Colorado
Fall 2000

TO MY

PARENTS,

WIFE JULIA,

AND DAUGHTER SOPHIA

ACKNOWLEDGEMENTS

Appreciation is extended to my advisor, Professor Charles D. Shackelford for his supervision and guidance on this dissertation. My co-advisor, Dr. James Warner instructed me in solving difficult problems piece by piece, and helped me on several occasions when I ran into troubles. Professor David Zachmann explained solving partial differential equations to me in a clear and "friendly" way. I enjoyed his class. He always gave his full support to students and allowed us to make mistakes and learn. Special thanks go to Dr. Thomas Solie. He helped me develop an understanding of irreversible thermodynamics and its applications. Many friends helped me in many ways during my stay at Aggie Village at Colorado State University. My friends shared their joy and pain with me enriching my international experience.

TABLE OF CONTENTS

LIST OF TABLES

LIST OF FIGURES

CHAPTER 1

INTRODUCTION

1.1 BACKGROUND

Historically, transport processes have been separated into isothermal processes and non-isothermal processes. Isothermal processes are related to many practical applications such as dewatering of the ground, and soft ground consolidation as well as injection, containment, and extraction of chemicals in the ground (e.g., Runnels and Larson, 1986; Lageman, 1993; Lageman et. al., 1989; Hamed, 1991; Pamukcu et al., 1990; Runnels and Wahli, 1993; Shapiro et al., 1989, and 1993; Acar et al., 1989, 1990, 1992, 1993, 1994, and 1996). Non-isothermal processes involving heat transport are of growing interest in the area of subsurface transport studies particularly for problems involving the impact upon heat resulting from power plants or nuclear waste isolation, and the extraction of heat from aquifers, etc. (e.g., Andrews and Anderson, 1980; Bernard et al., 1981; Gupta et al., 1987; Huyakorn and Gelhar, 1981; Huyakorn et al., 1986; Kipp, 1987; Milly, 1982; Reed, 1985; Voss, 1984; Walker et al., 1981).

The results of relatively recent engineering practice have indicated that coupled processes driven by hydraulic, chemical, electric, and thermal gradients are necessary to understand the controlling mechanism of electrokinetic remediation in fine-grained soils (e.g., Shapiro 1990, Yeung 1990, Alshawabkeh 1994, Menon 1996, and Hsu 1997). These findings are relevant with respect to current waste disposal practice, where fine-

grained soil barriers are used to contain toxic waste involving water, solutes, current, and heat. As a result, it may be a requirement in the near future that coupled transport processes be explicitly considered when designing earthen barriers.

A comprehensive theoretical model is required for coupled transport processes in fine-grained soils. This model should address contaminant transport under the combined effects of hydraulic, chemical, electrical, and thermal gradients. This model should provide a basis for a comprehensive design/analysis including different boundary conditions, site-specific contamination, and parameter sensitivity analysis in a full-scale field study.

1.2 GOAL AND OBJECTIVES OF THIS STUDY

The goal of this research is to develop a model that includes coupled hydraulic, chemical, electrical, and thermal gradients (HCET model) to investigate parameter sensitivity of coupled flow phenomena applied to fined-gained soils for applications involving waste disposal and remediation. To achieve this goal, the specific objectives were identified:

- to develop a model to consider the effects of not only hydraulic, chemical, or electrical potential gradients, but also thermal potential gradient on subsurface contaminant migration,
- to verify/validate with respect to analytical/numerical models and measured data, and
- to perform parameter sensitivity analysis on coupled processes phenomena.

1.3 UNDERLYING ASSUMPTIONS FOR THE HCET MODEL

- The soil medium is saturated.
- The temperatures of the fluid and the soil medium are equal.
- The temperature dependence of fluid density and viscosity may be neglected for the temperature ranges studied.
- Change in fluid density due to changing solute concentration may be neglected.
- The flow rate under investigation for Peclet number is less than 20, which is applied to fined-grained soils in which diffusion is the dominant transport process relative to advection and numerical dispersion by high flow rate can be neglected for solute transport.
- The parameter values used in the numerical simulations are based on those associated with fine-grained soil applications, which may not necessarily be applied to other situations without further study.

CHAPTER 2

LITERATURE REVIEW

2.1 CONDUCTION PHENOMENA

This section includes introduction on conduction phenomena area of direct flows and coupled flows.

2.1.1 Direct flow phenomena

There are four well-established laws of fluid, chemical, electricity, and heat flow:

Darcy's law between fluid flow and hydraulic gradient;

Fourier's law between heat flow and temperature gradient;

Ohm's law between electrical current and potential gradient;

Fick's law between flow of a solute and its concentration gradient, etc.

In these above examples, we see a simple, linear dependence of a flow, J_i, with its direct driving force X_i. For more complicated couple-relationship in irreversible thermodynamic theorem, there are additional phenomenological linear relationships between fluxes and cross-coupled driving forces. The conjugated driving force usually dominates than these cross-coupled effects that are less important and negligible.

2.1.2 Coupled flow phenomena

Simple direct flow relationship does not always hold when two or more flows are present. In the thermodynamics of irreversible processes, any driving force may give rise to any flux. For example, an electromotive force and hydraulic gradient both may cause the flow of water. In general, then, we must allow contributions to a given flux from other than its conjugated driving force. Onsager, in 1931, developed mathematical equations to express these relationships between fluxes and forces (see Bear in 1972 for early references):

$$\begin{aligned} J_1 &= L_{11}X_1 + L_{12}X_2 + \ldots + L_{1n}X_n \\ J_2 &= L_{21}X_1 + L_{22}X_2 + \ldots + L_{2n}X_n \\ &\vdots \\ J_n &= L_{n1}X_1 + L_{n2}X_2 + \ldots + L_{nn}X_n \end{aligned} \qquad [2\text{-}1]$$

or, in abbreviated form:

$$J_i = \sum_{j=1}^{n} L_{ij}X_j \qquad (i = 1,2,\ldots,n) \qquad [2\text{-}2]$$

where the J_is are fluxes, the X_js are thermodynamic driving forces, and the coefficients L_{ij}s are independent of both the fluxes J_is and the driving forces X_js. These L_{ij}s are properties that may or may not be of domination in any given soil. The coefficients of L_{ij}s are also be called phenomenological coefficients because the "phenomenological"

means that the coefficients must be experimentally determined. The L_{ii}s are called the conjugated conductivity coefficients for flows and Lij ($i \neq j$) are called coupling coefficients which give rise cross interaction phenomena. Onsager also stated that the phenomenological coefficients Lij (provided a proper choice is made for the fluxes Jis and driving forces Xj) must satisfy the symmetric relationship:

$$L_{ij} = L_{ji} \qquad (i, j = 1, 2, \ldots, n) \qquad [2\text{-}3]$$

Miller (1960) had reviewed experimental verification of Onsager's symmetry relations (Onsager reciprocal relations) and had shown it to be valid for a wide range of transport phenomena including electrokinetic coupling. When two or more of these transport phenomena occur simultaneously, they interfere and produce cross effects. These cross effects of coupled flows that can occur under the influences of hydraulic, thermal, electrical, and chemical gradients are summarized by Mitchell (1976) and Yeung (1993) as shown in Table 2-1.

These coupled and direct effects on flow phenomena can be described mathematically by adding terms proportional to their coupled driving forces to the corresponding conjugated flow equations. In each case, the experimentally observed empirical equation is a linear, homogeneous relationship between a flow and driving forces in the form of equation 2-1. In case of a system under flows of water, electric current, cation, and anion transport with their hydraulic, electrical, and chemical gradients across a membrane, equation 2-1 may be expressed as equations 2-4 (a-d) (Mitchell, 1976; Yeung, 1991):

Table 2-1: Coupled and direct flow phenomena (after Mitchell 1976, Yeung and Mitchell 1993).

Flux J_i	**Gradient X_j**			
	Hydraulic X_1	Electrical X_2	Thermal X_3	Chemical X_4
Fluid J_1	**Hydraulic conduction (Darcy's law)**	Electro-osmosis	Thermo-osmosis	Chemical osmosis
Electric current J_2	Streaming potential	**Electric conduction (Ohm's law)**	Seebeck effect	Diffusion and membrane potentials
Heat J_3	Isothermal heat transfer	Peltier effect	**Thermal conduction (Fourier's law)**	Dufour effect
Ion J_4	Ultra filtration	Electrophoresis	Soret effect	**Diffusion (Fick's law)**

$$J_w = L_{11}\nabla(-P) + L_{12}\nabla(-E) + L_{13}\nabla(-\mu_c^c) + L_{14}\nabla(-\mu_a^c) \quad [2\text{-}4a]$$

$$I = L_{21}\nabla(-P) + L_{22}\nabla(-E) + L_{23}\nabla(-\mu_c^c) + L_{24}\nabla(-\mu_a^c) \quad [2\text{-}4b]$$

$$J_c^d = L_{31}\nabla(-P) + L_{32}\nabla(-E) + L_{33}\nabla(-\mu_c^c) + L_{34}\nabla(-\mu_a^c) \quad [2\text{-}4c]$$

$$J_a^d = L_{41}\nabla(-P) + L_{42}\nabla(-E) + L_{43}\nabla(-\mu_c^c) + L_{44}\nabla(-\mu_a^c) \quad [2\text{-}4d]$$

These four equations contain four kinds of driving forces, and sixteen phenomenological coefficients. These unknown phenomenological coefficients can be reduced by Onsager's reciprocal relations.

$$L_{12} = L_{21} \quad [2\text{-}5]$$

$$L_{13} = L_{31} \quad [2\text{-}6]$$

$$L_{14} = L_{41} \quad [2\text{-}7]$$

$$L_{23} = L_{32} \quad [2\text{-}8]$$

$$L_{24} = L_{42} \qquad [2\text{-}9]$$

$$L_{34} = L_{43} \qquad [2\text{-}10]$$

There are ten independent coefficients characterizing the system. If any three of the driving forces can be set to zero in different experiments, the quantities of flows are determined by a single driving force. The ratio of the measured quantity of the flow to its driving force gives the L_{ij}. However, it is often more convenient to set two forces and one flow to zero so as to evaluate the appropriate unknown phenomenological coefficients, L_{ij}s, by implicit solution of the simultaneous equations. The calculation of these unknown phenomenological coefficients is presented for the situation of saturated zone of flow and solute transport in section 2.2.

2.2 PHENOMENOLOGICAL COEFFICIENTS

The derivations of phenomenological coefficients L_{ij}s in saturated flow situation are presented in sections from 2 2.1 to 2.2.5 (Yeung and Mitchell, 1993).

2.2.1 Phenomenological coefficient L_{11}

This coefficient is related to the hydraulic conductivity of the soil. Hydraulic conductivity is the most used variable parameter in geotechnical engineering (Olson and Daniel, 1981), ranging from 1 E-3 to 1 m/s for different soils (Freeze and Cherry, 1979). Using equations 2-4, if we suppose that only water flow and electrical current are

measured, and we assume that the concentration diffusional fluxes are zero because the gradients of cations and anions are zero; i.e., $\nabla(\mu_i^c) = 0$. Then, equations 2-4 reduce to

$$J_w = L_{11}\nabla(-P) + L_{12}\nabla(-E) \qquad [2\text{-}11a]$$

$$I = L_{21}\nabla(-P) + L_{22}\nabla(-E) \qquad [2\text{-}11b]$$

When I = 0 in equation 2-11b, we obtain

$$\nabla(-E) = -\frac{L_{21}}{L_{22}}\nabla(-P) \qquad [2\text{-}12]$$

for the gradient of streaming potential generated by the applied hydraulic gradient. Substitution of equation 2-12 into 2-11a gives

$$J_w = (L_{11} - \frac{L_{12}L_{21}}{L_{22}})\gamma_w\nabla(-h) \qquad [2\text{-}13]$$

where γ_w is the unit weight of water and h is the hydraulic head. J_w is the flow per unit total area which is related to the hydraulic gradient by Darcy's law

$$J_w = K_{hh}\nabla(-h) \qquad [2\text{-}14]$$

where K_{hh} is the hydraulic conductivity (L/T) of the soil, and h is the hydraulic head (L). Comparing the equations of 2-13 and 2-14, we obtain that

$$L_{11} = \frac{K_{hh}}{\gamma_w} + \frac{L_{12}L_{21}}{L_{22}} \qquad [2\text{-}15]$$

2.2.2 Phenomenological coefficients L_{12} (L_{21}) and L_{22}

In the measurements of the flow by electro-osmosis and the bulk electrical conductivity κ of a soil, electrodes are installed at both ends of the sample. Different electrical gradients are applied across the soil sample. The measurements are taken as flows and electric currents. In these situations, the solutions in the two reservoirs are maintained at the same hydraulic pressure; i.e., $\nabla(-P) = 0$. Moreover, if the solutions are of equal concentration, equal to that of the pore fluid in the soil, then $\nabla(\mu_c^c) = 0$. Therefore, equation 2-4 reduces to

$$J_w = L_{12}\nabla(-E) \qquad [2\text{-}16a]$$

$$I = L_{22}\nabla(-E) \qquad [2\text{-}16b]$$

In equation 2-16a, the right hand side is the fluid transport due to electrical gradients and the electro-osmotic permeability K_{he} ($m^2/V/s$). Casagrande (1983) gives the relation by

$$J_w = K_{he}\nabla(-E) \qquad [2\text{-}17]$$

where K_{he} for most soils is in the range of 1 E-9 to 1 E-8 m^2/Vs, and can be assumed to be about 5 E-9 m^2/Vs for practical purposes (Casagrande, 1983). Comparing the equations of 2-16a and 2-17, we obtain that

$$L_{12} = K_{he} \qquad [2\text{-}18]$$

The $L_{12} = L_{21}$ gives an equivalence of streaming potential and electro-osmosis obtained by the combination of equation 2-12 and 2-16 which is known as Saxen's law (De Groot, 1952)

$$\left(\frac{J_w}{I}\right)_{\Delta P=0} = -\left(\frac{\Delta E}{\Delta P}\right)_{I=0} \qquad [2\text{-}19]$$

This law has been verified experimentally for a number of clay-water-electrolyte systems (Miller, 1960; Gray, 1966).

Equation 2-16b is the same as the form of Ohm's law (Hayt, 1981) applied to the soil sample. Therefore,

$$L_{22} = \kappa \qquad [2\text{-}20]$$

From experience, it is known that κ is generally in the range 0.01-0.1 S/m for most soil (Yeung, 1990).

2.2.3 Phenomenological coefficients L_{33}, L_{34} (L_{43}) and L_{44}

Without hydraulic gradient and electrical gradient in the system, equations 2-4 reduce to

$$J_c^d = L_{33}\nabla(-\mu_c^c) + L_{34}\nabla(-\mu_a^c) \qquad [2\text{-}21a]$$

$$J_a^d = L_{43}\nabla(-\mu_c^c) + L_{44}\nabla(-\mu_a^c) \qquad [2\text{-}21b]$$

In order to discuss the equilibrium properties of liquid mixture, we need to know how the chemical potential of a solution depends on its composition. The concentration-dependent part of the chemical potential of species i can be expressed as

$$\mu_i^c = RT \ln \gamma_i C_i \qquad [2\text{-}22]$$

where R is the universal gas constant and γ_i is the activity coefficient of species i (Stumm and Morgan, 1981). The activity coefficient is function of the composition of the solution. When the solution is at infinite dilution (ideal dilute solution), the activity coefficient becomes unity; that is, $\gamma_i \rightarrow 1$ as $C_i \rightarrow 0$ (Atkins, 1990) so that

equation 2-22 becomes

$$\mu_i^c = RT \ln C_i \qquad [2\text{-}23]$$

By taking the derivative of both sides of equation 2-23, we obtain

$$\nabla(-\mu_i^c) = \frac{RT}{C_i}\nabla(-C_i) \qquad [2\text{-}24]$$

The transport of chemical species in solution in response to a gradient in its concentration is described by Fick's law of diffusion. According to the Fick's first law, the one dimensional transport can be written as:

$$J_i^d = D_i^0 \nabla(-C_i) \qquad [2\text{-}25]$$

where J_i^d is the diffusive mass flux, D_i^0 is the diffusion coefficient or diffusivity in free solution for species i. Because of the tortuous flow path in soil, the diffusion is slower than in free solution. A modification of Fick's first law is used for diffusion in saturated porous media:

$$J_i^d = n\tau D_i^0 \nabla(-C_i) \qquad [2\text{-}26]$$

or

$$J_i^d = nD_i^* \nabla(-C_i) \qquad [2\text{-}27]$$

where τ is an empirical coefficient which accounts for the tortuosity of soil, D_i^* is the effective diffusion coefficient of chemical species i in the soil, and n, the porosity term, is required since the diffusive flux, J_i^d, is defined with respect to the total cross-sectional area of the porous media. Values of τ are reported in the range 0.01 to 0.67 (Freeze and Cherry, 1979; Shackelford, 1989, and Shackelford and Daniel, 1991).

Another important mass transport of species flux is advection by the fluid in the porous media. The total species flux of i is related to the diffusional flux of species i and its relative flow advection to the water as follows:

$$J_i = J_i^d + C_i J_w \qquad [2\text{-}28]$$

As the process of interdiffusion is only the presence of concentration gradient, no water flow is associated (i.e. $J_w = 0$), the combination of equations 2-21, 2-24, and 2-28 gives

$$J_c = L_{33} \frac{RT}{C_c} \nabla(-C_c) + L_{34} \frac{RT}{C_a} \nabla(-C_a) \qquad [2\text{-}29a]$$

$$J_a = L_{43}\frac{RT}{C_c}\nabla(-C_c) + L_{44}\frac{RT}{C_a}\nabla(-C_a) \qquad [2\text{-}29b]$$

No interaction between ions is assumed in this dilute solution. Hence

$$L_{34} = L_{43} = 0 \qquad [2\text{-}30]$$

Substitution of equations 2-29 into equation 2-28 gives

$$J_c = L_{33}\frac{RT}{C_c}\nabla(-C_c) \qquad [2\text{-}31a]$$

$$J_a = L_{44}\frac{RT}{C_a}\nabla(-C_a) \qquad [2\text{-}31b]$$

Comparing equations 2-27 and 2-31, we get

$$L_{33} = \frac{nD_c^* C_c}{RT} \qquad [2\text{-}32a]$$

$$L_{44} = \frac{nD_a^* C_a}{RT} \qquad [2\text{-}32b]$$

2.2.4 Phenomenological coefficients L_{23} (L_{32}) and L_{24} (L_{42})

When no hydraulic gradient and no chemical gradient are present, i.e. $\nabla(-P) = 0$ and $\nabla(-\mu_i^c) = 0$, equations 2-4 become

$$J_c^d = L_{32}\nabla(-E) \qquad [2\text{-}33a]$$

$$J_a^d = L_{42}\nabla(-E) \qquad [2\text{-}33b]$$

where L_{32} and L_{42} are the proportionality constants relating the diffusional flows of the cation and the anion in response to an applied electric field. In soil science, there is no established test to measure the ionic species in response to an applied electrical gradient in soils to drive functional relations for L_{32} and L_{42} (Yeung, 1993). However, in physical chemistry, the ionic mobility u_i of an ion species i may be defined to be the velocity of ion in free solution under the influence of a unit electrical gradient as:

$$v_i = \frac{z_i}{|z_i|}u_i\nabla(-E) \qquad [2\text{-}34]$$

where z_i is the valence of species i. With no water flow, equations 2-33 equal

$$J_c = L_{32}\nabla(-E) \qquad [2\text{-}35a]$$

$$J_a = L_{42}\nabla(-E) \qquad [2\text{-}35b]$$

The ion flux migrating through the porous media is:

$$J_i = nC_i v_i \qquad [2\text{-}36]$$

Comparison of equations 2-35 and 2-36 gives

$$v_c = \frac{L_{32}}{nC_c}\nabla(-E) \qquad [2\text{-}37a]$$

$$v_a = \frac{L_{42}}{nC_a}\nabla(-E) \qquad [2\text{-}37b]$$

Let coefficients of equations 2-34 and 2-37 be equal so that

$$L_{32} = nu_c C_c \qquad [2\text{-}38a]$$

$$L_{42} = -nu_a C_a \qquad [2\text{-}38b]$$

Due to the tortuosity, the paths of ionic migration in soils are much longer than those in aqueous solutions so that equations 2-38 are modified to

$$L_{32} = nu_c^* C_c \qquad [2\text{-}39a]$$

$$L_{42} = -nu_a^* C_a \qquad [2\text{-}39b]$$

where u_i^* is the effective ionic mobility and can be theoretically estimated by assuming that the Nernst-Townsend-Einstein relation between D_i and u_i holds for ions in the pore fluid of soil (Holmes, 1962; Mitchell and Yeung, 1991; Alshawabkeh and Acar, 1992).

$$u_i^* = \frac{D_i^* |z_i| F}{RT} \qquad [2\text{-}40]$$

Substitution of equation 2-40 into equations 2-39 gives

$$L_{32} = n\frac{D_c^* z_c F}{RT} C_c \qquad [2\text{-}41a]$$

$$L_{42} = -n\frac{D_a^* z_a F}{RT} C_a \qquad [2\text{-}41b]$$

2.2.5 Phenomenological coefficients L_{13} (L_{31}) and L_{14} (L_{41})

Osmosis is the passage of a pure solvent into a solution separated from it by a semipermeable membrane, a membrane permeable to the solvent but not to the solute.

The flow of solvent through the membrane into the solution will stop when the hydraulic pressure difference developed is equal to the osmotic pressure π . The osmotic pressure π is the pressure that must be applied to the solution at the high concentration side to stop the flow of solvent into the solution. This osmotic pressure can be approximated by the Van't Hoff equation.

$$\pi = RT\sum_{i=1}^{n-1}\Delta C_i \qquad [2\text{-}42]$$

When the ionic concentration differences across the permeable membrane are caused by one cation and one anion, equation 2-42 is simplified to

$$\pi = RT\nabla C_c + RT\nabla C_a \qquad [2\text{-}43]$$

The measurement of osmotic pressure induced by the concentration difference across the semipermeable membrane is conducted through the saturated zone that the flows of solvent and electric current are zero; i.e.,

$$J_w = 0 \qquad [2\text{-}44a]$$

$$I = 0 \qquad [2\text{-}44b]$$

Substitution of equation 2-44b into equation 2-4b gives

$$\nabla[-E] = -\frac{L_{21}}{L_{22}}\nabla(-P) - \frac{L_{23}}{L_{22}}\nabla(-\mu_c^c) - \frac{L_{24}}{L_{22}}\nabla(-\mu_a^c) \qquad [2\text{-}45]$$

Substituting equations 2-24, 2-48a, and 2-45 into equation 2-4a, we have

$$\nabla P = -\left(\frac{L_{13}L_{22} - L_{12}L_{23}}{L_{11}L_{22} - L_{12}L_{21}}\right)\frac{RT}{C_c}\nabla C_c - \left(\frac{L_{14}L_{22} - L_{12}L_{24}}{L_{11}L_{22} - L_{12}L_{21}}\right)\frac{RT}{C_a}\nabla C_a \qquad [2\text{-}46]$$

For an ideal semipermeable membrane, no ions can pass. The pressure difference developed is the osmotic pressure,

$$\nabla P = \pi \qquad [2\text{-}47]$$

However, most the soil behave as leaky membranes, i.e. they enable passage of some ions, hence we have

$$\frac{\nabla P}{\pi} = \omega \qquad [2\text{-}48]$$

where ω is a measure of membrane efficiency, known as the reflection coefficient or osmotic selectivity coefficient (Kemper and Rollins, 1966). When $\omega = 1$, the membrane

is an ideal semipermeable and all the ions are reflected. When $\omega = 0$, the membrane is non-selective and no ions are reflected. The value of ω depend on the properties of both membrane and the ions (Katchalsky and Curran, 1967; Yeung, 1990). Substituting equation 2-48 into equation 2-46 and comparing the coefficients of equation 2-43, we have

$$L_{13} = -\frac{\omega C_c(L_{11}L_{22} - L_{12}L_{21}) - L_{12}L_{23}}{L_{22}} \qquad [2\text{-}49a]$$

$$L_{14} = -\frac{\omega C_a(L_{11}L_{22} - L_{12}L_{21}) - L_{12}L_{24}}{L_{22}} \qquad [2\text{-}49b]$$

In summary, the coupled flow processes through the saturated zone can be expressed by the phenomenological theory of irreversible processes in fluid systems composed of flow of water, current, and cations and anions under the driving forces of hydraulic, electrical, and chemical gradients as previous equations 2-4 as follows.

$$J_w = L_{11}\nabla(-P) + L_{12}\nabla(-E) + L_{13}\nabla(-\mu_c^c) + L_{14}\nabla(-\mu_a^c) \qquad [2\text{-}50a]$$

$$I = L_{21}\nabla(-P) + L_{22}\nabla(-E) + L_{23}\nabla(-\mu_c^c) + L_{24}\nabla(-\mu_a^c) \qquad [2\text{-}50b]$$

$$J_c^d = L_{31}\nabla(-P) + L_{32}\nabla(-E) + L_{33}\nabla(-\mu_c^c) + L_{34}\nabla(-\mu_a^c) \qquad [2\text{-}50c]$$

$$J_a^d = L_{41}\nabla(-P) + L_{42}\nabla(-E) + L_{43}\nabla(-\mu_e^c) + L_{44}\nabla(-\mu_a^c) \qquad [2\text{-}50d]$$

The sixteen phenomenological coefficients can be reduced to ten terms by the Onsager's reciprocal relations and be experimentally determined as:

$$L_{11} = \frac{K_{hh}}{\gamma_W} + \frac{L_{12}L_{21}}{L_{22}} = \frac{K_{hh}}{\gamma_W} + \frac{K_{he}^2}{\kappa} \qquad [2\text{-}51]$$

$$L_{12} = L_{21} = K_{he} \qquad [2\text{-}52]$$

$$\begin{aligned} L_{13} = L_{31} &= -\frac{\omega C_e(L_{11}L_{22} - L_{12}L_{21}) - L_{12}L_{23}}{L_{22}} \\ &= -\omega C_e\left(\frac{K_{hh}}{\gamma_W}\right) + \frac{L_{12}L_{23}}{L_{22}} \\ &= -\omega C_e\left(\frac{K_{hh}}{\gamma_W}\right) + \frac{K_{he}nu_e^*C_e}{\kappa} \end{aligned} \qquad [2\text{-}53]$$

$$\begin{aligned} L_{14} = L_{41} &= -\frac{\omega C_a(L_{11}L_{22} - L_{12}L_{21}) - L_{12}L_{24}}{L_{22}} \\ &= -\omega C_a\left(\frac{K_{hh}}{\gamma_W}\right) + \frac{L_{12}L_{24}}{L_{22}} \\ &= -\omega C_a\left(\frac{K_{hh}}{\gamma_W}\right) + \frac{K_{he}nu_a^*C_a}{\kappa} \end{aligned} \qquad [2\text{-}54]$$

$$L_{22} = \kappa \qquad [2\text{-}55]$$

$$L_{23} = L_{32} = nu_c^* C_c = n\frac{D_c^* z_c F}{RT} C_c \quad [2\text{-}56]$$

$$L_{24} = L_{42} = -nu_a^* C_c = -n\frac{D_a^* z_a F}{RT} C_a \quad [2\text{-}57]$$

$$L_{33} = \frac{nD_c^* C_c}{RT} \quad [2\text{-}58]$$

$$L_{34} = L_{43} = 0 \quad [2\text{-}59]$$

$$L_{44} = \frac{nD_a^* C_a}{RT} \quad [2\text{-}60]$$

where,

K_{hh} is the hydraulic conductivity

K_{he} is the coefficient of electro-osmotic permeability

κ is the bulk electrical conductivity of soil

ω is the coefficient of osmotic efficiency

γ_w is the unit weight of water

C_c is the concentration of cation

C_a is the concentration of anion

u_c^* is the effective ionic mobility of cation

u_a^* is the effective ionic mobility of anion

D_c^* is the effective diffusivity of cation

D_a^* is the effective diffusivity of anion

n is the porosity of soil

R is the universal gas constant

T is the absolute temperature

F is the Faraday's constant

Also, recall equation 2-28 that the total species concentration flux of i is the sum of the diffusive flux of species i and its relative flux to the water as follows:

$$J_i = J_i^d + C_i J_w \qquad [2\text{-}61]$$

Hence, the mass transport process of interdiffusion is the presence of concentrational gradient diffusion, and water flow advection. The combination of equations 2-4a and 2-50c, and 2-4a and 2-50d gives the flow equations for cations and anions under the influences of hydraulic, electrical, and chemical gradients,

$$J_c = (L_{31} + C_c L_{11})\gamma_w \nabla(-h) + (L_{32} + C_c L_{12})\nabla(-E) + (L_{33} + C_c L_{13})\frac{RT}{C_c}\nabla(-C_c) + (L_{34} + C_c L_{14})\frac{RT}{C_a}\nabla(-C_a) \qquad [2\text{-}62a]$$

$$J_a = (L_{41} + C_a L_{11})\gamma_w \nabla(-h) + (L_{42} + C_a L_{12})\nabla(-E) + (L_{43} + C_a L_{13})\frac{RT}{C_a}\nabla(-C_c) + (L_{44} + C_a L_{14})\frac{RT}{C_a}\nabla(-C_a) \quad [2\text{-}62b]$$

where $\nabla(-h)$ is the hydraulic gradient (dimensionless).

2.3 TRANSIENT TRANSPORT

The transient transport equations for the conservation of mass, charge, and energy in a continuum condition are used to model the saturated zone coupled processes transport of contaminant (Alshawabkeh and Acar, 1996).

$$S_s \frac{\partial h}{\partial t} = -\nabla \cdot J_w \quad [2\text{-}63a]$$

$$\frac{\partial T_e}{\partial t} = -\nabla \cdot I \quad [2\text{-}63b]$$

$$n\frac{\partial C_c}{\partial t} = -\nabla \cdot J_c + \sum \rho_b R_c \quad [2\text{-}63c]$$

$$n\frac{\partial C_a}{\partial t} = -\nabla \cdot J_a + \sum \rho_b R_a \quad [2\text{-}63d]$$

where T_e is the volumetric charge density of the soil medium (C/L^3), S_s is the specific storage of the aquifer (dimensionless), t is the time, ρ_b is the bulk density of soil

samples, and $\sum R_c$ and $\sum R_a$ (mole/L^3/T) are the production rates of the cations and anions per unit of fluid volume due to chemical reaction such as sorption/desorption, precipitation-dissolution, oxidation/reduction, and aqueous phase reactions.

The electrical gradients will be assumed constant throughout the process, and it will be assumed that the aqueous components are not involved in any chemical reactions except for linear sorption. Therefore, apply the continuity condition the equations 2-63a through 2-63d are simplified as follows:

$$S_s \frac{\partial h}{\partial t} = -\nabla \cdot J_w \qquad [2\text{-}64a]$$

$$= -\nabla \cdot \left[L_{11} \nabla(-P) + L_{12} \nabla(-E) + L_{13} \nabla(-\mu_c^c) + L_{14} \nabla(-\mu_a^c) \right] \qquad [2\text{-}64b]$$

$$\frac{\partial T_c}{\partial t} = -\nabla \cdot I \qquad [2\text{-}65a]$$

$$= -\nabla \cdot \left[L_{21} \nabla(-P) + L_{22} \nabla(-E) + L_{23} \nabla(-\mu_c^c) + L_{24} \nabla(-\mu_a^c) \right] \qquad [2\text{-}65b]$$

$$\frac{\partial C_c}{\partial t} = -\frac{1}{nR_d} \nabla \cdot [(L_{31} + C_c L_{11}) \gamma_w \nabla(-h) + (L_{32} + C_c L_{12}) \nabla(-E) + (L_{33} + C_c L_{13}) \frac{RT}{C_c} \nabla(-C_c) + (L_{34} + C_c L_{14}) \frac{RT}{C_a} \nabla(-C_a)] \qquad [2\text{-}66]$$

$$\frac{\partial C_a}{\partial t} = -\frac{1}{nR_d}\nabla\cdot[(L_{41}+C_aL_{11})\gamma_w\nabla(-h)+(L_{42}+C_aL_{12})\nabla(-E) \quad [2\text{-}67]$$
$$+(L_{43}+C_aL_{13})\frac{RT}{C_c}\nabla(-C_c)+(L_{44}+C_aL_{14})\frac{RT}{C_a}\nabla(-C_a)]$$

2.4 ELECTROKINETICS REMEDIATION

Coupled processes were discovered first by Rouss in 1801 (Bear 1972). He performed an experiment that showed that an applied electrical voltage may produce flows of electric charge and fluid in a porous medium. In contrast, an applied hydraulic head difference may produce not only a flow of fluid but also a flow of electric charge. By applying electric voltage, heavy metal contaminants may be removed from the soil, especially fined-grained soil.

2.4.1 Electrokinetics application

Application of coupled processes was first reported by Casagrande in 1947 (Mitchell, 1993). He used electroosmosis in consolidation and stabilization of soft fine-grained soils. Since 1947, environmental and geotechnical engineers have performed substantial research on coupled processes. Environmental engineers use electrophoresis to separate inorganic ions, amino acids, peptides, large protein molecules, and metal ions from contamination sites. Geotechnical engineers apply electrokinetics technique to stabilize soil at foundation or dam, to dewater and consolidate fine-grained soil at mine tailings, and to inject bentonite suspension into low hydraulic conductivity soils. Most recently, Yeung (1990) used electrokinetics technique to prevent contaminant leakage

through compacted clay liners. Chung (1994) used electrophores to stop leakage on synthetic liners by forming a bentonite clay plug that seals the hole. Hus (1997) investigated enhanced electrokinetics extraction of lead from a natural kaolinite soil with 90% removal. The electrokinetics technique to prevent or to remove environmental pollutants in the fine-grained soils was become more widely use.

2.4.2 Electrokinetics modeling

Modeling of coupled transport processes is currently limited because of the complex physical and chemical aspects of these processes. Nonetheless, four models have recently been presented for evaluating contaminant removal by coupled transport processes.

Acar et al. (1990) presented a one-dimensional finite element model used to predict the pH distribution under the combined effects of hydraulic, electrical, and chemical gradients. The model provides good agreement with experimental evaluation of hydrogen ion transport and distribution. However, it neglects the transient changes in electrical and hydraulic gradients.

Mitchell and Yeung (1991) described a one-dimensional finite difference model in a study evaluating the feasibility of using electroosmosis to retard the migration of contaminants across fine-grained soil barriers used in waste disposal facilities. Their model predictions of the transport of sodium and chloride ions across the barriers were in "fairly good" agreement with experimental data. The limitations of their model include those of the model presented by Acar et al. (1990). Furthermore, it did not include electrochemical reactions at the electrodes.

Shapiro et al. (1989) incorporated electrochemistry in transport processes in a one-dimensional finite element model that accounts for the aqueous phase reactions in the pore fluid. However, the model by Shapiro et al. (1989) does not include the sorption and complex chemistry.

Alshawabkeh and Acar (1996) presented a one-dimensional finite element model that includes multicomponent chemical reactions in the transport processes such as electrical neutrality and complexation. This model also predicted the chemical distributions for pilot scale experimental data fairly well. The limitations of this model are that it does not include pH buffer capacity, chemical sorption, and chemical precipitation. Also, the chemical reactions of this model account only for the case of lead removal.

Alshawabkeh and Acar (1996) addressed there were demand to deal with the thermal effects on the eletrokinetics technique. A potentially significant limitation in all the four models summarized above is that they do not consider thermal gradients during solute transport, i.e., all the models assume isothermal conditions. Also, their models handle only parameters partially of the coupled flow processes for the lack of laboratory and field data. Therefore, an improved theoretical formulation including nonisothermal conditions during coupled processes is proposed. This model will focus on the additional thermal coupled effects and the general purpose formulation of the contaminant transport.

In fine-grained soils, coupling among hydraulic, chemical, electric, and thermal gradients (HCET) can be responsible for other coupled processes. Some effects of coupled processes are significant in application for environmental/geotechnical

engineering, but are currently ignored in groundwater engineering (Shackelford, 1989; Mitchell, 1993). This research will deal with the above related problems for coupled processes contaminant transport using HCET model to explore the parameter sensitivity analysis.

CHAPTER 3

MATHEMATICAL DEVELOPMENT

This chapter we would like to development the mathmatical theory for HCET model which includes the govering equations, and its simplfied application. We will put its programing souce code in the Appendix for readers reference.

3.1 GOVERNING EQUATIONS

The primary field variables are: hydraulic head, h, total analytical concentration of components j, C_j, electrical voltage, E, and temperature, T. Thus, there is a total of four unknown variables, governed by four independent transport equations.

3.1.1 Flux equations

The flux of coupled flow processes through the subsurface zone can be expressed by the phenomenological theory of irreversible processes in fluid systems composed of flow of water, chemical, current, and heat under the driving forces of hydraulic head, concentration, electrical voltage, and temperature gradients as follows.

$$J_w = K_{hh}\nabla(-h) + \sum \omega_j \frac{K_{hh}}{\gamma_w} RT\nabla(-C_j) + K_{he}\nabla(-E) + K_{ht}\nabla(-T) \qquad [3\text{-}1a]$$

$$J_{C_j}^{d} = K_{ch}\gamma_w \nabla(-h) + n\sum D_j^{*}\nabla(-C_j) + n\sum C_j u_j^{*}\nabla(-E) + \lambda_{ct}\nabla(-T) \qquad [3\text{-}1b]$$

$$J_I^{d} = K_{eh}\gamma_w \nabla(-h) + nF\sum z_j D_j^{*}\nabla(-C_j) + \sigma_{ee}\nabla(-E) + \sigma_{et}\nabla(-T) \qquad [3\text{-}1c]$$

$$J_T^{d} = K_{th}\gamma_w \nabla(-h) + \sum \lambda_{te}\frac{RT}{C_j}\nabla(-C_j) + \sigma_{te}\nabla(-E) + \lambda_{tt}\nabla(-T) \qquad [3\text{-}1d]$$

Where,

C_j = the total molar concentration of the j^{th} component (M),

D_j^* = the effective diffusion coefficient of the j^{th} component ($m^2 sec^{-1}$),

E = the electrical potential (volt),

F = the Faraday's constant (96,485 C per mole electrons),

h = the hydraulic head (m),

J_I^d = the current density ($C\ sec^{-1} m^{-2}$),

$J_{C_j}^d$ = diffusional chemical flux per unit cross sectional area of the soil (moles $m^{-2} sec^{-1}$),

J_T^d = diffusional heat flux per unit cross sectional area of the soil ($J\ sec^{-1} m^{-2}$),

J_W = fluid flux per unit cross sectional area of the soil ($m^3\ sec^{-1} m^{-2}$),

K_{ch} = the coefficient of ultra filtration ($mole\ m\ sec^{-1} N^{-1}$),

K_{eh} = the coefficient of streaming potential ($m\ C\ N^{-1} sec^{-1}$),

K_{hh} = the coefficient of hydraulic conductivity ($m\ sec^{-1}$),

K_{he} = the coefficient of electro-osmotic permeability ($m^2\ sec^{-1}\ volt^{-1}$),

K_{ht} = the coefficient of thermoosmosis ($m^2\ sec^{-1} K^{-1}$),

K_{th} = the coefficient of isothermo heat transfer ($J\ m\ sec^{-1} N^{-1}$),

n = the soil porosity (dimensionless),

R = the universal gas constant ($8.314 J\ mol^{-1} K^{-1}$),

T = the absolute temperature (K),

u_j^* = the effective ionic mobility of the j^{th} chemical species ($m^2 volt^{-1} sec^{-1}$)

$= \frac{D_j^* z_j F}{RT}$,

z_j = the charge of the j^{th} component,

λ_{ct} = the coefficient of Soret effect ($moles\ m^{-1} sec^{-1} K^{-1}$),

λ_{tt} = the coefficient of thermal conductivity ($J\ m^{-1} sec^{-1} K^{-1}$),

λ_{tc} = the coefficient of Dufour effect ($mol\ sec^{-1} m^{-1}$),

γ_W = the unit weight of water ($9.81 N\ m^{-3}$),

σ_{ee} = the effective electric conductivity of the porous media ($C\ m^{-1} sec^{-1} volt^{-1}$),

σ_{et} = the coefficient of thermal electricity ($C\ m^{-1} sec^{-1} K^{-1}$),

σ_{te} = the coefficient of Peltier effect ($J\ volt^{-1} sec^{-1} m^{-1}$), and

ω or ω_j = the coefficient of osmotic efficiency (0 to 1).

To simplify the notation, we can express the flux of coupled flows as:

$$J_w = K_{hh}\nabla(-h) + K_{hco}\nabla(-C_j) + K_{he}\nabla(-E) + K_{ht}\nabla(-T) \quad [3\text{-}2a]$$

$$J_{C_j}^d = D_{cho}^*\nabla(-h) + n\sum D_j^*\nabla(-C_j) + n\sum C_j u_j^*\nabla(-E) + D_{cto}^*\nabla(-T) \quad [3\text{-}2b]$$

$$J_I^d = \sigma_{eho}\nabla(-h) + \sigma_{eco}\nabla(-C_j) + \sigma_{ee}\nabla(-E) + \sigma_{eto}\nabla(-T) \quad [3\text{-}2c]$$

$$J_T^d = \lambda_{th}\nabla(-h) + \lambda_{tco}\nabla(-C_j) + \lambda_{teo}\nabla(-E) + \lambda_{tt}\nabla(-T) \quad [3\text{-}2d]$$

where,

$$K_{hco} = \sum \omega_j RT\frac{K_{hh}}{\gamma_w} \quad [3\text{-}2e]$$

$$\sigma_{eho} = K_{eh}\gamma_w \quad [3\text{-}2f]$$

$$\sigma_{eto} = \sigma_{et} \quad [3\text{-}2g]$$

$$\sigma_{eco} = nF\sum z_j D_j^* \quad [3\text{-}2h]$$

$$\lambda_{th} = K_{th}\gamma_w \quad [3\text{-}2i]$$

$$\lambda_{teo} = \sigma_{te} \quad [3\text{-}2j]$$

$$\lambda_{tco} = \sum \lambda_{tc}\frac{RT}{C_j} \quad [3\text{-}2k]$$

$$D_{cho}^* = K_{ch}\gamma_w \quad [3\text{-}2l]$$

$$D_{cto}^* = \lambda_{ct} \quad [3\text{-}2m]$$

3.1.2 Absolute chemical flux

One important mass transport of comopnent flux in the subsurface zone is advection by the fluid in the porous media. The absolute chemical flux of C_j (i.e., flux relative to a stationary solid phase) is related to the diffusional flow flux of component C_j and its relative flow advection to the water (Alshawabkeh and Acar, 1992; Yeung and Mitchell, 1993) as:

$$J_{C_j} = J^d_{C_j} + C_j J_w \qquad [3\text{-}3a]$$

Substituting equations.3-2a and 3-2b into 3-3a, we obtain absolute chemical flux

$$J_{C_j} = D^*_{cho}\nabla(-h) + n\sum D^*_j\nabla(-C_j) + n\sum C_j u^*_j\nabla(-E) + D^*_{cto}\nabla(-T) \qquad [3\text{-}3b]$$
$$+ C_j[K_{hh}\nabla(-h) + K_{hco}\nabla(-C_j) + K_{he}\nabla(-E) + K_{ht}\nabla(-T)]$$

3.1.3 Absolute charge flux

The absolute charge flux (i.e., flux relative to a stationary solid phase) is the sum of the diffusional charge flux and its convective charge flux (Shapiro 1990; Acar and Akram 1993) as:

$$J_i = J^d_i + \sum^{N} z_i F \frac{C_i}{C_w} J_w \qquad [3-4a]$$

Employ the perservation of electrical neutrality,

$$\sum^{N} C_i z_j = 0 \qquad [3-4b]$$

The contibution of convective charge flux, the second term of equation 3-4a, is zero. Therefore, the absolute charge flux is equal to the diffusional charge flux when electricial neutrality is applied.

3.1.4 Absolute thermal flux

The absolute thermal flux (i.e., flux relative to a stationary solid phase) is related to the diffusional thermal flux of component C_j and its relative thermal advection to the water (De Groot, 1952) as:

$$J_T = J_T^d + TJ_w \qquad [3\text{-}5a]$$

J_T is the absolute thermal flux that includes diffusional and advective flux of heat, but does not include radiation, evaporation/condensation or freezing/thawing effects. Substituting equations 3-2a and 3-2d into 3-5a, we obtain absolute thermal flux

$$J_T = \lambda_{th}\nabla(-h) + \lambda_{tco}\nabla(-C_j) + \lambda_{te}\nabla(-E) + \lambda_{tt}\nabla(-T) \qquad [3\text{-}5b]$$
$$+ T[K_{hh}\nabla(-h) + K_{hco}\nabla(-C_j) + K_{he}\nabla(-E) + K_{ht}\nabla(-T)]$$

3.1.5 Transient transport

Continuity of water, mass, charge, and energy in a unit volume of the soil pore fluid under the set of assumptions employed required that

$$S_s\frac{\partial h}{\partial t} = -\nabla\cdot J_w \qquad [3\text{-}6a]$$

$$n\frac{\partial C_j}{\partial t} = -\nabla\cdot J_{C_j} \qquad [3\text{-}6b]$$

$$\frac{\partial T_e}{\partial E}\frac{\partial E}{\partial t} = \frac{1}{C_{IP}}\frac{\partial E}{\partial t} = -\nabla\cdot J_I \qquad [3\text{-}6c]$$

$$C_{TP}\left(\frac{\partial T}{\partial t}\right) = -\nabla\cdot J_T \qquad [3\text{-}6d]$$

where,

$\frac{\partial C_j}{\partial t}$ = the rate of storage change of the j^{th} chemical component per volume of solution ($M\ sec^{-1}$),

C_{IP} = the electrical capacitance per unit volume ($farad\ L^{-1}$),

C_{TP} = the heat capacity of the porous medium ($J\ ^0C^{-1}\ m^{-3}$),

n = the porosity of porous medium (dimensionless),

S_s = the specific storage of the porous medium (m^{-1}),

Te = the volumetric charge density of the soil medium ($C\ L^{-1}$), and

t = sec.

By substitutions of 3-2 (a-d), 3-3b, and 3-4a, 3-5b into the eqs. 3-6a through 3-6d, the continuity conditions become:

$$S_s \frac{\partial h}{\partial t} = -\nabla \cdot J_w \qquad [3\text{-}7a]$$

$$= -\nabla \cdot \left[K_{hh} \nabla(-h) + K_{he} \nabla(-E) + K_{ht} \nabla(-T) + K_{hco} \nabla(-C_j) \right] \qquad [3\text{-}7b]$$

$$= K_{hh} \frac{\partial^2 h}{\partial x^2} + K_{he} \frac{\partial^2 E}{\partial x^2} + K_{ht} \frac{\partial^2 T}{\partial x^2} + K_{hco} \frac{\partial^2 C_j}{\partial x^2} \qquad [3\text{-}7c]$$

$$n \frac{\partial C_j}{\partial t} = -\nabla \cdot J_{C_j} \qquad [3\text{-}8a]$$

$$= -\nabla \cdot \{ D^*_{cho} \nabla(-h) + n \sum C_j u_j^* \nabla(-E) + D^*_{ctn} \nabla(-T) + n \sum D_j^* \nabla(-C_j) + C_j [K_{hh} \nabla(-h) + K_{he} \nabla(-E) + K_{ht} \nabla(-T) + K_{hco} \nabla(-C_j)] \} \qquad [3\text{-}8b]$$

$$\frac{1}{C_{IP}} \frac{\partial E}{\partial t} = -\nabla \cdot J_I \qquad [3\text{-}9a]$$

$$= -\nabla \cdot \left[\sigma_{eho} \nabla(-h) + \sigma_{eco} \nabla(-C_j) + \sigma_{ee} \nabla(-E) + \sigma_{eto} \nabla(-T) \right] \qquad [3\text{-}9b]$$

$$= \sigma_{eho} \frac{\partial^2 h}{\partial x^2} + \sigma_{eco} \frac{\partial^2 C_j}{\partial x^2} + \sigma_{ee} \frac{\partial^2 E}{\partial x^2} + \sigma_{eto} \frac{\partial^2 T}{\partial x^2} + \frac{\partial \sigma_{ee}}{\partial x} \frac{\partial E}{\partial x} \qquad [3\text{-}9c]$$

$$C_{TP}\frac{\partial T}{\partial t} = -\nabla \cdot J_T \qquad [3\text{-}10a]$$

$$= -\nabla \cdot \{\lambda_{th}\nabla(-h) + \lambda_{teo}\nabla(-E) + \lambda_{tt}\nabla(-T) + \lambda_{tco}\nabla(-C_j) \qquad [3\text{-}10b]$$
$$+ T[K_{hh}\nabla(-h) + K_{he}\nabla(-E) + K_{ht}\nabla(-T) + K_{hco}\nabla(-C_j)]\}$$

3.2 SIMPLIFIED APPLICATION

3.2.1 Advection-dispersion flux

If, under isothermal condition, without electrical gradient, without effects of streaming potential and chemical osmosis, the equation 3-3b becomes

$$J_{(C_j)} = C_j K_{hh}\nabla(-h) + nD_j^*\nabla(-C_j) \qquad [3\text{-}11]$$

Equation 3-11 is the familiar advection-dispersion flux describing the migration of nonreactive contaminants through a porous medium (Freeze and Cherry, 1979; Folkes, 1982; Gillham and Cherry, 1982; Gillham et al., 1984; Yeung and Mitchell 1993).

3.2.2 Transient flow equation

If the thermal gradient, electrical gradient, and chemical osmosis are neglect, the equation 3-7c becomes

$$S_s\frac{\partial h}{\partial t} = K_{hh}\frac{\partial^2 h}{\partial x^2} \qquad [3\text{-}12]$$

Equation 3-12 is the familiar unsteady state flow equation describing the one dimensional flow through a homogeneous porous media (McWhorter and Sunada, 1977; Freeze and Cherry, 1979; Istok, 1989).

3.2.3 Solute transient transport equation

If, under isothermal condition, without electrical gradient, without effects of streaming potential and chemical osmosis, the equation 3-8b becomes

$$n\frac{\partial C_j}{\partial t} = -\frac{\partial}{\partial x}\left(C_j q_w\right) + nD_j^* \frac{\partial^2 C_j}{\partial x^2} \qquad [3\text{-}13]$$

Equation 3-13 is the familiar unsteady state solute transport equation for nonuniform flow describing the one dimensional solute transient transport through a porous media (McWhorter and Sunada, 1977; Freeze and Cherry, 1979; Istok, 1989; Shackelford, 1989).

3.2.4 Heat transport equation

Without electrical gradient, chemical gradient, effects of isothermal heat transfer and thermal osmosis, the equation 3-10b becomes

$$C_{TP}\frac{\partial T}{\partial t} = -\frac{\partial}{\partial x}\left(T q_w\right) + \lambda_m \frac{\partial^2 T}{\partial x^2} \qquad [3\text{-}14]$$

Equation 3-14 is the general heat transport equation describing the liquid heat transport without phase change (van der Heijde, 1993). The heat flux in the right hand side of equation 3-14 is the convective heat flux and diffusional heat flux.

CHAPTER 4

FINITE ELEMENT FORMULATION

Since there is no analytical solution for thermodynamically complex systems as the derived governing equations present in Chapter 3, a numerical algorithm is demand to solve these equations. A finite element method is chosen to serve a numerical tool for the solutions of these governing equations. The finite element formulation has some advantages than other numerical methods (Reddy, 1993; Thompson 1995; Entwistle, 1999). For example, it is more flexible to handle boundary conditions and it is more stability to solve a coupled governing equations (Fletcher, 1991). Following finite element formulation for given governing equations will includes semidiscrete formulation of spatial variation, time approximation, and imposing of initial and boundary conditions (Huyakorn and Pinder, 1983).

Recall equations of 3-7c, 3-8b, 3-9c, and 3-10b and repeat them here:

$$S_s \frac{\partial h}{\partial t} = K_{hh} \frac{\partial^2 h}{\partial x^2} + K_{he} \frac{\partial^2 E}{\partial x^2} + K_{ht} \frac{\partial^2 T}{\partial x^2} + K_{hco} \frac{\partial^2 C_j}{\partial x^2} \qquad [3\text{-}7c]$$

$$n\frac{\partial C_j}{\partial t} = -\nabla\cdot\{D^*_{cho}\nabla(-h) + n\sum C_j u_j^*\nabla(-E) + D^*_{cto}\nabla(-T) + n\sum D_j^*\nabla(-C_j) + C_j[K_{hh}\nabla(-h) + K_{he}\nabla(-E) + K_{ht}\nabla(-T) + K_{hco}\nabla(-C_j)]\} \quad [3\text{-}8b]$$

$$\frac{1}{C_{IP}}\frac{\partial E}{\partial t} = \sigma_{eho}\frac{\partial^2 h}{\partial x^2} + \sigma_{eco}\frac{\partial^2 C_j}{\partial x^2} + \sigma_{ee}\frac{\partial^2 E}{\partial x^2} + \sigma_{eto}\frac{\partial^2 T}{\partial x^2} + \frac{\partial\sigma_{ee}}{\partial x}\frac{\partial E}{\partial x} \quad [3\text{-}9c]$$

$$C_{TP}\frac{\partial T}{\partial t} = -\nabla\cdot\{\lambda_{th}\nabla(-h) + \lambda_{teo}\nabla(-E) + \lambda_{tt}\nabla(-T) + \lambda_{tco}\nabla(-C_j) + T[K_{hh}\nabla(-h) + K_{he}\nabla(-E) + K_{ht}\nabla(-T) + K_{hco}\nabla(-C_j)]\} \quad [3\text{-}10b]$$

These above equations can be written in matrix form as:

$$\begin{bmatrix} K_{hh} & K_{hco} & K_{he} & K_{ht} \\ D^*_{cho} + C_j K_{hh} & nD_j^* + C_j K_{hco} & nC_j u_j^* + C_j K_{he} & D^*_{cto} + C_j K_{ht} \\ \sigma_{eho} & \sigma_{eco} & \sigma_{ee} & \sigma_{eto} \\ \lambda_{th} + TK_{hh} & \lambda_{tco} + TK_{hco} & \lambda_{teo} + TK_{he} & \lambda_{tt} + TK_{ht} \end{bmatrix}\begin{bmatrix} h^* \\ C_j^* \\ E^* \\ T^* \end{bmatrix}$$

$$+\begin{bmatrix} 0 & 0 & 0 & 0 \\ 0 & +K_{hh}\nabla h + K_{hco}\nabla C_j & 0 & 0 \\ & +K_{he}\nabla E + K_{ht}\nabla T & & \\ 0 & 0 & \nabla\sigma_{ee} & 0 \\ 0 & 0 & 0 & +K_{hh}\nabla h + K_{hco}\nabla C_j \\ & & & +K_{he}\nabla E + K_{ht}\nabla T \end{bmatrix}\begin{bmatrix} h^* \\ C_j^* \\ E^* \\ T^* \end{bmatrix} = \frac{\partial}{\partial t}\begin{bmatrix} S_s h \\ nC_j \\ \frac{1}{C_{IP}}E \\ C_{TP}T \end{bmatrix} \quad [4\text{-}1]$$

The notation, in equation 4-1, is simplified by writing

$$\begin{bmatrix} A^{11} & B^{12} & C^{13} & D^{14} \\ A^{21} & B^{22} & C^{23} & D^{24} \\ A^{31} & B^{32} & C^{33} & D^{34} \\ A^{41} & B^{42} & C^{43} & D^{44} \end{bmatrix}\begin{bmatrix} h^* \\ C_j^* \\ E^* \\ T^* \end{bmatrix} + \begin{bmatrix} 0 & 0 & 0 & 0 \\ 0 & V^{44} & 0 & 0 \\ 0 & 0 & V^{33} & 0 \\ 0 & 0 & 0 & V^{44} \end{bmatrix}\begin{bmatrix} h^* \\ C_j^* \\ E^* \\ T^* \end{bmatrix} = \begin{bmatrix} S_s\frac{\partial h}{\partial t} \\ n\frac{\partial C_j}{\partial t} \\ \frac{1}{C_{IP}}\frac{\partial E}{\partial t} \\ C_{TP}\frac{\partial T}{\partial t} \end{bmatrix} \quad [4\text{-}2]$$

where,

$$A^{11} = K_{hh} \quad [4\text{-}3a]$$

$$B^{12} = K_{hco} \quad [4\text{-}3b]$$

$$C^{13} = K_{he} \quad [4\text{-}3c]$$

$$D^{14} = K_{ht} \quad [4\text{-}3d]$$

$$A^{21} = D^{\bullet}_{cho} + C_j K_{hh} \quad [4\text{-}3e]$$

$$B^{22} = nD^{\bullet}_{j} + C_j K_{hco} \quad [4\text{-}3f]$$

$$C^{23} = nC_j u^{\bullet}_{j} + C_j K_{he} \quad [4\text{-}3g]$$

$$D^{24} = D^{\bullet}_{cto} + C_j K_{ht} \quad [4\text{-}3h]$$

$$A^{31} = \sigma_{cho} \quad [4\text{-}3i]$$

$$B^{32} = \sigma_{cco} \quad [4\text{-}3j]$$

$$C^{33} = \sigma_{ce} \quad [4\text{-}3k]$$

$$D^{34} = \sigma_{cto} \quad [4\text{-}3l]$$

$$A^{41} = \lambda_{th} + TK_{hh} \quad [4\text{-}3m]$$

$$B^{42} = \lambda_{tco} + TK_{hco} \quad [4\text{-}3n]$$

$$C^{43} = \lambda_{tco} + TK_{he} \quad [4\text{-}3o]$$

$$D^{44} = \lambda_{tt} + TK_{ht} \quad [4\text{-}3p]$$

$$V^{33} = \nabla\sigma_{ee} \quad [4\text{-}3q]$$

$$V^{44} = K_{hh}\nabla h + K_{hco}\nabla C + K_{he}\nabla E + K_{ht}\nabla T \qquad [4\text{-}3r]$$

4.1 SEMIDISCRETE FINITE ELEMENT MODEL

The semidiscrete formulation involves approximation of the spatial variation of the dependent variables, which construct the weak form of differential equation 4-2 over an element (Reddy, 1993). Integration by parts is used on the left hand side term once to distribute the spatial derivatives equally between the weight function M_i and the dependent variables h, C_j, E, and T. By substituting approximation functions of h, C_j, E, and T, we obtain the spatial approximation of the governing equation 4-2 as following equation 4-4:

$$\begin{bmatrix} [P^{11}] & [0] & [0] & [0] \\ [0] & [P^{22}] & [0] & [0] \\ [0] & [0] & [P^{33}] & [0] \\ [0] & [0] & [0] & [P^{44}] \end{bmatrix} \begin{Bmatrix} \{\dot{h}\} \\ \{\dot{C}_j\} \\ \{\dot{E}\} \\ \{\dot{T}\} \end{Bmatrix} + \begin{bmatrix} [K^{11}] & [K^{12}] & [K^{13}] & [K^{14}] \\ [K^{21}] & [K^{22}] & [K^{23}] & [K^{24}] \\ [K^{31}] & [K^{32}] & [K^{33}] & [K^{34}] \\ [K^{41}] & [K^{42}] & [K^{43}] & [K^{44}] \end{bmatrix} \begin{Bmatrix} \{h\} \\ \{C_j\} \\ \{E\} \\ \{T\} \end{Bmatrix}$$

$$= \begin{Bmatrix} \{F^1\} \\ \{F^2\} \\ \{F^3\} \\ \{F^4\} \end{Bmatrix} \qquad [4\text{-}4]$$

In short matrix form, we have

$$[P]\{\dot{\Delta}\} + [K]\{\Delta\} = \{F\} \qquad [4\text{-}5]$$

where an overdot indicates a time derivative, and

$$P_{ij}^{11} = \int_{\Omega^e} S_s(M_i M_j)dx \qquad [4\text{-}6a]$$

$$P_{ij}^{22} = \int_{\Omega^e} \left(nM_i M_j\right) dx \qquad [4\text{-}6b]$$

$$P_{ij}^{33} = \int_{\Omega^e} \frac{\partial T_e}{\partial E}\left(M_i M_j\right)dx = \int_{\Omega^e} \frac{1}{C_{TP}}\left(M_i M_j\right)dx \qquad [4\text{-}6c]$$

$$P_{ij}^{44} = \int_{\Omega^e} C_{TP}\left(M_i M_j\right)dx \qquad [4\text{-}6d]$$

$$K_{ij}^{11} = \int_{\Omega^e} \left(A^{11}\frac{\partial M_i}{\partial x}\frac{\partial M_j}{\partial x}\right)dx \qquad [4\text{-}7a]$$

$$K_{ij}^{12} = \int_{\Omega^e} \left(B^{12}\frac{\partial M_i}{\partial x}\frac{\partial M_j}{\partial x}\right)dx \qquad [4\text{-}7b]$$

$$K_{ij}^{13} = \int_{\Omega^e} \left(C^{13}\frac{\partial M_i}{\partial x}\frac{\partial M_j}{\partial x}\right)dx \qquad [4\text{-}7c]$$

$$K_{ij}^{14} = \int_{\Omega^e} \left(D^{14}\frac{\partial M_i}{\partial x}\frac{\partial M_j}{\partial x}\right)dx \qquad [4\text{-}7d]$$

$$K_{ij}^{21} = \int_{\Omega^e} \left(A^{21}\frac{\partial M_i}{\partial x}\frac{\partial M_j}{\partial x}\right)dx \qquad [4\text{-}7e]$$

$$K_{ij}^{22} = \int_{\Omega^e} \left(B^{22}\frac{\partial M_i}{\partial x}\frac{\partial M_j}{\partial x}\right)dx + \int_{\Omega^e} \left(V^{44}M_i\frac{\partial M_j}{\partial x}\right)dx \qquad [4\text{-}7f]$$

$$K_{ij}^{23} = \int_{\Omega^e} \left(C^{23} \frac{\partial M_i}{\partial x} \frac{\partial M_j}{\partial x} \right) dx \qquad [4\text{-}7g]$$

$$K_{ij}^{24} = \int_{\Omega^e} \left(D^{24} \frac{\partial M_i}{\partial x} \frac{\partial M_j}{\partial x} \right) dx \qquad [4\text{-}7h]$$

$$K_{ij}^{31} = \int_{\Omega^e} \left(A^{31} \frac{\partial M_i}{\partial x} \frac{\partial M_j}{\partial x} \right) dx \qquad [4\text{-}7i]$$

$$K_{ij}^{32} = \int_{\Omega^e} \left(B^{32} \frac{\partial M_i}{\partial x} \frac{\partial M_j}{\partial x} \right) dx \qquad [4\text{-}7j]$$

$$K_{ij}^{33} = \int_{\Omega^e} \left(C^{33} \frac{\partial M_i}{\partial x} \frac{\partial M_j}{\partial x} \right) dx + \int_{\Omega^e} \left(V^{33} M_i \frac{\partial M_j}{\partial x} \right) dx \qquad [4\text{-}7k]$$

$$K_{ij}^{34} = \int_{\Omega^e} \left(D^{34} \frac{\partial M_i}{\partial x} \frac{\partial M_j}{\partial x} \right) dx \qquad [4\text{-}7l]$$

$$K_{ij}^{41} = \int_{\Omega^e} \left(A^{41} \frac{\partial M_i}{\partial x} \frac{\partial M_j}{\partial x} \right) dx \qquad [4\text{-}7m]$$

$$K_{ij}^{42} = \int_{\Omega^e} \left(B^{42} \frac{\partial M_i}{\partial x} \frac{\partial M_j}{\partial x} \right) dx \qquad [4\text{-}7n]$$

$$K_{ij}^{43} = \int_{\Omega^e} \left(C^{43} \frac{\partial M_i}{\partial x} \frac{\partial M_j}{\partial x} \right) dx \qquad [4\text{-}7o]$$

$$K_{ij}^{44} = \int_{\Omega^e} \left(D^{44} \frac{\partial M_i}{\partial x} \frac{\partial M_j}{\partial x} \right) dx + \int_{\Omega^e} \left(V^{44} M_i \frac{\partial M_j}{\partial x} \right) dx \qquad [4\text{-}7p]$$

Note: $K_{ij} = K_{ji}$, but $K^{ij} \neq K^{ji}$.

$$F_i^1 = \int_{\Omega^e} M_i A^{11} h_j \frac{\partial M_j}{\partial x} dx + \int_{\Omega^e} M_i B^{12} C_{tj} \frac{\partial M_j}{\partial x} dx + \int_{\Omega^e} M_i C^{13} E_j \frac{\partial M_j}{\partial x} dx + + \int_{\Omega^e} M_i D^{14} T_j \frac{\partial M_j}{\partial x} dx = q_{hh} + q_{hco} + q_{he} + q_{ht} \quad [4\text{-}8a]$$

$$F_i^2 = \int_{\Omega^e} M_i A^{21} h_j \frac{\partial M_j}{\partial x} dx + \int_{\Omega^e} M_i B^{22} C_{tj} \frac{\partial M_j}{\partial x} dx + \int_{\Omega^e} M_i C^{23} E_j \frac{\partial M_j}{\partial x} dx + + \int_{\Omega^e} M_i D^{24} T_j \frac{\partial M_j}{\partial x} dx = q_{cho} + C_j q_{hh} + q_{cc}^{\bullet} + C_j q_{hco} + q_{ce}^{\bullet} + C_j q_{he} + q_{cto} + C_j q_{ht} \quad [4\text{-}8b]$$

$$F_i^3 = \int_{\Omega^e} M_i A^{31} h_j \frac{\partial M_j}{\partial x} dx + \int_{\Omega^e} M_i B^{32} C_{tj} \frac{\partial M_j}{\partial x} dx + \int_{\Omega^e} M_i C^{33} E_j \frac{\partial M_j}{\partial x} dx + + \int_{\Omega^e} M_i D^{34} T_j \frac{\partial M_j}{\partial x} dx = q_{eho} + q_{eco} + q_{ee} + q_{eto} \quad [4\text{-}8c]$$

$$F_i = \int_{\Omega^e} M_i A^{41} h_j \frac{\partial M_j}{\partial x} dx + \int_{\Omega^e} M_i B^{42} C_{tj} \frac{\partial M_j}{\partial x} dx + \int_{\Omega^e} M_i C^{43} E_j \frac{\partial M_j}{\partial x} dx + + \int_{\Omega^e} M_i D^{44} T_j \frac{\partial M_j}{\partial x} dx = q_{th} + Tq_{hh} + q_{tco} + Tq_{hco} + q_{teo} + Tq_{he} + q_{tt} + Tq_{ht} \quad [4\text{-}8d]$$

4.2 TIME APPROXIMATION

In solving partial differential equations 4-2, the time derivative is approximated by using a first order correct implicit, finite difference scheme (Reddy, 1993). The approximation is

$$\frac{dh}{dt} = \frac{h^{t+\Delta t} - h^t}{\Delta t} \quad [4\text{-}9a]$$

$$\frac{dC_j}{dt} = \frac{C_j^{t+\Delta t} - C_j^t}{\Delta t} \qquad [4\text{-}9b]$$

$$\frac{dE}{dt} = \frac{E^{t+\Delta t} - E^t}{\Delta t} \qquad [4\text{-}9c]$$

$$\frac{dT}{dt} = \frac{T^{t+\Delta t} - T^t}{\Delta t} \qquad [4\text{-}9d]$$

The vector [h], [C_j], [E], and [T] are known at the time t and are evaluated at time $t + \Delta t$. Substitution in equation 4-6 yields

$$\left[\begin{bmatrix} \left[\frac{P^{11}}{\Delta t}\right] & [0] & [0] & [0] \\ [0] & \left[\frac{P^{22}}{\Delta t}\right] & [0] & [0] \\ [0] & [0] & \left[\frac{P^{33}}{\Delta t}\right] & [0] \\ [0] & [0] & [0] & \left[\frac{P^{44}}{\Delta t}\right] \end{bmatrix} + \alpha \begin{bmatrix} [K^{11}] & [K^{12}] & [K^{13}] & [K^{14}] \\ [K^{21}] & [K^{22}] & [K^{23}] & [K^{24}] \\ [K^{31}] & [K^{32}] & [K^{33}] & [K^{34}] \\ [K^{41}] & [K^{42}] & [K^{43}] & [K^{44}] \end{bmatrix}\right] \begin{Bmatrix} h \\ C_j \\ E \\ T \end{Bmatrix}^{t+\Delta t} \qquad [4-10]$$

$$= \begin{Bmatrix} \{F^1\} \\ \{F^2\} \\ \{F^3\} \\ \{F^4\} \end{Bmatrix}^t + \begin{bmatrix} \left[\frac{P^{11}}{\Delta t}\right] & [0] & [0] & [0] \\ [0] & \left[\frac{P^{22}}{\Delta t}\right] & [0] & [0] \\ [0] & [0] & \left[\frac{P^{33}}{\Delta t}\right] & [0] \\ [0] & [0] & [0] & \left[\frac{P^{44}}{\Delta t}\right] \end{bmatrix} \begin{Bmatrix} h \\ C_j \\ E \\ T \end{Bmatrix}^t$$

$$-(1-\alpha) \begin{bmatrix} [K^{11}] & [K^{12}] & [K^{13}] & [K^{14}] \\ [K^{21}] & [K^{22}] & [K^{23}] & [K^{24}] \\ [K^{31}] & [K^{32}] & [K^{33}] & [K^{34}] \\ [K^{41}] & [K^{42}] & [K^{43}] & [K^{44}] \end{bmatrix} \begin{Bmatrix} h \\ C_j \\ E \\ T \end{Bmatrix}^t$$

4.3 INITIAL AND BOUNDARY CONDITIONS

Basically, there are three kinds of boundary conditions to deal with (Huyakorn and Pinder, 1983, Istok, 1989, Reddy 1993, and Thompson 1995; Entwistle, 1999):

(1) First type of boundary U (Dirichlet boundary condition) is a specified variable along a given boundary. The procedure for imposing first kind of boundary U involves resetting unknown variables at the left hand side of assembled governing equations with given values (i.g. U is equal to h, E, T, or C_j at any given boundary) and blasting both sides of equations to ensure that the specified constants are maintained along the boundary.

(2) Second type of boundary F_u^n (Neumann boundary condition) is a specified flux along a given boundary. The values of imposed second kind of boundary F_u^n at the right hand side of assembled governing equations are either zero's if no external point source is applied or is the given values if an external point source is applied.

(3) Third type of boundary (Cauchy boundary condition) is a mixed form of first kind and second kind along a given boundary. This third kind boundary is treated with two parts as first kind moves to the left hand side of assembled governing equations as well as second kind remains at the right hand side.

4.3.1 Initial and boundary conditions for hydraulic driving force

The solution of equation 3-7c requires knowledge of the initial distribution of the pressure head within the flow domain, Ω:

$$h(x, t) = h_O(x) \qquad \text{for} \qquad t = 0 \qquad [4\text{-}11]$$

where h_O is a prescribed function of spatial coordinate, x.

Three types of boundary conditions are considered in the water transport equation. The first kind of boundary condition is specified pressure head (Dirichlet type) of the form

$$h(x, t) = h_1(x, t) \qquad \text{on} \qquad \Gamma_D \qquad [4\text{-}12]$$

where h_1 is the known function of time and space at all points of the boundary. The second kind of boundary condition is specified pressure flux (Neumann type) of the form

$$-K_{hh}\frac{\partial h}{\partial x} = \begin{cases} q_{hh} \\ 0 \text{ for imperable boundary} \end{cases} \text{ on } \quad \Gamma_{\searrow} \qquad [4\text{-}13]$$

where q_{hh} is the known as the second boundary condition, also referred to as Neumann condition. The third kind of boundary condition is a mixed form of first and second kind along a given boundary.

$$-K_{hh}\frac{\partial h}{\partial x} + h' = h_3 \quad \text{on} \quad \Gamma_C \qquad [4\text{-}14]$$

where, h' is a leakage head loss, and h_3 (x, t) is the known as the third boundary condition, also referred to as Cauchy condition.

4.3.2 Initial and boundary conditions for chemical driving force

The solution of equation 4-2 requires knowledge of the initial distribution of the concentration within the flow domain, Ω, i.e.,

$$C_j(x, t) = C_o(x) \quad \text{for} \quad t = 0 \qquad [4\text{-}15]$$

where C_O is a prescribed function of x.

Chemical transport equation implements three types of boundary conditions. The first kind of boundary condition is specified concentration (Dirichlet type) of the form

$$C_j(x, t) = C_1(x, t) \quad \text{on} \quad \Gamma_D \qquad [4\text{-}16]$$

where $C_1(x, t)$ is the known at all points of the boundary. The second kind of boundary condition is specified concentration flux (Neumann type) of the form

$$-nD_j^* \frac{\partial C_j}{\partial x} = \begin{cases} q_{cc}^* \\ 0 \text{ for impermeable boundary} \end{cases} \quad \text{on} \quad \Gamma_N \qquad [4\text{-}17]$$

The third kind of boundary condition is a mixed form of first and second kind along a given boundary.

$$-nD_j^* \frac{\partial C_j}{\partial x} + q_{hh} C_j = q_{hh} C_3 \quad \text{on} \quad \Gamma_C \qquad [4\text{-}18]$$

where $q_{hh}C_3$ (x, t) is the known as the third boundary condition, also referred to as Cauchy type of condition.

4.3.3 Initial and boundary conditions for electrical driving force

The solution of equation 3-9c requires knowledge of the initial distribution of the current within the flow domain, Ω:

$$E(x, t) = E_0(x) \quad \text{for} \quad t = 0 \qquad [4\text{-}19]$$

where E_O is a prescribed function of spatial coordinate, x.

Current transport equation implements three types of boundary conditions. The first kind of boundary condition is specified current (Dirichlet type) of the form

$$E(x, t) = E_1(x, t) \quad \text{on} \quad \Gamma_D \qquad [4\text{-}20]$$

where $E_1(x, t)$ is the known function of time and space at all points of the boundary. The second kind of boundary condition is specified current flux (Neumann type) of the form

$$\text{ee}\frac{\partial E}{\partial x} = \begin{cases} q_{ee}(x,t) \\ 0 \text{ for impermeable boundary}_{\text{ary}} \end{cases} \quad \text{on} \quad \Gamma_N \qquad [4\text{-}21]$$

where q_{ee} (x, t) is the known as the second boundary condition, also referred to as Neumann condition. The third kind of boundary condition is a mixed form of first and second kind along a given boundary.

$$-\sigma_{ee}\frac{\partial E}{\partial x} + E^{'} = E_3 \quad \text{on} \quad \Gamma_C \qquad [4\text{-}22]$$

where $E^{'}$ is a barrier loss, and $E_3(x, t)$ is the known as the third boundary condition, also referred to as Cauchy condition.

4.3.4 Initial and boundary conditions for thermal driving force

The solution of equation 4-4 requires knowledge of the initial distribution of the temperature within the heat domain, Ω:

$$T(x, t) = T_o(x) \quad \text{for} \quad t = 0 \qquad [4\text{-}23]$$

where T_O is a prescribed function of spatial coordinate, x.

Heat transport equation implements three types of boundary conditions. The first kind of boundary condition is specified temperature (Dirichlet type) of the form

$$T(x, t) = T_1(x, t) \quad \text{on} \quad \Gamma_D \qquad [4\text{-}24]$$

where $T_1(x, t)$ is the known function of time and space at all points of the boundary. The second kind of boundary condition is specified heat flux (Neumann type) of the form

$$-\lambda_{tt}\frac{\partial T}{\partial x} = \begin{cases} q_{tt}(x,t) \\ 0 \text{ for impermeable boundary} \end{cases} \quad \text{on} \quad \Gamma_N \qquad [4\text{-}25]$$

where $q_{tt}(x, t)$ is the known as the second boundary condition, also referred to as Neumann condition. The third kind of boundary condition is a mixed form of first and second kind along a given boundary.

$$-\lambda_{tt}\frac{\partial T}{\partial x} + q_{hh}T = q_{hh}T_3 \quad \text{on} \quad \Gamma_C \qquad [4\text{-}26]$$

where $q_{hh}T_3(x, t)$ is the known as the third boundary condition, also referred to as Cauchy condition.

CHAPTER 5

EVALUATION OF THE HCET MODEL

5.1 INTRODUCTION

This chapter presents the validation, shows the flexibility, and demonstrates the sensitivity of the HCET model. The computer program structure, the FORTRAN source code, and a user's guide are provided in Appendices A through C.

Results of HCET model simulations are compared with results obtained from analytical/numerical simulations for flow and solute transport. Several cases are considered, ranging from a single variable water flow equation to multiple-variable coupled transport equations. These comparisons are performed to verify the FORTRAN code, to calibrate the parameters and boundary conditions for input data and output results, and to illustrate the capabilities for sensitivity analysis of the HCET model. When possible, the HCET model results are compared with experimental data.

To serve the purpose of evaluation of the HCET model, we use three major sub-sections: 1) comparison with analytical/numerical solutions for flow or solute transport, 2) extension of solute transport equation for coupling electric osmosis and thermal osmosis, and 3) sensitivity analysis as illustrated in Tables 5-1 and 5-2.

Table 5-1. Summarizing comparisons for the HCET model.

Class of simulation	Case number	Description of case	Basis for comparison	Reference
Comparison with analytical /numerical solutions for flow or solute transport	1.1	Flow equation (h as variable, where C_j, E, and T are constants) to verify HCET model	Analytical solution	Bird et al. (1960)
	1.2	Flow equation (h as variable, where C_j, E, and T are constants) to verify Hydrus model	Analytical solution	Bird et al. (1960)
	1.3	Flow equation to verify different boundary conditions.	Hydrus model	Vogel et al. (1996)
	1.4	Dimensionless relative resident concentrations as a function of dimensionless distance versus HCET model.	Analytical solutions	Van Genuchten and Parker (1984)
	1.5	Dimensionless relative resident concentrations as a function of dimensionless time versus HCET model.	Analytical solutions	Parker and Van Genuchten (1984)
	1.6	HCET model with dimensionless relative flux concentrations.	Analytical expressions	Van Genuchten (1981); Shackelford (1995)
Extension of solute transport equation for more variables	1.7	Current transport (h, C_t, E as variables, T constant) at fixed time.	Experimental data	Alshawabkeh and Acar (1996)
	1.8	Transient current transport (h, C_t, E as variables, T constant).	Experimental data	Alshawabkeh (1994)
	1.9	Heat transport (h, C_t, T as variables, E constant).	Hydrus model	Vogel et al. (1996)
	1.10	Heat effect on four-variable electrokinetics remediation (h, C_t, E, and T as variables).	Experimental data	Alshawabkeh (1994)

Table 5-2. Sensitivity analysis by HCET model.

Case number	Description of case	References
2.1	Chemical osmotic efficiency for different solute transport time at hydraulic conductivity of 1E-10 m/s (L=1m; C_0=100 mg/l).	Mitchell (1993)
2.2	Chemical osmotic efficiency for different hydraulic conductivities at fixed solute transport time 10,000 days (L=1m; C_0=100mg/l).	Mitchell (1993)
2.3	Coupled chemical osmotic efficiency for different solute transport time at hydraulic conductivity of 1E-10 m/s (L=1m; C_0=100 mg/l).	Mitchell (1993); Hsu (1997)
2.4	Coupled chemical osmotic efficiency for different hydraulic conductivities at fixed solute transport time 10,000 days (L=1m; C_0=100mg/l).	Mitchell (1993); Hsu (1997)
2.5	Coupled electric-osmotic conductivity for different solute remediation time at hydraulic conductivity of 1E-10 m/s (L=1m; C_0=100 mg/l).	Mitchell (1993); Hsu (1997)
2.6	Coupled electric-osmotic conductivity for different hydraulic conductivities at fixed solute remediation time 1000 days (L=1m; C_0=100 mg/l).	Mitchell (1993); Hsu (1997)
2.7	Coupled thermal osmosis coefficient for different solute transport time at hydraulic conductivity of 1E-11 m/s (L=1m; C0=1000 mg/l).	Dirksen (1969)
2.8	Coupled thermal osmosis coefficient for different hydraulic conductivities at fixed solute transport time 10,000 days (L=1m; C_0=1000 mg/l).	Dirksen (1969)
2.9	Contaminant transport from a nuclear waste repository.	See Table 5-10

5.2 COMPARISON OF HCET MODEL WITH FLOW OR SOLUTE TRANSPORT ANALYTICAL/NUMERICAL SOLUTIONS

Case 1.1: Flow equation (h as variable, where C_j, E, and T are constants) to verify HCET model

The governing equation 4-5 is repeated here:

$$\begin{bmatrix} K_{hh} & K_{hco} & K_{he} & K_{ht} \\ D^{*}_{cho} + C_j K_{hh} & nD^{*}_{j} + C_j K_{hco} & nC_j u^{*}_{j} + C_j K_{he} & D^{*}_{cto} + C_j K_{ht} \\ \sigma_{eho} & \sigma_{eco} & \sigma_{ee} & \sigma_{eto} \\ \lambda_{th} + TK_{hh} & \lambda_{tco} + TK_{hco} & \lambda_{te} + TK_{he} & \lambda_{tt} + TK_{ht} \end{bmatrix} \begin{bmatrix} h^{*} \\ C^{*}_{j} \\ E^{*} \\ T^{*} \end{bmatrix}$$

$$+ \begin{bmatrix} 0 & 0 & 0 & 0 \\ 0 & +K_{hh}\nabla h + K_{hco}\nabla C_j + K_{he}\nabla E + K_{ht}\nabla T & 0 & 0 \\ 0 & 0 & \nabla\sigma & 0 \\ 0 & 0 & 0 & +K_{hh}\nabla h + K_{hco}\nabla C_j + K_{he}\nabla E + K_{ht}\nabla T \end{bmatrix} \begin{bmatrix} h \\ C_j \\ E \\ T \end{bmatrix} = \frac{\partial}{\partial t} \begin{bmatrix} S_s h \\ nC_j \\ \frac{1}{C_{ii}} E \\ C_{TP} T \end{bmatrix} \qquad [4\text{-}5]$$

For one-dimensional flow, the governing equation 4-5, with C_j, E, and T as constants, reduces to equation 5-1

$$[K_{hh}]\frac{\partial^2 h}{\partial x^2} = \frac{\partial}{\partial t}[S_s h] \qquad [5\text{-}1]$$

We compare analytical and HCET model solutions of the flow equation for a homogenous hydraulic conductivity

For equation 5-1, appropriate initial and boundary conditions are,

$$h(0,t) = h_0 \qquad \text{at } t \geq 0; \tag{5-2a}$$

$$\frac{\partial h(L,t)}{\partial x} = 0 \qquad \text{at } t \geq 0; \tag{5-2b}$$

$$h(x,0) = 0 \qquad \text{at } x \geq 0; \tag{5-2c}$$

The analytical solution under the above boundary conditions and initial condition is (Bird et. al., 1960):

$$\frac{h(x,t)}{h_0} = 1 - \sum_{m=1}^{\infty} \frac{2\alpha_m \sin\left(\frac{\alpha_m x}{L}\right) \exp\left[-\frac{\alpha_m^2 K_{hh} t}{S_s L^2}\right]}{\left[\alpha_m^2\right]} \tag{5-3}$$

where the eigenvalues α_m are the positive roots of $\alpha_m \cot(\alpha_m) = 0$

The numerical formulation for equation 5-1 (Istok, 1989) is:

$$[K]\{h\} - \{F\} = 0 \tag{5-4}$$

where $[K]$ is the global hydraulic conductance matrix, $\{h\}$ is the vector of unknown hydraulic heads, and $\{F\}$ is a vector containing the specified fluxes at Neumann nodes. In the HCET model, we set the following parameters: NEM=20, NNM=21, NEQ=21, NSIZE=2, NDF=1, MXEBC=8, MXNBC=8, and MNDT=200

where, NEM=number of element, NNM=node number maximum, NEQ=number of equation, NSIZE=number size per element, NDF= number degree of freedom, MXEBC=maximum essential boundary condition, MXNBC= maximum natural boundary condition, and MNDT=maximum number of delta time.

To fit the HCET model solution with the analytical solution, the time steps and delta times selected are:

- for 1 day (50 steps, 0.02 day each delta time),
- for 10 days (10 steps, 1 day each delta time),
- for 100 days (100 steps, 1day each delta time), and
- for 1000 days (1000 steps, 1 day each delta time).

Figure 5-1 represents the plots for one-dimensional homogeneous transient flow with four time periods of 1 day, 10 days, 100 days, and 1000 days, respectively. They illustrate the evolution of the water head profile. The plot for the time period of 1000 days is a straight line, which indicates that the hydraulic head does not change after that time. For the HCET model, we set L=100 m for study domain, h_o = 100 m for the left hand side boundary condition, zero hydraulic head gradient for the right hand side boundary, and zero hydraulic head for the initial condition. Hydraulic conductivity is 6 meters per day. The symbol dots represent the HCET model solution in Figure 5-1. The HCET model solution is in good agreement with the analytical solution.

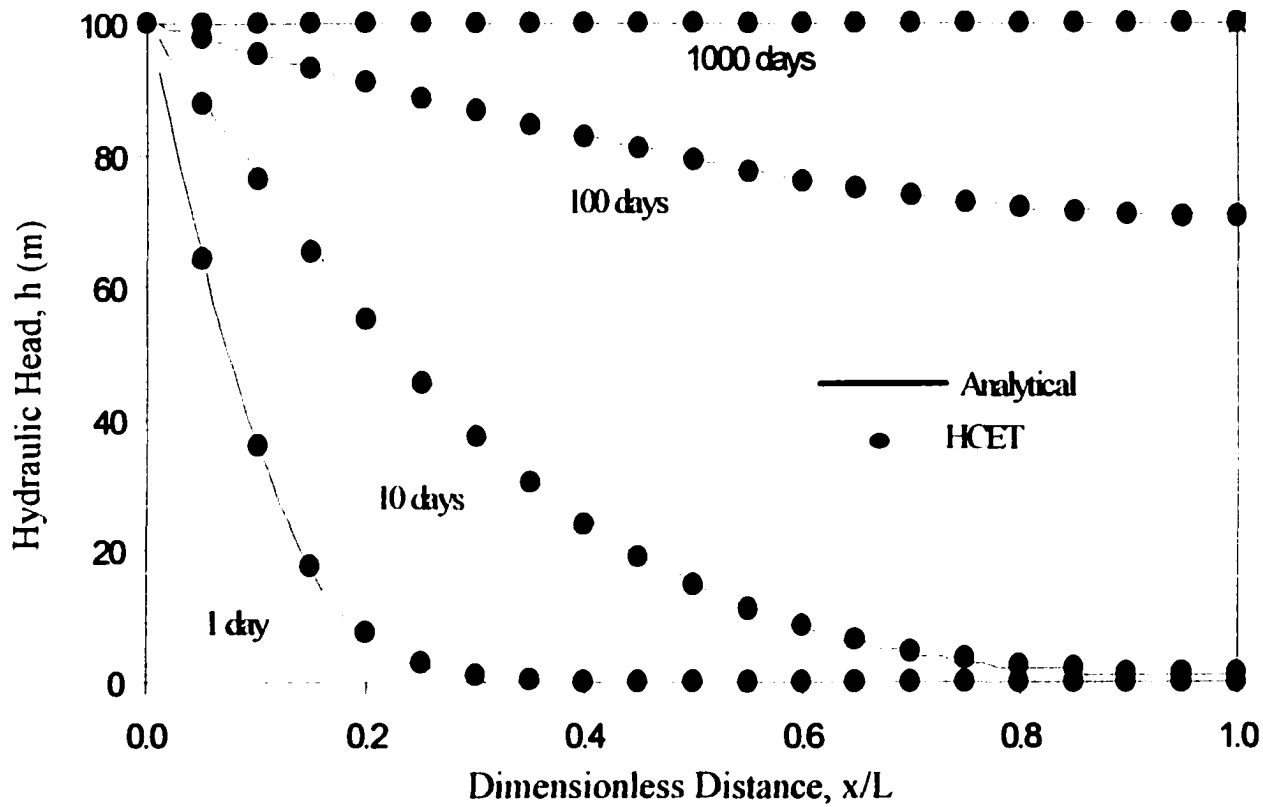

Figure 5-1: Plot of hydraulic head versus dimensionless distance for a comparison of analytical solutions with HCET model simulations of homogeneous transient flow equation for different time periods (L=100 m).

Case 1.2: Flow equation (h as variable, where C_j, E, and T are constants) to verify Hydrus model.

Equation 5-1 may be dimensionless as:

$$\frac{\partial^2 H}{\partial X^2} = S_q \frac{\partial H}{\partial T_q} \qquad [5\text{-}5a]$$

or

$$\frac{\partial^2 H}{\partial X^2} = S_d \frac{\partial H}{\partial T_d} \qquad [5\text{-}5b]$$

where,

$$T_q \left(= \frac{q_o t}{L} \right) = \text{dimensionless time based on bulk velocity,} \qquad [5\text{-}6a]$$

$$T_d \left(= \frac{t}{t_o} \right) = \text{dimensionless time,} \qquad [5\text{-}6b]$$

$$X \left(= \frac{x}{L} \right) = \text{dimensionless distance,} \qquad [5\text{-}7]$$

$$H \left(= \frac{h}{h_o} \right) = \text{dimensionless hydraulic head,} \qquad [5\text{-}8]$$

$$S_q \left(= \frac{S_s q_o L}{K_{hh}} \right) = \text{dimensionless number based on bulk velocity, and} \qquad [5\text{-}9]$$

$$S_d \left(= \frac{S_s L^2}{K_{hh} t_o} \right) = \text{dimensionless number.} \qquad [5\text{-}10]$$

We evaluate the accuracy of Hydrus model by calculating the hydraulic head at ratios x/L and different time at three S_d values. Tables 5-3.1 to 5-3.3 show the

comparison of analytical solutions versus Hydrus model simulations for different ratios x/L and different time at fixed S_d=2,10, 40 respectively. Figure 5-2 illustrates the plot for a comparison of analytical solutions with Hydrus model simulations at three dimensionless numbers, S_d = 2, 10, and 40. These calculations in Tables 5-3.1 to 5-3.3 and the plot in Figure 5-2 show Hydrus model is accuracy comparing with analytical solutions.

Table 5-3.1. Comparison of analytical solutions versus Hydrus model simulations for flow equation for different distance and domain length ratios at S_d=2.

S_d	t_0 (yr)	x (m)	L (m)	X (=x/L)	Analytical, h/h_0	Hydrus, h/h_0	Error
2	1	2	10	0.2	0.88542	0.88900	0.00358
2	4	4	20	0.2	0.88542	0.88453	0.00089
2	16	8	40	0.2	0.88542	0.88532	0.00010
2	1	4	10	0.4	0.78205	0.78900	0.00695
2	4	8	20	0.4	0.78205	0.78036	0.00169
2	16	16	40	0.4	0.78205	0.78187	0.00018
2	1	6	10	0.6	0.70003	0.71100	0.01097
2	4	12	20	0.6	0.70003	0.69771	0.00232
2	16	24	40	0.6	0.70003	0.69977	0.00026
2	1	8	10	0.8	0.64737	0.66300	0.01563
2	4	16	20	0.8	0.64737	0.64465	0.00272
2	16	32	40	0.8	0.64737	0.64707	0.00030
2	1	10	10	1.0	0.62922	0.65000	0.02078
2	4	20	20	1.0	0.62922	0.62637	0.00285
2	16	40	40	1.0	0.62922	0.62891	0.00031

Error = abs (Analytical - Hydrus).

Table 5-3.2. Comparison of analytical solutions versus Hydrus model simulations for flow equation for different distance and domain length ratios at S_d=10.

S_d	t_0 (yr)	x (m)	L (m)	X (=x/L)	Analytical, h/h_0	Hydrus, h/h_0	Error
10	1	2	10	0.2	0.65478	0.65400	0.00078
10	4	4	20	0.2	0.65478	0.65353	0.00125
10	16	8	40	0.2	0.65478	0.65454	0.00024
10	1	4	10	0.4	0.37144	0.37000	0.00144
10	4	8	20	0.4	0.37144	0.37017	0.00127
10	16	16	40	0.4	0.37144	0.37130	0.00014
10	1	6	10	0.6	0.18146	0.18200	0.00054
10	4	12	20	0.6	0.18146	0.18124	0.00022
10	16	24	40	0.6	0.18146	0.18168	0.00022
10	1	8	10	0.8	0.08093	0.08500	0.00407
10	4	16	20	0.8	0.08093	0.08182	0.00089
10	16	32	40	0.8	0.08093	0.08149	0.00056
10	1	10	10	1.0	0.05069	0.06000	0.00931
10	4	20	20	1.0	0.05069	0.05202	0.00133
10	16	40	40	1.0	0.05069	0.05138	0.00069

Error = abs (Analytical - Hydrus).

Table 5-3.3. Comparison of analytical solutions versus Hydrus model simulations for flow equation for different distance and domain length ratios at S_d=40.

	t_0 (yr)	x (m)	L (m)	X (=x/L)	Analytical, h/h_0	Hydrus, h/h_0	Error
40	1	2	10	0.2	0.37109	0.37000	0.00109
40	4	4	20	0.2	0.37109	0.36961	0.00148
40	16	8	40	0.2	0.37109	0.37077	0.00032
40	1	4	10	0.4	0.07364	0.07500	0.00136
40	4	8	20	0.4	0.07364	0.07504	0.00141
40	16	16	40	0.4	0.07364	0.07497	0.00133
40	1	6	10	0.6	0.00729	0.00800	0.00071
40	4	12	20	0.6	0.00729	0.00832	0.00103
40	16	24	40	0.6	0.00729	0.00806	0.00077
40	1	8	10	0.8	0.00035	0.00100	0.00065
40	4	16	20	0.8	0.00035	0.00053	0.00018
40	16	32	40	0.8	0.00035	0.00047	0.00012
40	1	10	10	1.0	0.00002	0.00000	0.00002
40	4	20	20	1.0	0.00002	0.00004	0.00002
40	16	40	40	1.0	0.00002	0.00003	0.00002

Error = abs (Analytical - Hydrus).

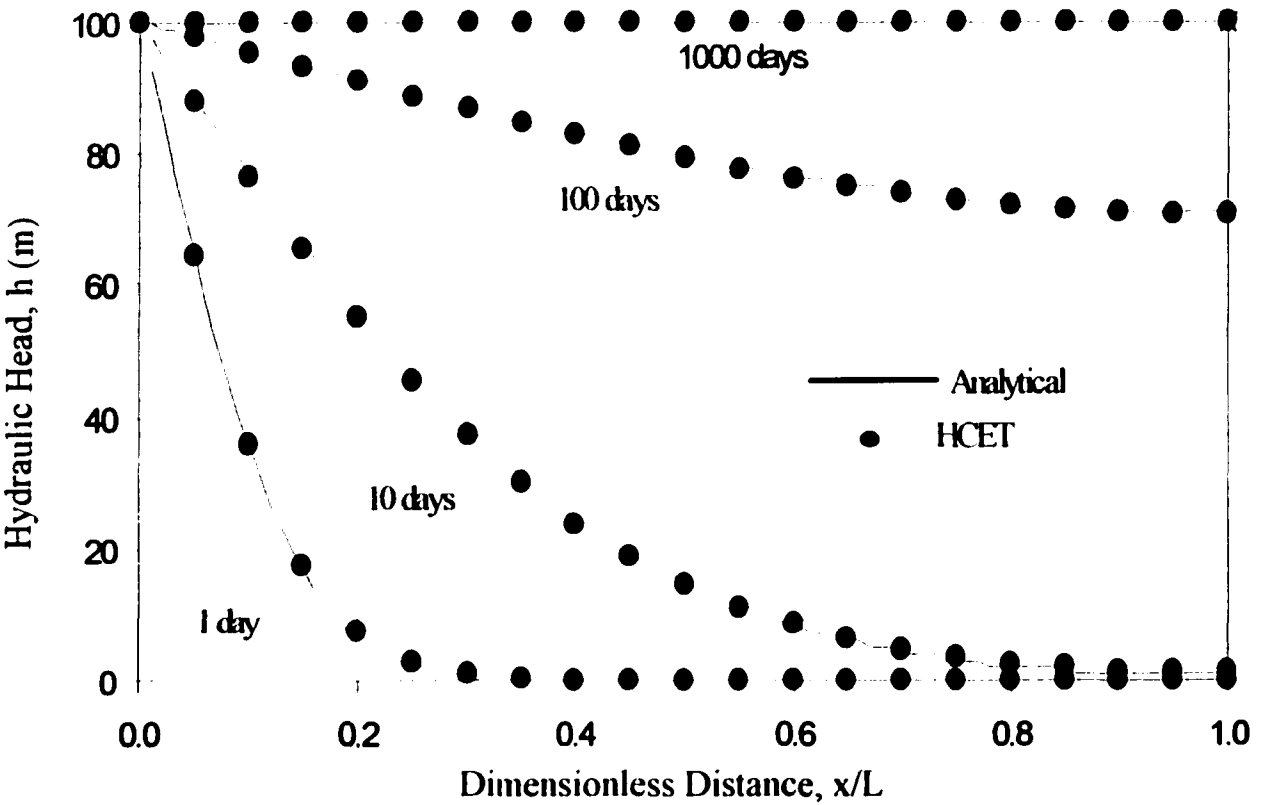

Figure 5-1: Plot of hydraulic head versus dimensionless distance for a comparison of analytical solutions with HCET model simulations of homogeneous transient flow equation for different time periods (L=100 m).

Case 1.3: Flow equation to verify different boundary conditions.

Table 5-4 shows the commonly used boundary conditions for flow equation (Anderson and Woessner 1992; Liu et. al, 2000).

Table 5-4. Boundary conditions for flow equation.

Case	Boundary conditions	
	upper	lower
S1	$h(0, t)=h_0$	$\frac{\partial h}{\partial x}(\infty, t) = 0$
S2	$-K_{hh}\frac{\partial h}{\partial x} = q_0$	$\frac{\partial h}{\partial x}(\infty, t) = 0$
S3	$h(0, t)=h_0$	$\frac{\partial h}{\partial x}(L, t) = 0$
S4	$-K_{hh}\frac{\partial h}{\partial x} = q_0$	$\frac{\partial h}{\partial x}(L, t) = 0$

The upper boundary represents either a specific value (S1 or S3) or a flux-type (S2 or S4) condition. The lower boundary is a zero-gradient boundary condition at a fixed length (e.g. column test) or at an infinite length (e.g. field-scale transport). Figures 5-3, 5-4, and 5-5 illustrate the comparisons of Hydrus model with HCET model for different boundary conditions at given S_d values of 2, 10, and 40, respectively. When we impose zero-gradient at the lower boundary conditions for S1 and S2, a ten times length of finite distance is calculated instead of semi-infinite length. The results in these Figures show excellent agreement between Hydrus model and HCET model. They also indicate S3 is always equal or great than S1, and S4 is always equal or great than S2. In other words, a column test is always more conservative than field evaluation.

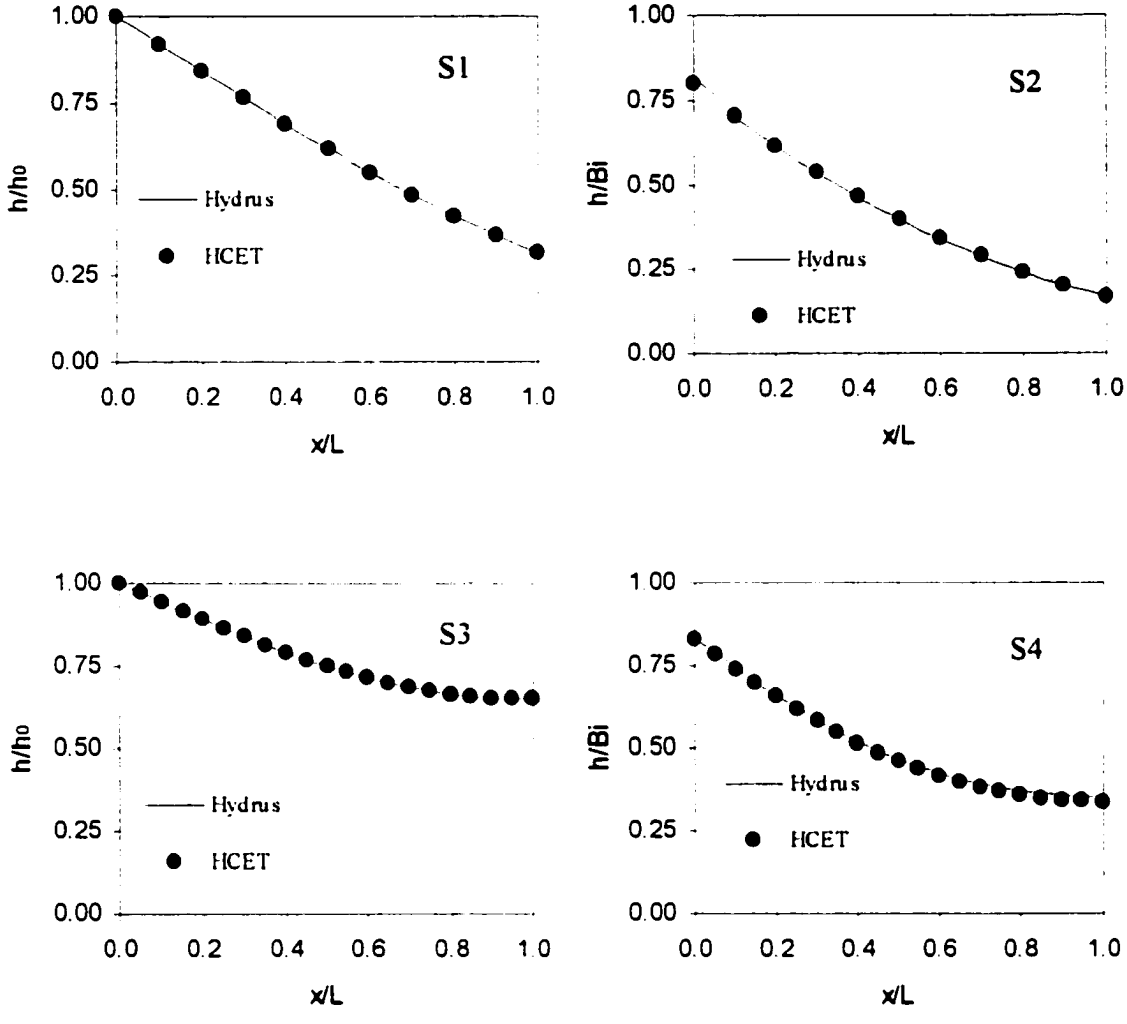

Figure 5-3: Plot for dimensionless hydraulic head versus dimensionlessdistance for a comparison of Hydrus model versus HCET model for different boundary conditions at dimensionless number S_d=2. Bi is a Biot number = $q_0 L/K_{hh}$.

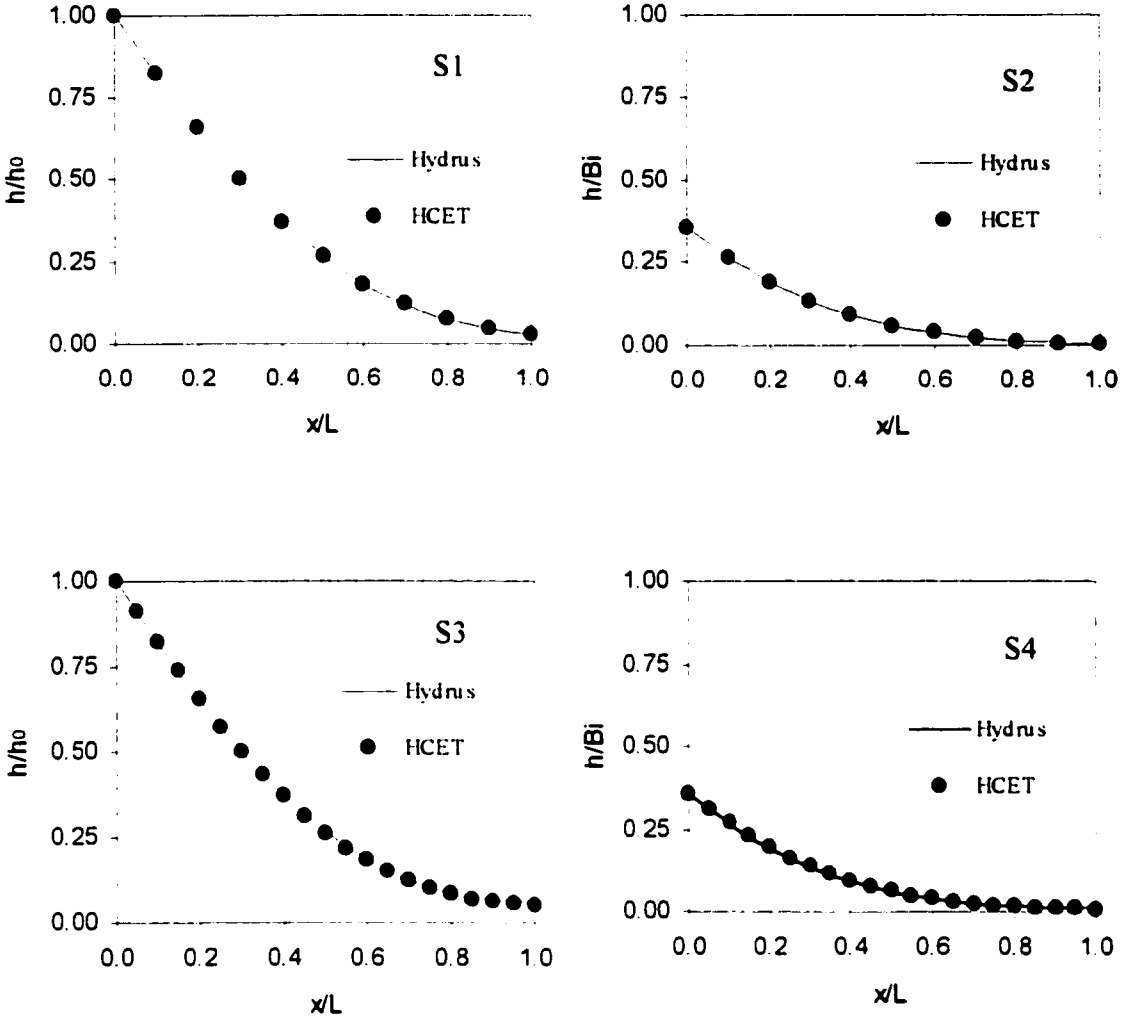

Figure 5-4: Plot for dimensionless hydraulic head versus Dimensionless distance for a comparison of Hydrus model versus HCET model for different boundary conditions at dimensionless number S_d=10. Bi is a Biot number = $q_0 L/K_{hh}$.

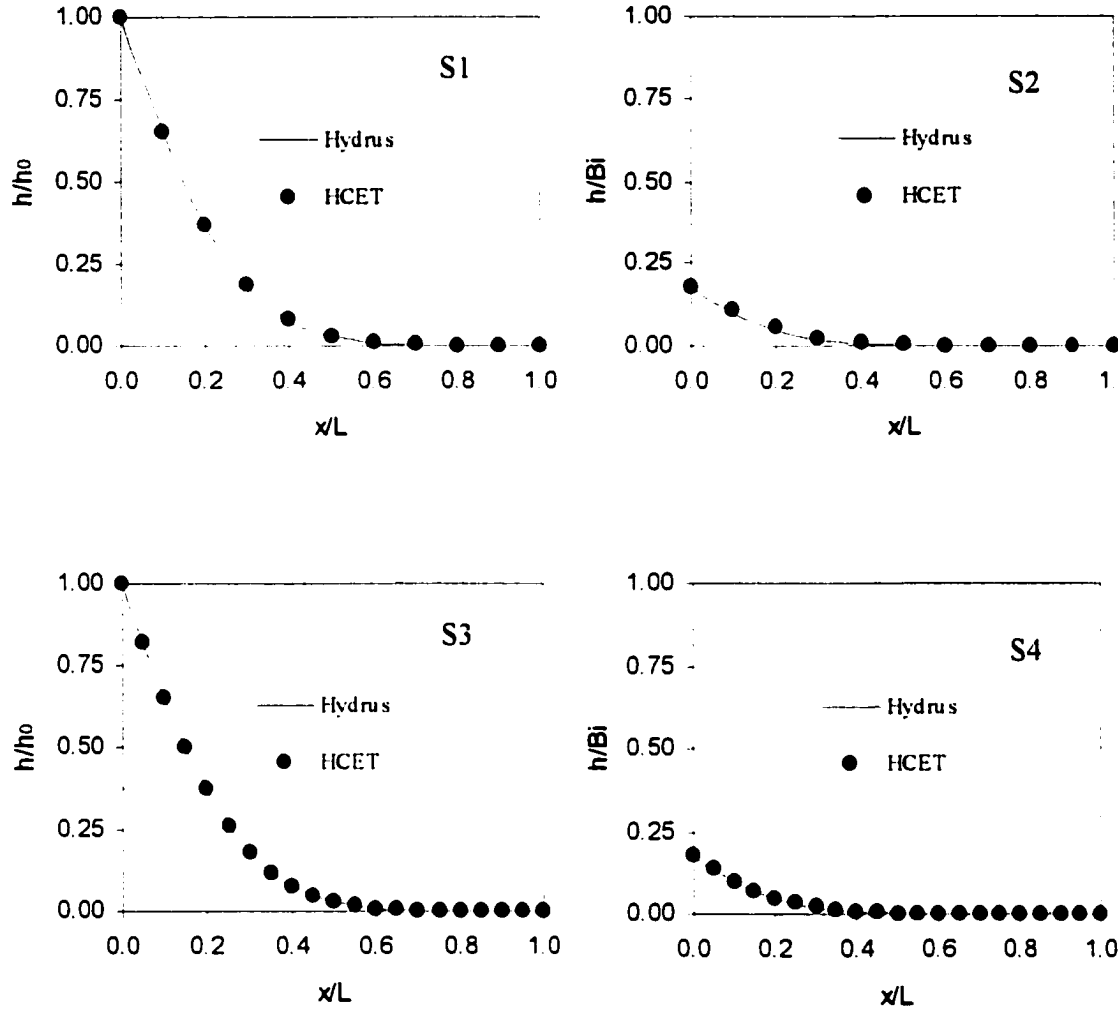

Figure 5-5: Plot for dimensionless hydraulic head versus Dimensionless distance for a comparison of Hydrus model versus HCET model for different boundary conditions at dimensionless number S_d=40. Bi is a Biot number = q_0L/K_{hh}.

Case 1.4: Dimensionless relative resident concentration models versus HCET model

We will discuss the dimensionless relative resident concentrations as a function of dimensionless distance. To validate the HCET model for relative resident concentration models for solute transport, when E, T are set at constants, governing equation 4-5 reduces to equation 5-11

$$R_d \frac{\partial C_r}{\partial t} = D \frac{\partial^2 C_r}{\partial x^2} - v \frac{\partial C_r}{\partial x} \qquad [5-11]$$

The equation 5-11 is the usually discussed advection-dispersion transport equation with water velocity, v, constant. For a one-dimensional system at saturated soil and steady-state uniform flow, the appropriate parameters for advection-dispersion transport equations are: C_r is the solute concentration in the pore water of the soil, also known as the "resident concentration" (van Genuchten and Paker 1984, Shackelford, 1995), t is the time, x is the macroscopic distance in the direction of transport, v is the average linear or seepage velocity, $D\left(= D^* = D_l^*\right)$ is the dispersion/diffusion coefficient, and R_d is the retardation factor.

Four analytical solutions to equation 5-11, as summarized in Table 5-5, are extensively cited by researchers (van Genuchten 1981; van Genuchten and Paker 1984; Shackelford, 1995). Each solution is based upon a different set of initial and boundary conditions. Models A.1 and A.3 are based on a first-kind or concentration-type inlet boundary conditions whereas models A.2 and A.4 are based on third-kind or flux-type inlet boundary condition. In addition, models A.1 and A.2 impose a semi-infinite kind of lower boundary and models A.3 and A.4 impose a finite kind of boundary.

Table 5-5. Resident concentration models for one-dimensional advection-dispersion equation (van Genutchten 1981; van Genuchten and Paker 1984; Shackelford 1995).

Upper Boundary	Lower Boundary	Concentration Models [for c(x,0)=0]	Model Designation
$C_r(0,t) = C_0$	$\frac{\partial C_r}{\partial x}(\infty, t) = 0$	$\frac{C_r(x,t)}{C_0} = 0.5\left\{\operatorname{erfc}\left[\frac{R_d x - vt}{2\sqrt{DR_d t}}\right] + \exp\left(\frac{vx}{D}\right)\operatorname{erfc}\left[\frac{R_d x + vt}{2\sqrt{DR_d t}}\right]\right\}$	A.1
$\left(vC_r - D\frac{\partial C_r}{\partial x}\right)\Big\|_{x=0} = vC_0$	$\frac{\partial C_r}{\partial x}(\infty, t) = 0$	$\frac{C_r(x,t)}{C_0} = 0.5\left\{\operatorname{erfc}\left[\frac{R_d x - vt}{2\sqrt{DR_d t}}\right] + 2\sqrt{\frac{v^2 t}{\pi DR_d}}\exp\left[-\frac{(R_d - vt)^2}{4DR_d t}\right] - \left(1 + \frac{vx}{D} + \frac{v^2 t}{DR_d}\right)\exp\left(\frac{vx}{D}\right)\operatorname{erfc}\left[\frac{R_d x + vt}{2\sqrt{DR_d t}}\right]\right\}$	A.2
$C_r(0,t) = C_0$	$\frac{\partial C_r}{\partial x}(L, t) = 0$	$\frac{C_r(x,t)}{C_0} = 1 - \sum_{m=1}^{\infty}\frac{2\alpha_m \sin\left(\frac{\alpha_m x}{L}\right)\exp\left[\frac{vx}{2D} - \frac{v^2 t}{4DR_d} - \frac{\alpha_m^2 Dt}{L^2 R_d}\right]}{\left[\alpha_m^2 + \left(\frac{vL}{2D}\right)^2 + \frac{vL}{2D}\right]}$ where the eigenvalues α_m are the positive roots of $\alpha_m \cot(\alpha_m) + \frac{vL}{2D} = 0$	A.3
$\left(vC_r - D\frac{\partial C_r}{\partial x}\right)\Big\|_{x=0} = vC_0$	$\frac{\partial C_r}{\partial x}(L, t) = 0$	$\frac{C_r(x,t)}{C_0} = 1 - \sum_{m=1}^{\infty}\frac{\frac{2vL}{D}\beta_m\left[\beta_m \cos\left(\frac{\beta_m x}{L}\right) + \frac{vL}{2D}\sin\left(\frac{\beta_m x}{L}\right)\right]\exp\left[\frac{vx}{2D} - \frac{v^2 t}{4DR_d} - \frac{\beta_m^2 Dt}{L^2 R_d}\right]}{\left[\beta_m^2 + \left(\frac{vL}{2D}\right)^2 + \frac{vL}{2D}\right]\left[\beta_m^2 + \left(\frac{vL}{2D}\right)^2\right]}$ where the eigenvalues β_m are the positive roots of $\beta_m \cot(\beta_m) - \frac{\beta_m^2 D}{vL} + \frac{vL}{4D} = 0$	A.4

The different analytical solutions in Table 5-5 are expressed in terms of the original variables (x, t, R_d, v, D). Prediction of solute transport in groundwater engineering is often obtained in dimensionless form by solving the advection-dispersion transport equations 5-11. It would be more convenient to introduce the dimensionless parameters T_r and P_L, where T_r is the pore volume of flow,

$$T_r = \frac{vt}{L} \qquad [5-12]$$

and the dimensionless group P_L is referred to as the column Peclet number defined as

$$P_L = \frac{vL}{D}, \qquad [5-13]$$

where v is the seepage velocity, L is the column length, and D is the dispersion/diffusion coefficient. Making these substitutions results in dimensionless expressions of the analytical solutions in Table 5-5 as presented in Table 5-6. These analytical solutions can be used to validate numerical models in field studies. Figures 5-6, 5-7, and 5-8 illustrate plots of relative resident concentration versus dimensionless distance for the comparisons of analytical solutions with HCET model simulations at Peclet number vary from 1, 5, and 20, respectively. These Figures indicate good agreement between analytical solutions and HCET model simulations. For the large Peclet numbers, the solution A1 is close to solution A3. Similarly, for the large Peclet numbers, the solution A2 is close to solution A4.

Table 5-6. Dimensionless form of resident concentrations based on models in Table 5-5.

Concentration Model (1)	Dimensionless form for Concentration Models (2) [for c(X,0)=0]
A.1	$$\frac{C_r(X,T_r)}{C_0} = 0.5\left\{\operatorname{erfc}\left[\frac{X-T_r}{2\sqrt{T_r/P_L}}\right] + \exp(P_L X)\operatorname{erfc}\left[\frac{X+T_r}{2\sqrt{T_r/P_L}}\right]\right\}$$
A.2	$$\frac{C_r(X,T_r)}{C_0} = 0.5\left\{\operatorname{erfc}\left[\frac{X-T_r}{2\sqrt{T_r/P_L}}\right] + 2\sqrt{\frac{P_L T_r}{\pi}}\exp\left[-\left(\frac{X-T_r}{2\sqrt{T_r/P_L}}\right)^2\right] - (1+P_L X+P_L T_r)\exp(P_L X)\operatorname{erfc}\left[\frac{X+T_r}{2\sqrt{T_r/P_L}}\right]\right\}$$
A.3	$$\frac{C_r(X,T_r)}{C_0} = 1-\sum_{m=1}^{\infty}\frac{2\alpha_m \sin(\alpha_m X)\exp\left[\frac{P_L X}{2} - \frac{P_L T_r}{4} - \frac{\alpha_m^2 T_r}{P_L}\right]}{\left[\alpha_m^2 + \left(\frac{P_L}{2}\right)^2 + \frac{P_L}{2}\right]}$$ where the eigenvalues α_m are the positive roots of $\alpha_m \cot(\alpha_m) + \frac{P_L}{2} = 0$
A.4	$$\frac{C_r(X,T_r)}{C_0} = 1-\sum_{m=1}^{\infty}\frac{2P_L\beta_m\left[\beta_m\cos(\beta_m X)+\frac{P_L}{2}\sin(\beta_m X)\right]\exp\left[\frac{P_L X}{2} - \frac{P_L T_r}{4} - \frac{\beta_m^2 T_r}{P_L}\right]}{\left[\beta_m^2 + \left(\frac{P_L}{2}\right)^2 + \frac{P_L}{2}\right]\left[\beta_m^2 + \left(\frac{P_L}{2}\right)^2\right]}$$ where the eigenvalues β_m are the positive roots of $\beta_m \cot(\beta_m) - \frac{\beta_m^2}{P_L} + \frac{P_L}{4} = 0$

(1) Models given in Table 5-5. (2) $X = \frac{x}{L}$; $T_r = \frac{vt}{L}$; $P_L = \frac{vL}{D}$.

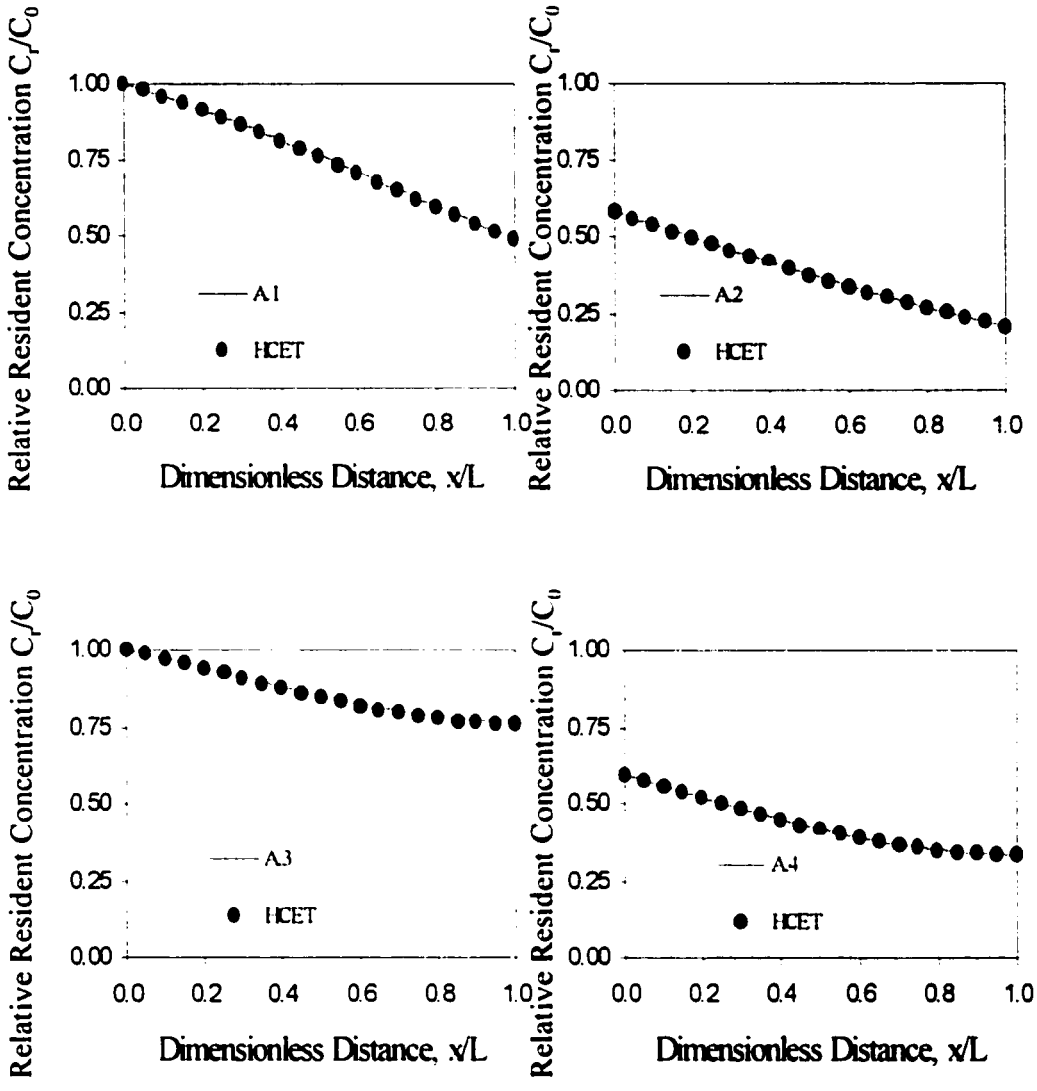

Figure 5-6: Plot for relative resident concentration, C_r/C_0, versus dimensionless distance, X=x/L, for a comparison of analytical solutions with HCET model simulations for a dimensionless Peclet number, P_L=1, and dimensionless time, T_r = 0.5.

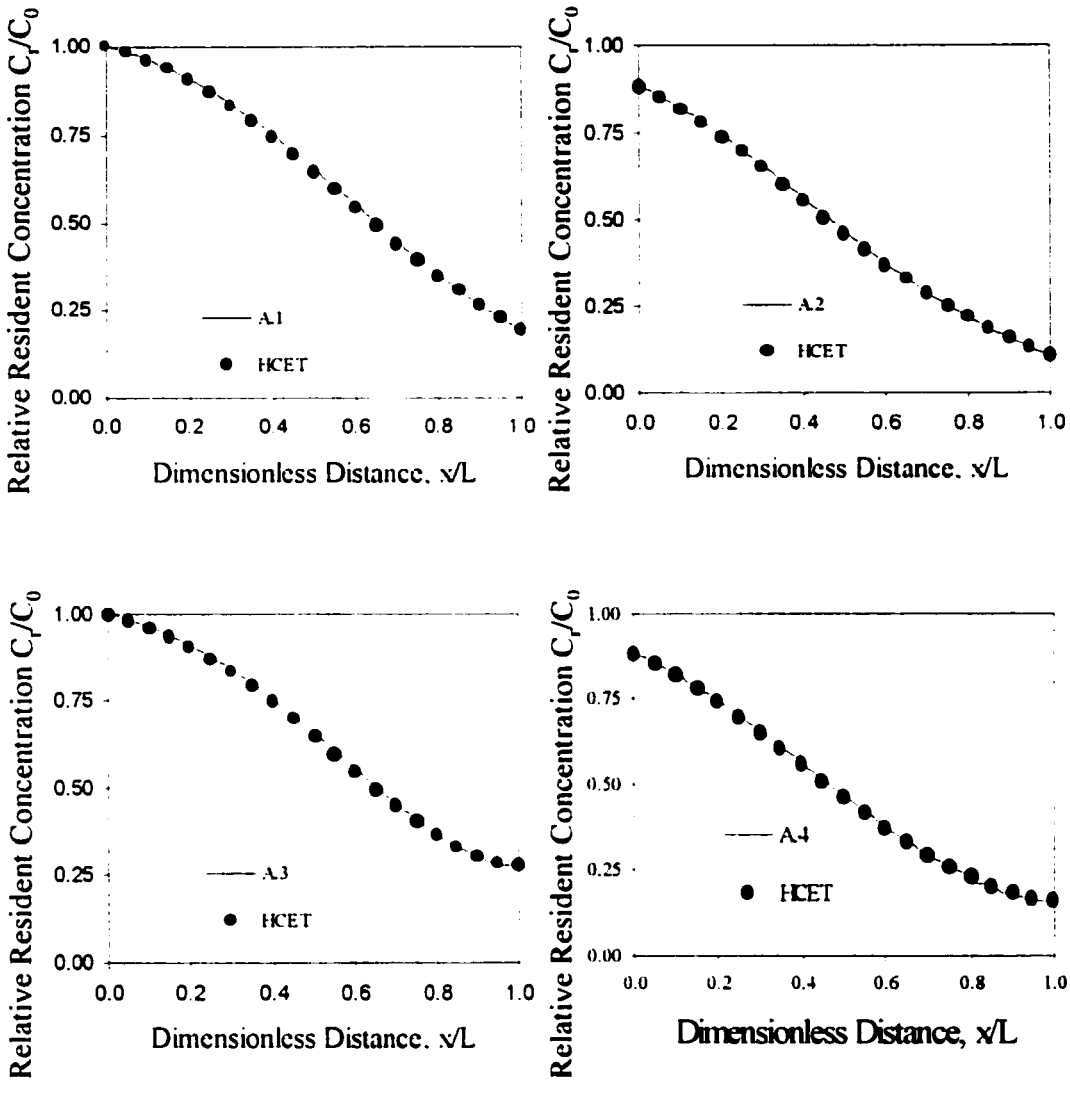

Figure 5-7: Plot for relative resident concentration, C_r/C_0, versus dimensionless distance, X=x/L, for a comparison of analytical solutions with HCET model simulations for a dimensionless Peclet number, P_L=5, and dimensionless pore volume of flow, T_r = 0.5.

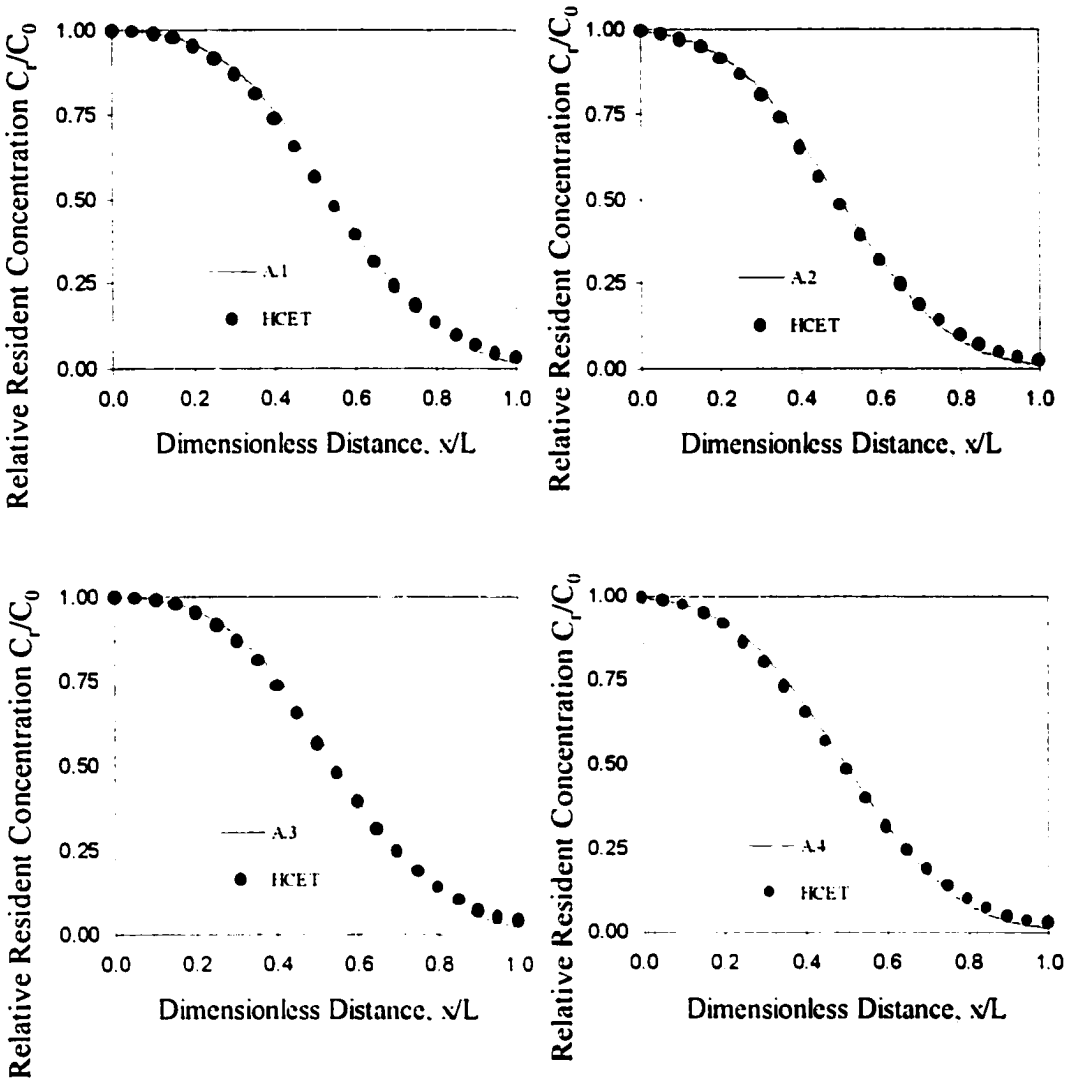

Figure 5-8: Plot for relative resident concentration, C_r/C_0, versus dimensionless distance, X=x/L, for a comparison of analytical solutions with HCET model simulations for a dimensionless Peclet number, P_L=20, and dimensionless pore volume of flow, T_r = 0.5.

Case 1.5: Dimensionless relative resident concentrations as a function of dimensionless time versus HCET model

The resident concentration models listed in Table 5-5 are evaluated by van Genuchten and Parker (1984) with respect to Peclet numbers, P_L, varying as 1, 5, and 20. These Peclet numbers are valid within the range of practical applications involving low permeability soil barriers for waste containment and remediation (van Genuchten and Parker 1984, and Shackelford, 1995). By assuming the resident concentration equal to effluent concentration at the lower boundary ($C_r/C_0 = C_e/C_0$ at $x = L$), van Genuchten and Parker 1984, and Shackelford, 1995, show the dimensionless relative concentration curves at the lower boundary as a function of pore volume of flow, T_r (or dimensionless time). The analytical solutions as lines are plotted in Figures 5-9 through 5-11. The HCET model solutions as symbols are plotted in Figures 5-9 through 5-11, too. These Figures indicate the analytical model solutions are in good agreement with the HCET model solutions.

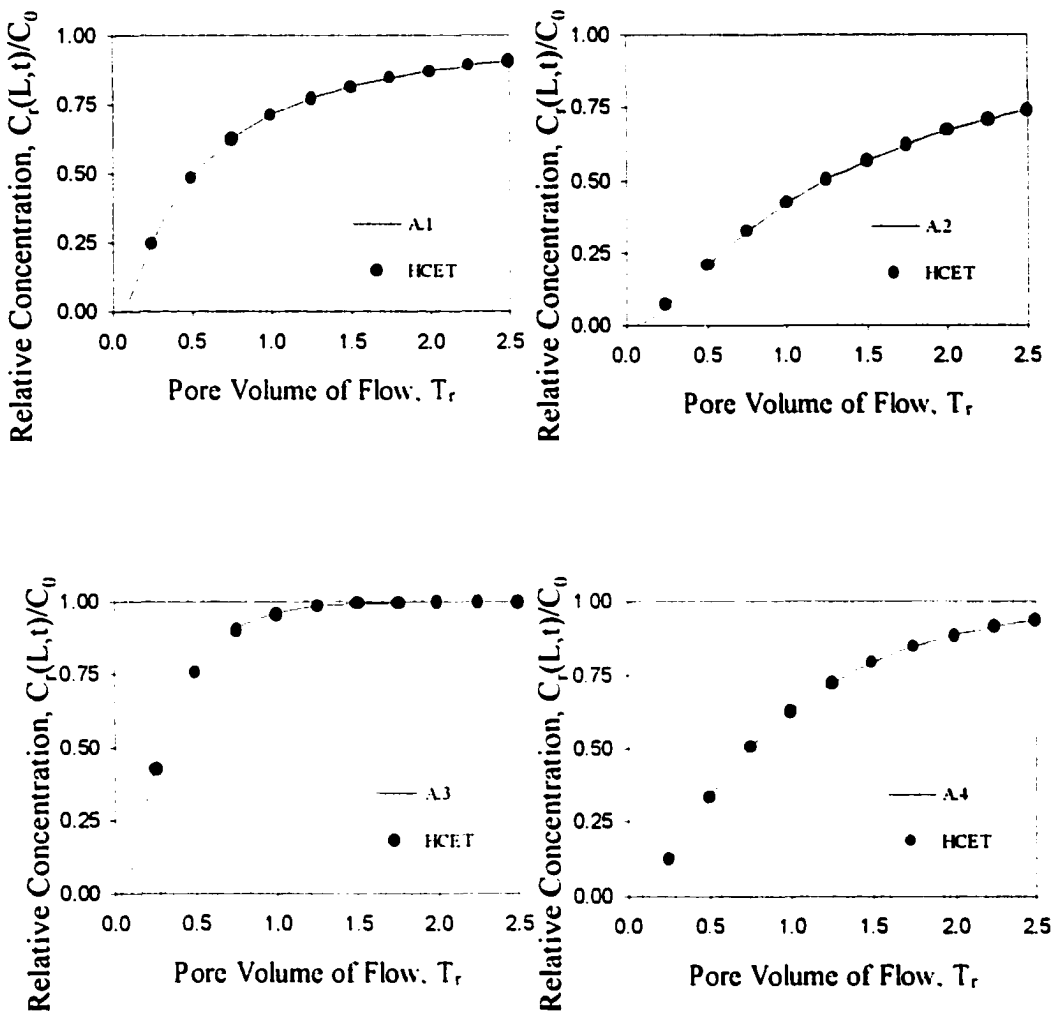

Figure 5-9: Plot for relative concentration, $C_r(L, t)/C_0$, versus pore volume of flow, T_r, for a comparison of analytical solutions with HCET model simulations for a dimensionless Peclet number, P_L=1.

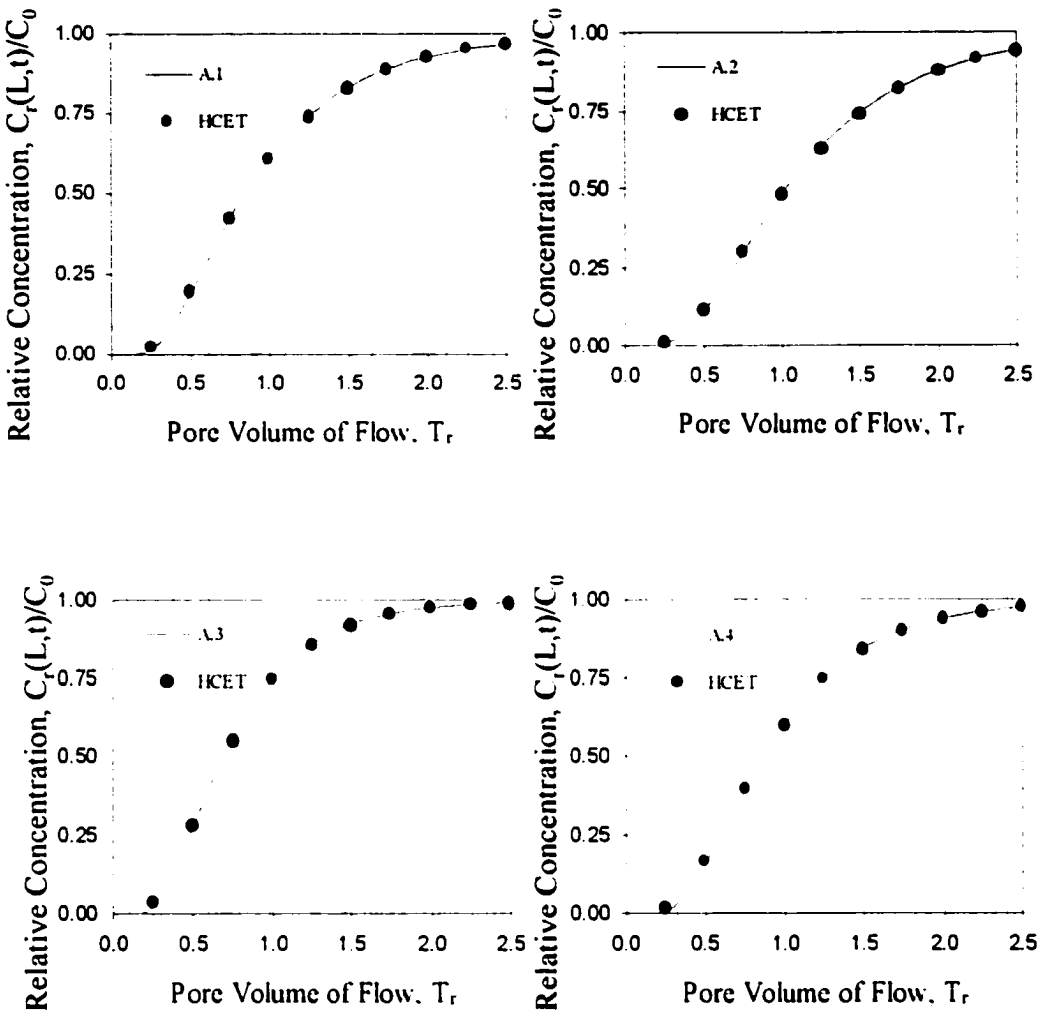

Figure 5-10: Plot for relative concentration, $C_r(L, t)/C_0$, versus pore volume of flow, T_r, for a comparison of analytical solutions with HCET model simulations for a dimensionless Peclet number, P_L=5.

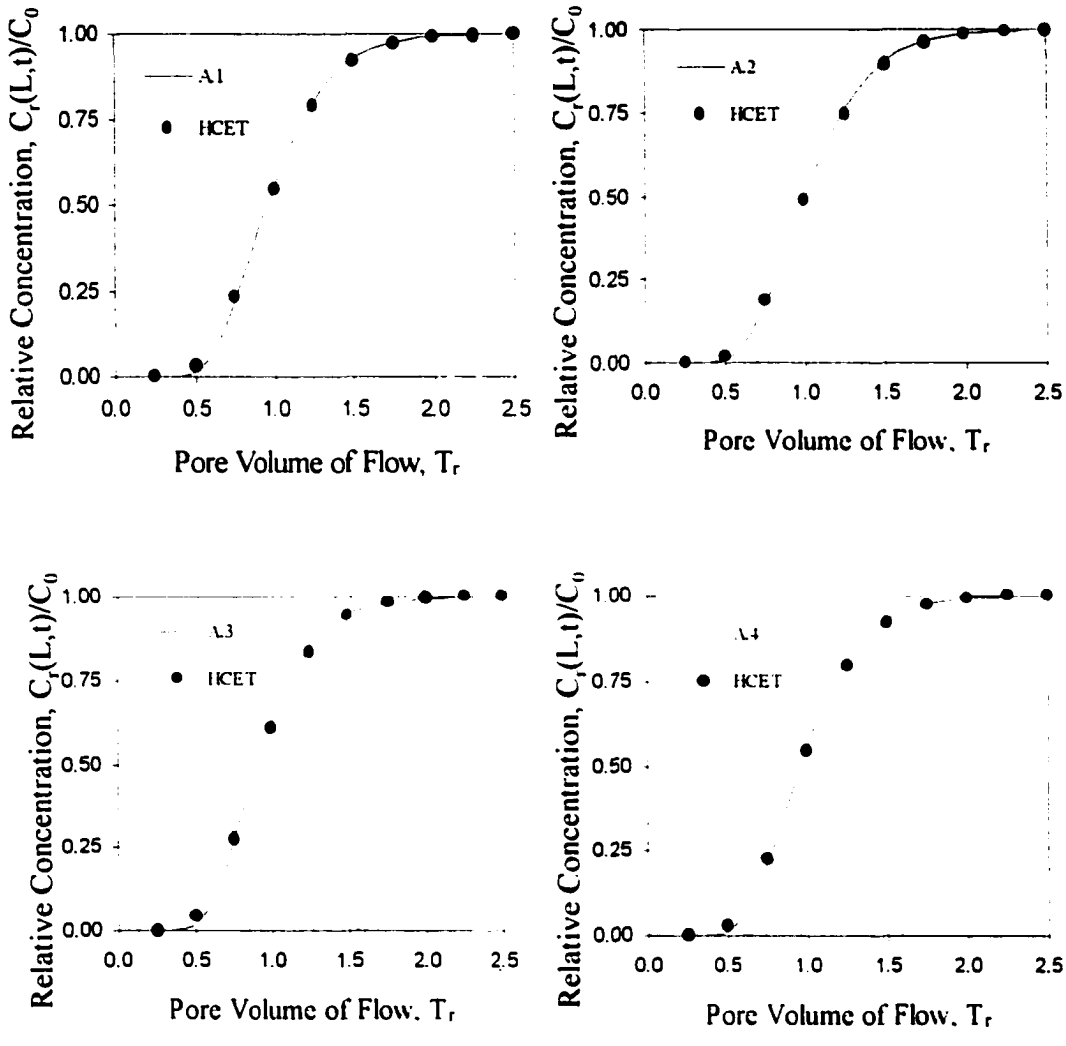

Figure 5-11: Plot for relative concentration, $C_r(L, t)/C_0$, versus pore volume of flow, T_r, for a comparison of analytical solutions with HCET model simulations for a dimensionless Peclet number, P_L=20.

Case 1.6: HCET model with dimensionless relative flux concentrations

We compare other commonly used models based on flux-averaged concentrations with HCET model. In most column tests, the effluent is collected in a reservoir from which liquid samples are recovered on a periodic basis and analyzed for chemical concentrations of specified chemical species. As a result, evaluation of effluent concentrations utilizing analytical solutions based on resident concentrations is conceptually incorrect (Parker and van Genuchten 1984, van Genuchten and Parker 1984, and Shackelford 1995). The usage of flux-averaged concentration or flowing concentration is common in analysis of soil column effluent data in laboratory experiments. The flux-averaged concentration, C_c, is defined as the mass flux of solute passing through the effluent end of the soil column per unit fluid flux during an elementary time interval, or

$$C_c = \frac{J(L,t)}{q_0} \qquad [5-14]$$

where J (L, t) is the solute mass flux evaluated just inside the effluent end of the column of soil of length L, t is time, and q_0 is the fluid flux given by Darcy's law, or

$$q_0 = \frac{Q}{A} = -K_{hh} i \qquad [5-15]$$

where Q is the volumetric flow rate, A is the total cross sectional area of the soil column perpendicular to the direction of flow, K_{hh} is the hydraulic conductivity of

the soil, and i is the hydraulic gradient (< 0). For a saturated soil in which all of the pore spaces are available for transport, the transient solute flux at the effluent end of the column of soil, J (L, t), is the sum of the transient advective solute flux, J_a (L, t), and the transient dispersive/diffusive solute flux, J_d (L, t), or

$$J(L,t) = J_a(L,t) + J_d(L,t) = q_o C_r(L,t) - nD\frac{\partial C_r(L,t)}{\partial x} \qquad [5-16]$$

where n is the total porosity of the soil. Thus, evaluation of flux-averaged effluent concentrations in accordance with equation 5-14 requires an evaluation of the solute flux, J (L, t) in equation 5-16.

Normalization of the effluent concentrations in equation 5-14 with respect to the influent concentration, C_0, results in the following expression:

$$\frac{C_e}{C_o} = \frac{J(L,t)}{q_o C_o} = RF \qquad [5-17]$$

where RF is the relative solute flux defined as follows (Shackelford 1992, Manassero and Shackelford 1994):

$$RF = \frac{J(L,t)}{q_o C_o} = \frac{J_a(L,t) + J_d(L,t)}{q_o C_o} \qquad [5-18]$$

where q_0C_0 is the steady-state solute flux (i.e., at steady-state transport, J (L, t) = q_0C_0, and RF = 1). The relative solute flux models resulting from the concentration-based models in Table 5-6 are listed in Table 5-7 in terms of the dimensionless parameters T_r and P_L.

The relative flux at effluent expressed by equation 5-18 can be rewritten numerically for the HCET model as

$$RF = \frac{J_{(x\ L,t)}}{q_0C_0} = \frac{K_{hh}}{q_0C_0}\frac{h_{nem+1} - h_{nem}}{x_{nem+1} - x_{nem}}C_L - \frac{nD_L^*}{q_0C_0}\frac{C_{nem+1} - C_{nem}}{x_{nem+1} - x_{nem}} \qquad [5-19]$$

where, nem is the number of elements studied, nem+1 is the total nodes in the domain in one-dimensional formulation, and D_L^* is the diffusion coefficient at the effluent. The relative flux models, RF (= C_L/C_0) in Figures 5-12 through 5-14, are compared for Peclet number values of 1, 5, and 20, respectively. Again, these Figures indicate the analytical expressions (lines) are in good agreement with the HCET model solutions (symbols).

Table 5-7. Relative Flux (RF) Models at x=L based on models in Table 5-5 (after Shackelford,1995).

Concentration Model (1)	Relative Flux, RF $\left(=\frac{J(L,t)}{q_0 c_0}\right)$, for Concentration Models (2)	Relative Flux Model
A.1	$RF = 0.5\left\{\operatorname{erfc}\left[\frac{1-T_t}{2\sqrt{T_t/P_L}}\right] + \frac{2}{\sqrt{\pi T_t P_L}}\exp\left[-\left(\frac{1-T_t}{2\sqrt{T_t/P_L}}\right)^2\right]\right.$	RF.1
A.2	$RF = 0.5\left\{\operatorname{erfc}\left[\frac{1-T_t}{2\sqrt{T_t/P_L}}\right] + \exp(P_L)\operatorname{erfc}\left[\frac{1+T_t}{2\sqrt{T_t/P_L}}\right]\right\}$	RF.2
A.3	$RF = 1 - \sum_{m=1}^{\infty} \frac{\alpha_m\left[\sin(\alpha_m) - \frac{2\alpha_m}{P_L}\cos(\alpha_m)\right]\exp\left[\frac{P_L}{2} - \frac{P_L T_t}{4} - \frac{\alpha_m^2 T_t}{P_L}\right]}{\left[\alpha_m^2 + \left(\frac{P_L}{2}\right)^2 + \frac{P_L}{2}\right]}$ where the eigenvalues α_m are the positive roots of $\alpha_m \cot(\alpha_m) + \frac{P_L}{2} = 0$	RF.3
A.4	$RF = 1 - \sum_{m=1}^{\infty} \frac{2\beta_m\left[\sin(\beta_m)\right]\exp\left[\frac{P_L}{2} - \frac{P_L T_t}{4} - \frac{\beta_m^2 T_t}{P_L}\right]}{\left[\beta_m^2 + \left(\frac{P_L}{2}\right)^2 + P_L\right]}$ where the eigenvalues β_m are the positive roots of $\beta_m \cot(\beta_m) - \frac{\beta_m^2}{P_L} + \frac{P_L}{4} = 0$	RF.4

(1) Models given in Table 5-5. (2) $T_t = \frac{vt}{L}$; $P_L = \frac{vL}{D}$; $q_0 = nv$.

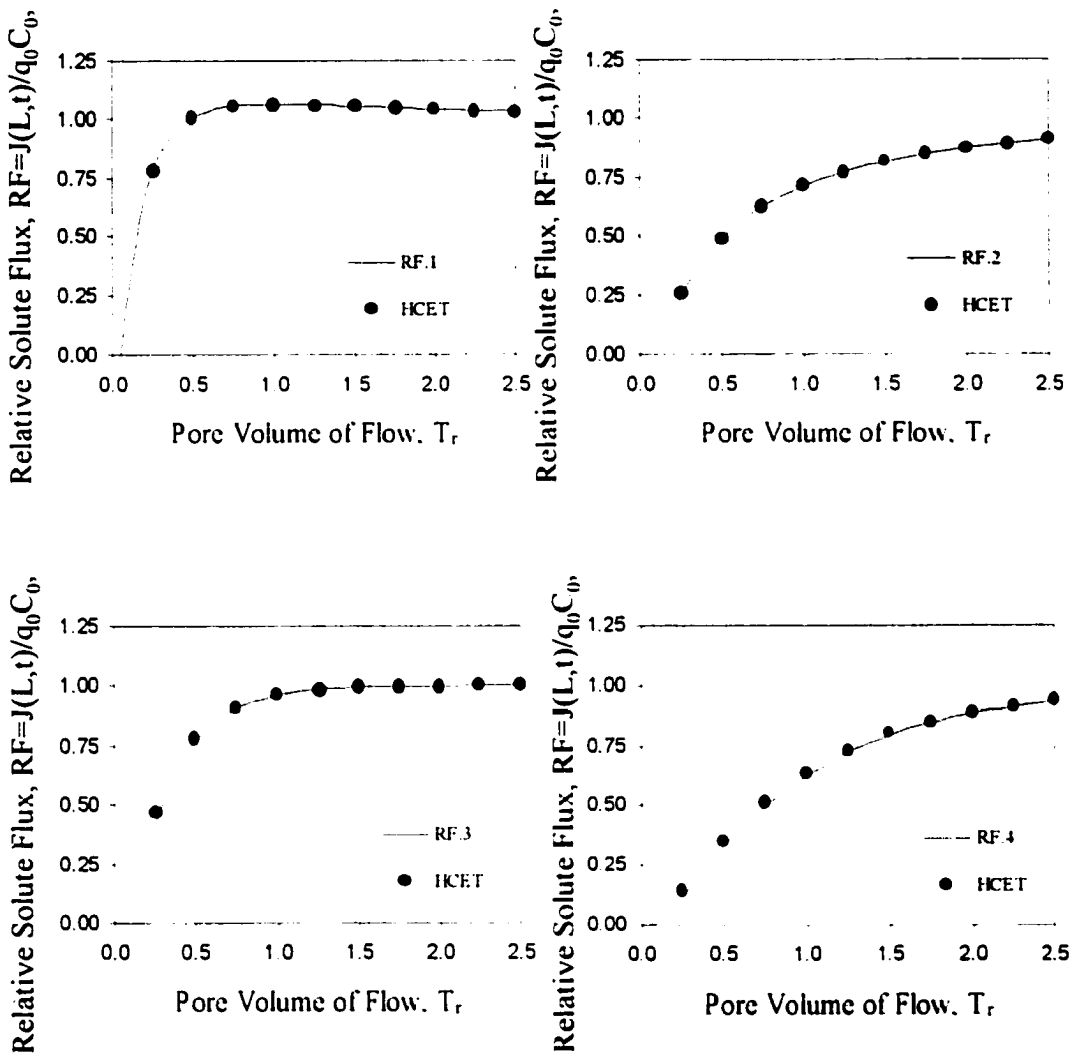

Figure 5-12: Plot for relative solute flux, $RF=J(L,t)/q_0C_0$ versus pore Volume of flow, T_r, for a comparison of analytical solutions with HCET model simulations for a dimensionless Peclet number, $P_L=1$.

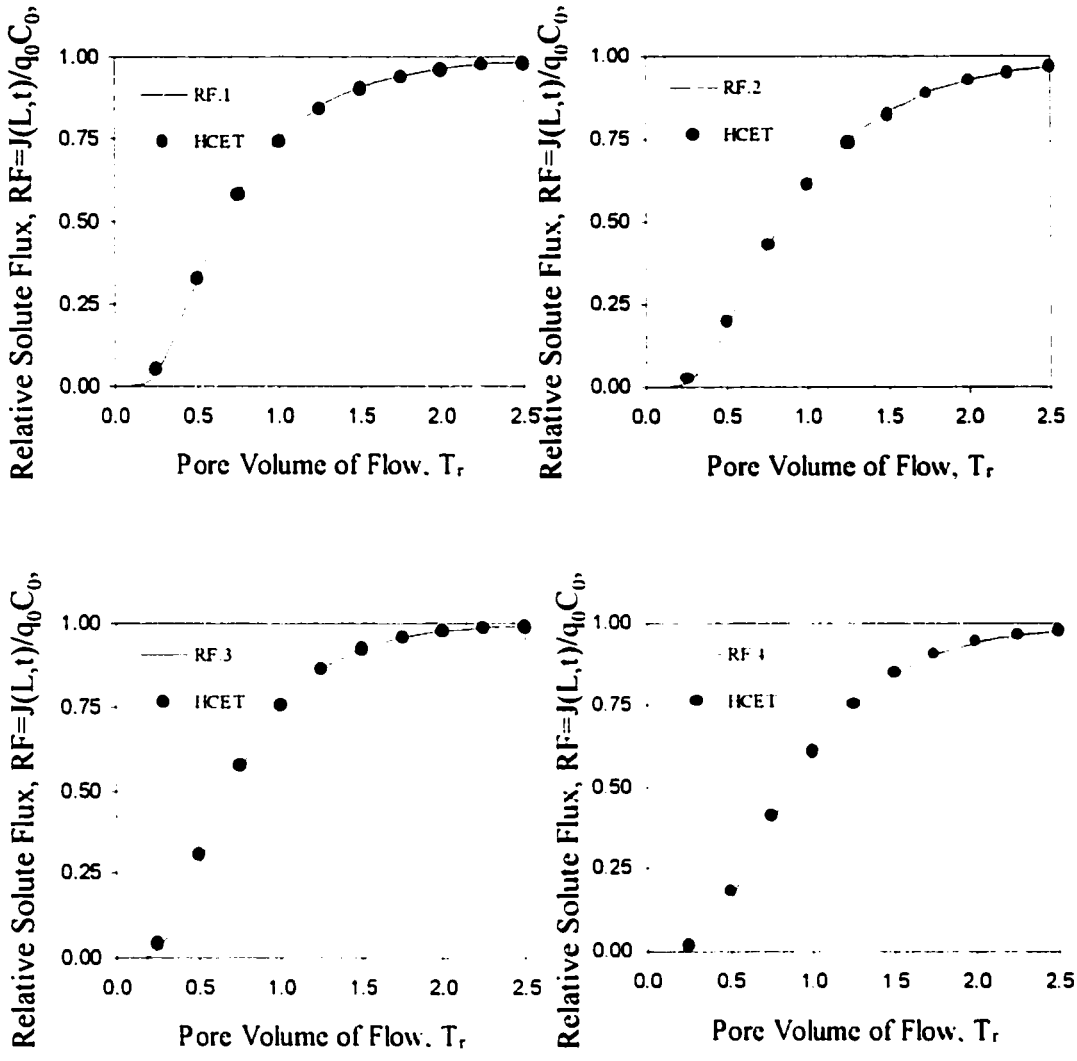

Figure 5-13: Plot for relative solute flux, $RF=J(L,t)/q_0C_0$ versus pore Volume of flow, T_r, for a comparison of analytical solutions with HCET model simulations for a dimensionless Peclet number, $P_L=5$.

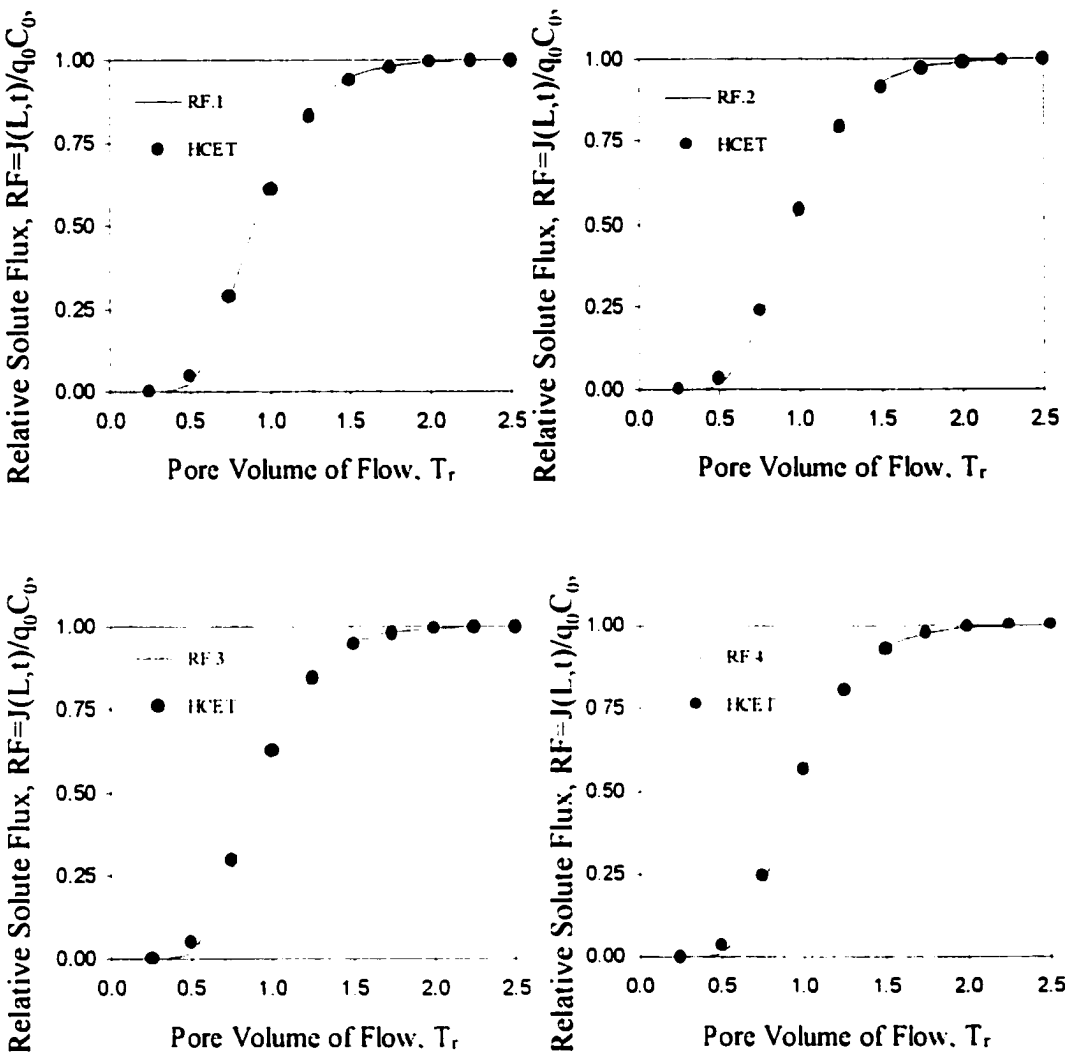

Figure 5-14: Plot for relative solute flux, $RF=J(L,t)/q_0C_0$ versus pore Volume of flow, T_r, for a comparison of analytical solutions with HCET model simulations for a dimensionless Peclet number, $P_L=20$.

5.3 EXTENSION OF SOLUTE TRANSPORT EQUATION FOR MORE VARIABLES

Case 1.7: Current transport (h, C_j, E as variables, T constant) at fixed time

The objective of this section is to use the HCET model to simulate the variation of electric potential as a function of distance from the anode. Allowing three variables, h, C_j, and E with T constant, there is no analytical solution for the governing equation 4-5 We compare the simulated voltage distribution with experimental data obtained in a pilot plant study by Alshawabkeh (Alshawabkeh and Acar, 1996). Alshawabkeh's pilot plant study is one of the extensive researches on electrokinetic remediation to remove contaminants from soils. Electrokinetic remediation is considered to be an innovative and cost-effective technology in waste management.

For the HCET model with constant temperature, equation 4-5 reduces to equation 5-20:

$$\begin{bmatrix} K_{hh} & K_{hc_j} & K_{he} \\ D^*_{cho} + C_j K_{hh} & nD^*_j + C_j K_{hc_j} & D^*_{cto} + C_j K_{ht} \\ \sigma_{eho} & \sigma_{ec_j} & \sigma_{ee} \end{bmatrix} \begin{bmatrix} h \\ C_j \\ E \end{bmatrix}$$

$$+ \begin{bmatrix} 0 & 0 & 0 \\ 0 & +K_{hh}\nabla h + K_{hc}\nabla C_j \\ & +K_{he}\nabla E + 0 & 0 \\ 0 & 0 & \nabla\sigma_{ee} \end{bmatrix} \begin{bmatrix} h \\ C_j \\ E \end{bmatrix} = \frac{\partial}{\partial t} \begin{bmatrix} S_s h \\ nC_j \\ \frac{1}{C_{tp}} E \end{bmatrix} \qquad [5\text{-}20]$$

To meet the boundary conditions set in Alshawabkeh's experiments, equation 5-20 must be reduced to equation 5-21.

$$\begin{bmatrix} K_{hh} & 0 & 0 \\ 0 & nD_j^* & 0 \\ 0 & 0 & \sigma_{ee} \end{bmatrix} \begin{bmatrix} h \\ C_j \\ E \end{bmatrix} + \begin{bmatrix} 0 & 0 & 0 \\ 0 & K_{hh}\nabla h & 0 \\ 0 & 0 & \nabla\sigma_{ee} \end{bmatrix} \begin{bmatrix} h \\ C_j \\ E \end{bmatrix} = \frac{\partial}{\partial t} \begin{bmatrix} S_s h \\ nC_j \\ 0 \end{bmatrix} \quad [5\text{-}21]$$

One cannot obtain a general analytical solution for equation 5-21. However, a HCET model numerical solution can be obtained to compare with the experimental data collected by Alshawabkeh. The initial condition expressed in Alshawabkeh's research is given by

$$E(x,0) = 0 \qquad \text{at } x \geq 0; \quad [5\text{-}22]$$

that is, electric potential is not applied at the beginning of the removal process. The boundary conditions of electric potential expressed in Alshawabkeh's experiment is given by

$$E(0, t < 1200h) = I_o * f(R) \text{ or } \frac{E}{f(R)} = I_o \quad \text{at } x = 0;$$

$$E(0, t \geq 1200h) = I_o * R \text{ or } \frac{E}{R} = I_o \quad \text{at } x = 0 \quad [5\text{-}23a]$$

$$E(L, t) = 0 \qquad \text{at } t \geq 0 \quad \text{and} \quad x = L. \quad [5\text{-}23b]$$

where $f(R)$ represents how resistance changes as a function of other variables. However, resistance, R, is constant after 1200 hours of processing. Figure 5-15 illustrates a plot of electrical potential versus distance from anode by Alshawabkeh's experimental data, Alshawabkeh and Acar model calculations, and the HCET model simulation.

The HCET model offers a reasonable fit to the experiment data; Alshawabkeh's model calculation does not. Alshawabkeh indicates the electric potential is a function of chemical concentration in solution. He argues the difference between the experimental data and his calculations result from not accounting for the effect of retardation, and for chemical precipitation of species close to the anode. He did not caution that the resistance could be a function of temperature, T, too. According to Lindeburg (1990) electric potential can be a function of temperature following an empirical equation

$$E = A + BT + CT^2 \qquad [5\text{-}24]$$

where the constants A, B, and C must be determined for the particular material of interest. Once calibrated this relationship may be used to forecast the relationship of electric potential and temperature.

In conclusion, based on the HCET model simulation, we agree with Alshawabkeh and Lindeburg that the electric potential across the soil column at constant current is a function of chemical concentration in solution, e.g. Pb^{++}, retardation, chemical precipitation of species close to the anode, temperature, and electric resistance of soil.

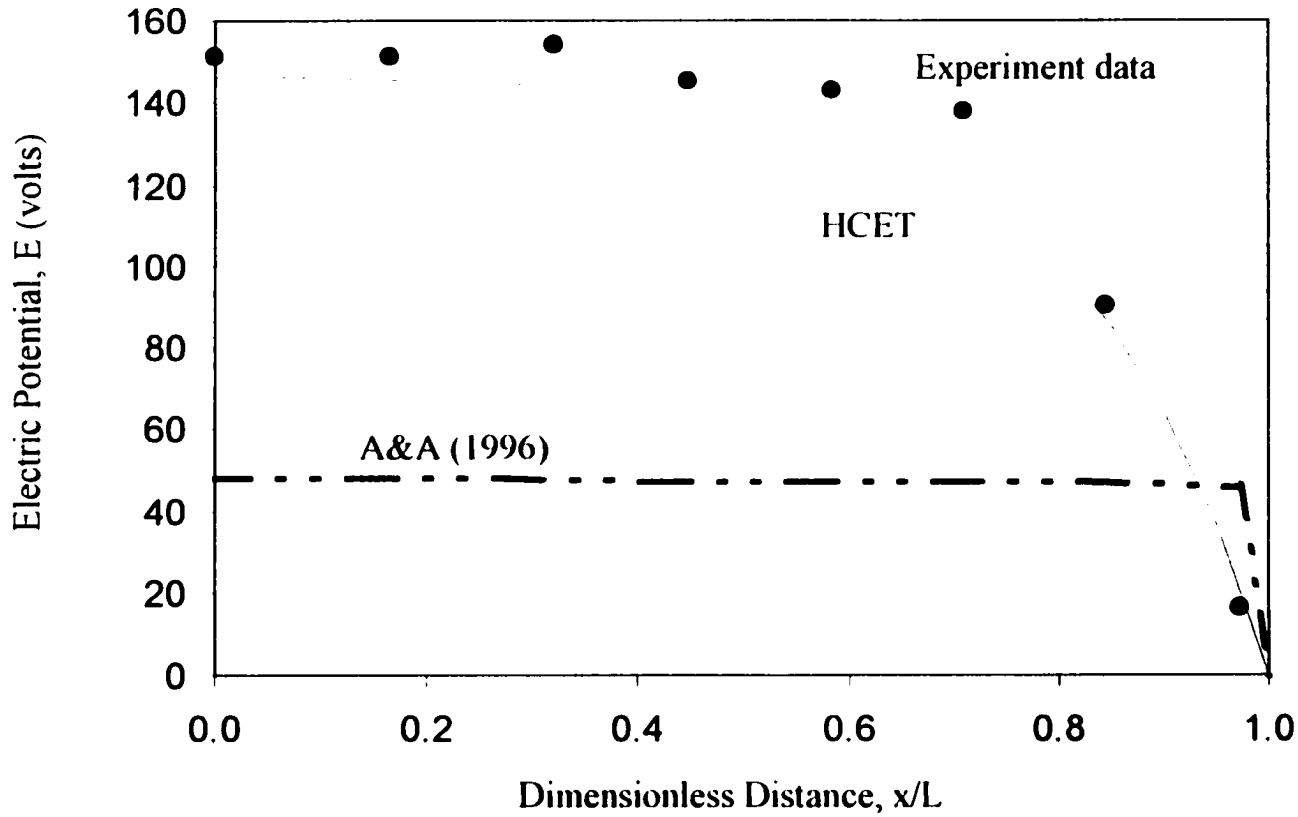

Figure 5-15: Plot of electrical potential versus dimensionless distance from anode for a comparison among Alshawabkeh's experimental data, Alshawabkeh and Acar (A&A) model calculation, and the HCET model simulation, L=72 cm.

Case 1.8: Transient current transport (h, C_i, E as variables, T constant)

We also compare the HCET model simulation with experiment data (Alshawabkeh 1994) for the transient electrical potential distribution versus distance. These lines, in Figure 5-16, show the HCET model simulation of the transient electric potential distributions up to 1200 hours of processing. The symbols are Alshawabkeh's experimental data.

We see a decrease of electric potential from left to right represents both experimental data and the HCET model. That is, the soil electric resistance lowers the voltage of power supply. However, the experiment data does not behave like the HCET model within the 20 cm range of anode. The reason may be the acid added and the chemical reaction at the anode end, which are not counted by either numerical modeling or by experimental error. However, it statistically closely matches the experimental data and the simulation of HCET model. Further reasons, which affect the soil resistance as a function of time and space, are the soil resistance changed with time, some heat effect changed the soil properties or the chemical precipitation at the soil column. By Ohm's law, electric potential distribution across the study domain is linear dropped at a fixed time and a fixed resistance for a constant current (electric potential is equal to current multiples resistance). However, in this study domain, chemical reactions change soil properties and electric conductivities. In turn, it changes the electric potential distribution away from linearity. It recommends the chemical reaction to be specified/included to do a better modeling. A soil electric conductivity gradient of 0.1 S/m^2 is assumed to fit HCET model with experimental data away from the linearity of Ohm's law.

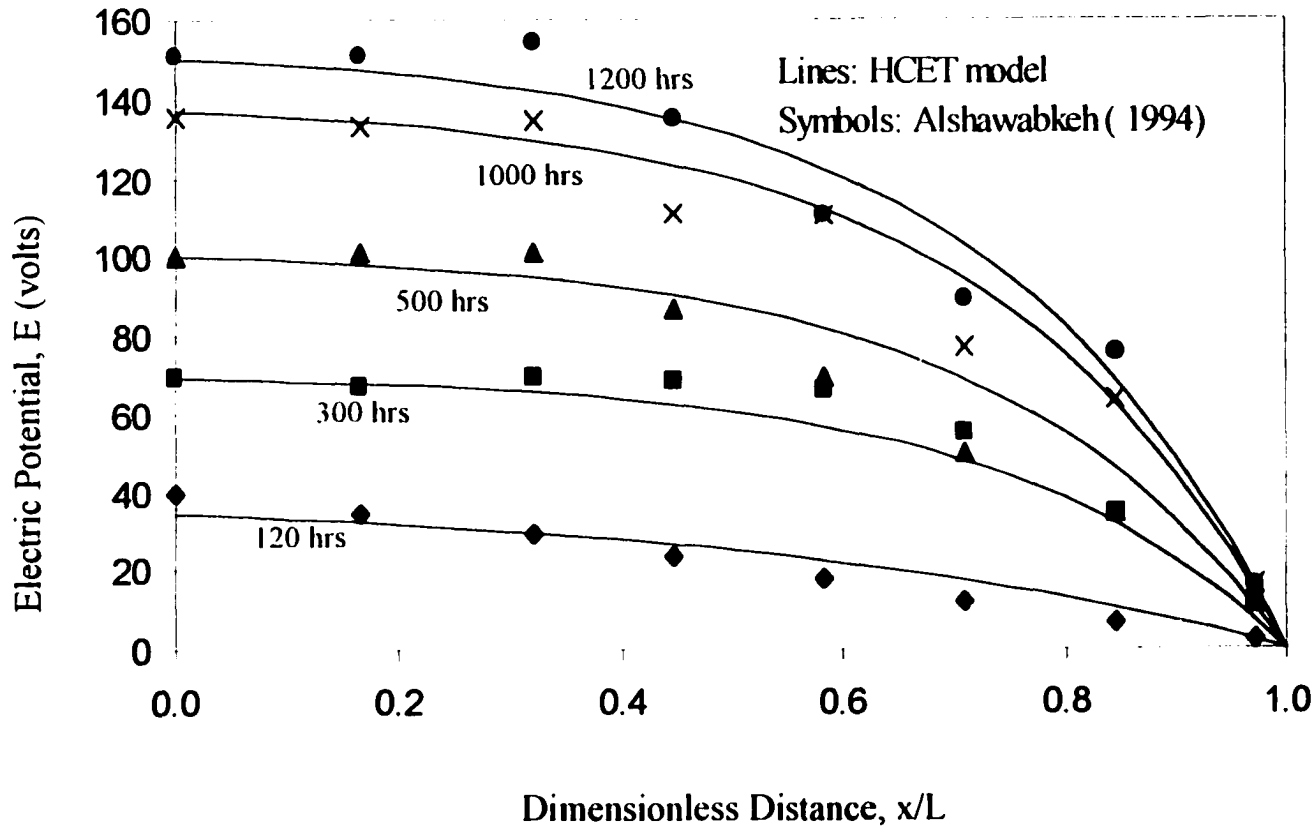

Figure 5-16: Comparison of Alshawabkeh's experimental data with HCET model calculations for the plot of voltage distribution versus dimensionless distance after 120, 300, 500, 1000, and 1200 hours processing (L=72 cm).

The boundary conditions, in Figures 5-15 and 5-16, need to be addressed. For the left hand side boundary condition like equation 5-23a, electric potential is changing with time and is site dependent. We establish this relationship of electric potential and time based on Alshawabkeh's experiments. Figure 5-17 shows the regression values of electric potential versus time, using Alshawabkeh's experimental measurement boundary condition in 1994. The solid line fitted Alshawabkeh's data with regression square of 0.99. At transient state, the electrical potential varies with the time, and reaches a stable value of 150 volts after 1200 hours of processing at a constant current.

For the right hand side boundary condition in equation 5-23b, we assume it is first kind specified value with zero electric potential based on the followings facts.

- Electric capacitance is very small and close to zero compared with electric conductivity (Acar and Alshawabkeh, 1996).
- Experimental measurement indicates that the electric potential at the right hand side boundary condition is zero (Alshawabkeh, 1994).
- Current movement is very fast and electrical potential balance occurs very rapidly. At the right hand side boundary, changes in electrical potentials close to a steady zero value for any time of interest.
- Electrical potential is a relative value. To solve numerical solutions, boundary conditions are required to be set according to the site's conditions.

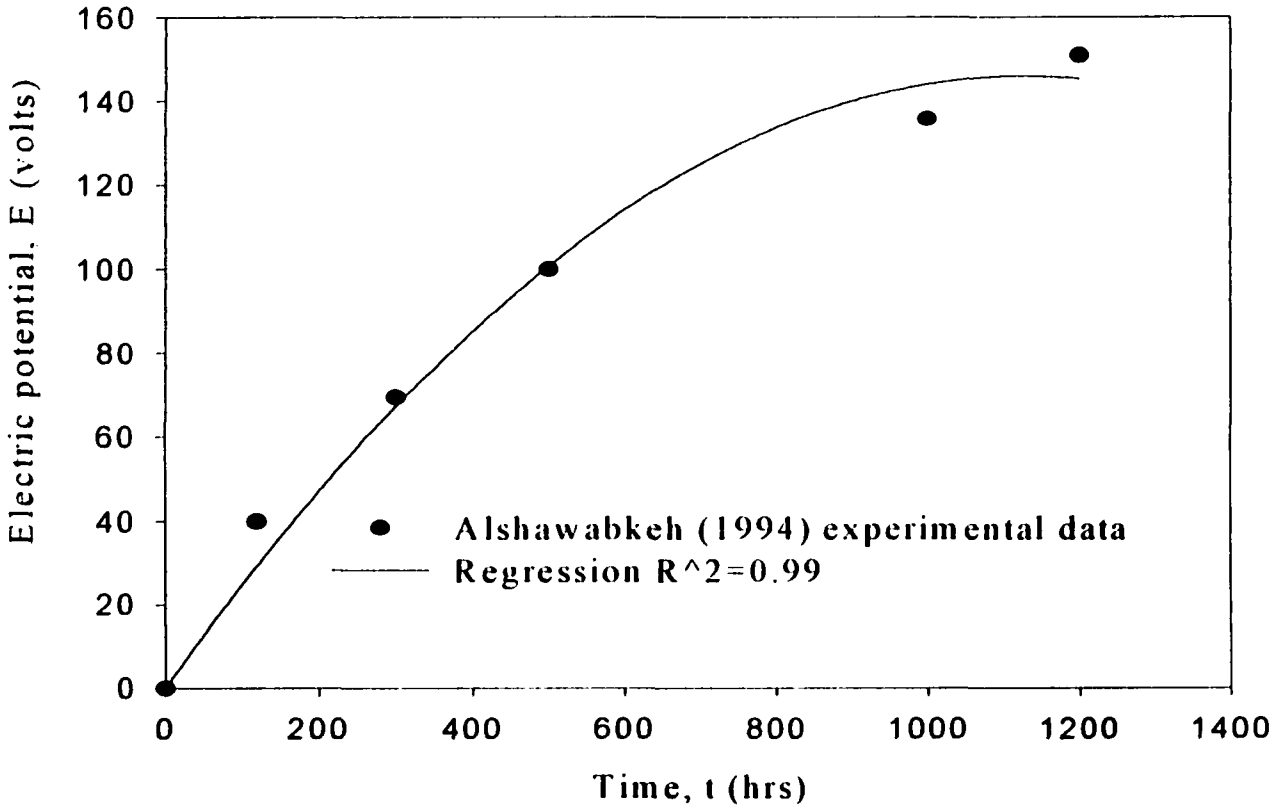

Figure 5-17: Regression value of electric potential versus time using Alshawabkeh's experimental data

Case 1.9: Heat Transport (h, C_j, T as variables with E constant)

The objective of this case is to validate the governing equation 4-5 compared with HYDRUS model 5.0. The HYDRUS model 5.0 is developed by the United States Department of Agriculture, USDA. HYDRUS is a public domain code and has been used and validated extensively (Huang, Zhang, and van Genutchten, 1996).

For the HCET model with constant electric potential, equation 4-5 reduces to equation 5-25:

$$\begin{bmatrix} K_{hh} & K_{hco} & K_{ht} \\ D^{*}_{cho} + C_j K_{hh} & nD^{*}_{j} + C_j K_{hco} & D^{*}_{cht} + C_j K_{ht} \\ \lambda_{th} + TK_{hh} & \lambda_{tco} + TK_{hco} & \lambda_{tt} + TK_{ht} \end{bmatrix} \begin{bmatrix} h \\ C_j \\ T \end{bmatrix} + \begin{bmatrix} 0 & 0 & 0 \\ 0 & \begin{matrix} +K_{hh}\nabla h + K_{hco}\nabla C_j \\ + \ 0 \ + K_{ht}\nabla T \end{matrix} & 0 \\ 0 & 0 & \begin{matrix} +K_{hh}\nabla h + K_{hco}\nabla C_j \\ + \ 0 \ - K_{ht}\nabla T \end{matrix} \end{bmatrix} \begin{bmatrix} h \\ C_j \\ T \end{bmatrix} = \frac{\partial}{\partial t} \begin{bmatrix} S_s h \\ nC_j \\ C_{TP} T \end{bmatrix} \qquad [5\text{-}25]$$

The HYDRUS model uses less parameters than HCET model. To compare HYDRUS model with HCET model, the parameters in equation 5-25 will be further reduced to equation 5-26.

$$\begin{bmatrix} K_{hh} & 0 & 0 \\ 0 & nD^{*}_{j} & 0 \\ 0 & 0 & \lambda_{tt} \end{bmatrix} \begin{bmatrix} h \\ C_j \\ T \end{bmatrix} + \begin{bmatrix} 0 & 0 & 0 \\ 0 & K_{hh}\nabla h & 0 \\ 0 & 0 & K_{ht}\nabla T \end{bmatrix} \begin{bmatrix} h \\ C_j \\ T \end{bmatrix} = \frac{\partial}{\partial t} \begin{bmatrix} S_s h \\ nC_j \\ C_{TP} T \end{bmatrix} \qquad [5\text{-}26]$$

We compare the HCET model simulation with the HYDRUS model simulation involving the hydraulic head, chemical concentration, and temperature. The solution of 5-26 requires the specification of initial and boundary conditions for the soil temperature, T. The initial condition of soil temperature expressed in the HYDRUS 5.0 is given by

$$T(x,0) = T_i(x) \qquad \text{at } x \geq 0; \tag{5-27a}$$

where T_i is a prescribed function of x.

The boundary conditions of soil temperature to solve governing equations 5-26 expressed in the HYDRUS 5.0 is given by

$$T(x,t) = T_o(t) \qquad \text{at } x = 0 \text{ or } x = \ell; \tag{5-27b}$$

where, $T_o(t)$ is the prescribed temperature as a function of time. Atmospheric boundary conditions for daily fluctuations in soil temperature are often approximated by a sine function as follows (Vogel etc., 1996):

$$T_o = \overline{T} + A\sin\left(\frac{2\pi t}{t_p} - \omega_o\right) \tag{5-28}$$

where, t_p is the period of time required to complete one full cycle of the temperature sine wave (taken to be one day), $\overline{T}$ is the average temperature of the soil surface

during time period t_p and A is the amplitude of the sine wave. The phase ω_0 in equation 5-28 may be used to specify the times at which the daily temperature minima and maxima occur. For example, $\omega_0 = 7\pi/12$ allows the highest temperature to occur at one p.m. (Vogel etc., 1996).

The input parameters for numerical simulation were $\overline{T}$ = 15 °C, A = 5 °C, v =100 cm/d, ω = 24hr, $\omega_0 = 7\pi/12$, and D_h =50 cm^2/d. We further assumed a finite profile of 150 cm, so that the effect of the lower boundary can be ignored for the results presented here. Figure 5-18 shows a comparison of HYDRUS 5.0 model solution with HCET model solution. The illustrated temperature distribution versus depth curves are for different times and for an initial temperature T_i of 10 °C in the top100 cm of the soil profile. The results indicate a close match of the HYDRUS 5.0 and HCET models at all times.

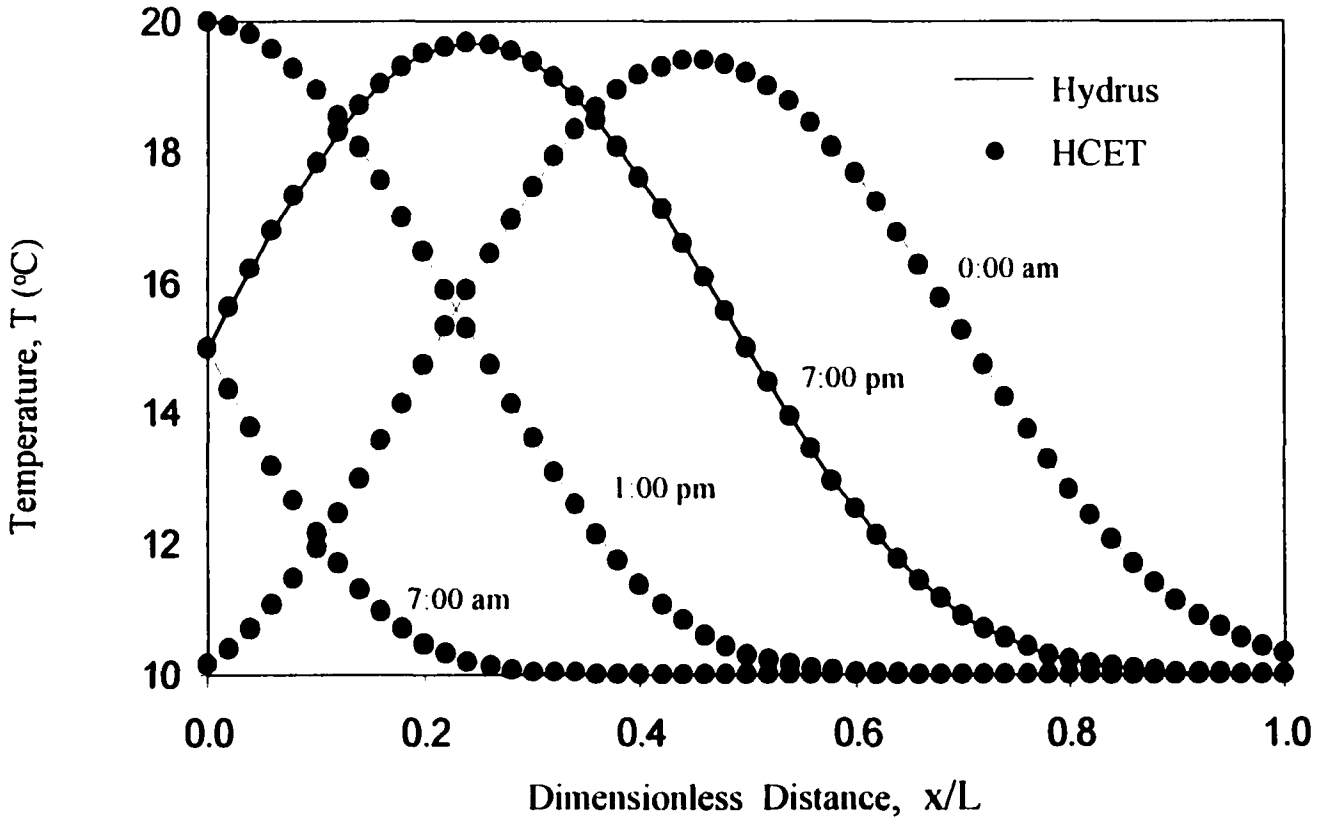

Figure 5-18: Plot of temperature versus dimensionless distance for a comparison of Hydrus model with HCET model simulations for different times (L=100cm).

Case 1.10: Heat effect on four-variable electrokinetics remediation (h, C_j, E, and T as variables).

We first describe Alshawabkeh's experimental data of heat effects on electrokinetic remediation, and then we present a numerical prediction by the HCET model.

One of the first attempts to explore the effects of four variables is Alshawabkeh's pilot plant studies of an enhanced electroosmosis effect. In his experiments, he measured each of the four variables versus distance within the pilot plant setup. His example considers water, solute, current, and heat movement.

Now we consider all four variables for the governing equation 4-5 Some simplification is required to be able to compare with the experimental data collected by Alshawabkeh in 1994:

$$\begin{bmatrix} K_{hh} & 0 & 0 & 0 \\ 0 & nD_j^* & 0 & 0 \\ 0 & 0 & \sigma_{ee} & 0 \\ 0 & 0 & 0 & \lambda_{tt} \end{bmatrix} \begin{bmatrix} \dot{h} \\ \dot{C}_j \\ \dot{E} \\ \dot{T} \end{bmatrix} + \begin{bmatrix} 0 & 0 & 0 & 0 \\ 0 & +K_{hh}\nabla h & 0 & 0 \\ 0 & 0 & 0 & 0 \\ 0 & 0 & 0 & +K_{ht}\nabla T \end{bmatrix} \begin{bmatrix} h \\ C_j \\ E \\ T \end{bmatrix} = \frac{\partial}{\partial t} \begin{bmatrix} 0 \\ nC_j \\ 0 \\ C_{tp}T \end{bmatrix} \qquad [5\text{-}29]$$

For the HCET model simulation, the parameters that need to be set in the main program are: NEM=20, NNM=21, NEQ=84, NSIZE=8, NDF=4, MXEBC=8, MXNBC=8, MNN=20, and MNDT=20

where, NEM=number of element, NNM=node number maximum, NEQ=number of equation, NSIZE=number size per element, NDF= number degree of freedom.

MXEBC=maximum essential boundary condition, MXNBC= maximum natural boundary condition, and MNDT=maximum number of delta time.

The symbols in Figures 5-19a, and 5-19b illustrate the experimental data conducted by Alshawabkeh. The solid and dashed lines in Figures 5-19a, and 5-19b are predicted by HCET model.

At anolyte and catholyte boundaries, heat is generated by resistivity and lost to the ambient. Two cases, 5-19a and 5-19b, of boundary conditions are studied. For case a, calculations are performed by assuming the heat boundary condition at the anolyte and at the catholyte is a simple linear function of time. For case b, a polynomial relationship is established between the boundary condition and time, to simulate seasonal variation of ambient temperature. Figure 5-19a shows that the temperature increases due to resistivity at the anolyte and catholyte. The HCET model simulation shows a relatively poor fit of the experiment data for case a. Case b shows the heat exchange due to resistivity with seasonally ambient temperature variation at the anolyte and at the catholyte. In case b, the data fit the simulation curves reasonably well.

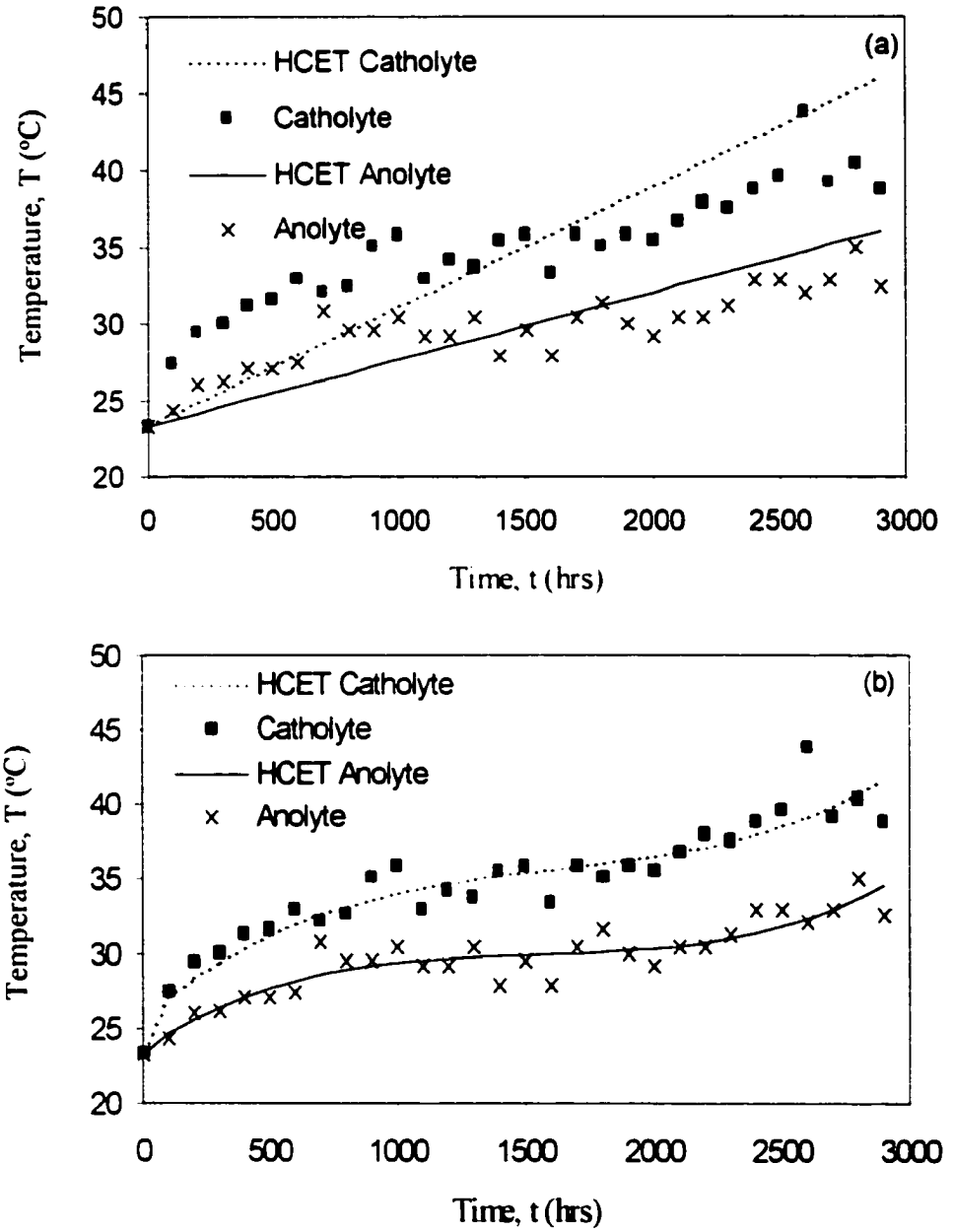

Figure 5-19: Plot of the temperature versus time curves for the HCET model simulations: (a) linearly increasing boundary condition, (b) seasonal variation boundary condition.

5.4 SENSITIVITY ANALYSIS OF COUPLED DRIVING FORCES TO SOLUTE TRANSPORT

One of the important and useful aspects of the HCET model is that parameter sensitivity analysis can be simulated and evaluated economically before undertaking the field engineering. This section explores the HCET model's capability for analysis of the relative contribution of coupled effects in transport processes.

Figure 5-20 illustrates two scenarios: contaminant remediation and contaminant transport. For the scenario of contaminant remediation we will illustrate the sensitivity of electric osmosis's contributions to solute transport. For contaminant transport we will illustrate the potential contribution of chemical osmosis and thermal osmosis coupling with hydraulic flow impacting on solute transport. The compared parameters for sensitivity analysis are collected in Table 5-8, with key parameters in bold print. The input data used in simulation for sensitivity analysis cases 2.1 to 2.8 are detailed in Table 5-9.

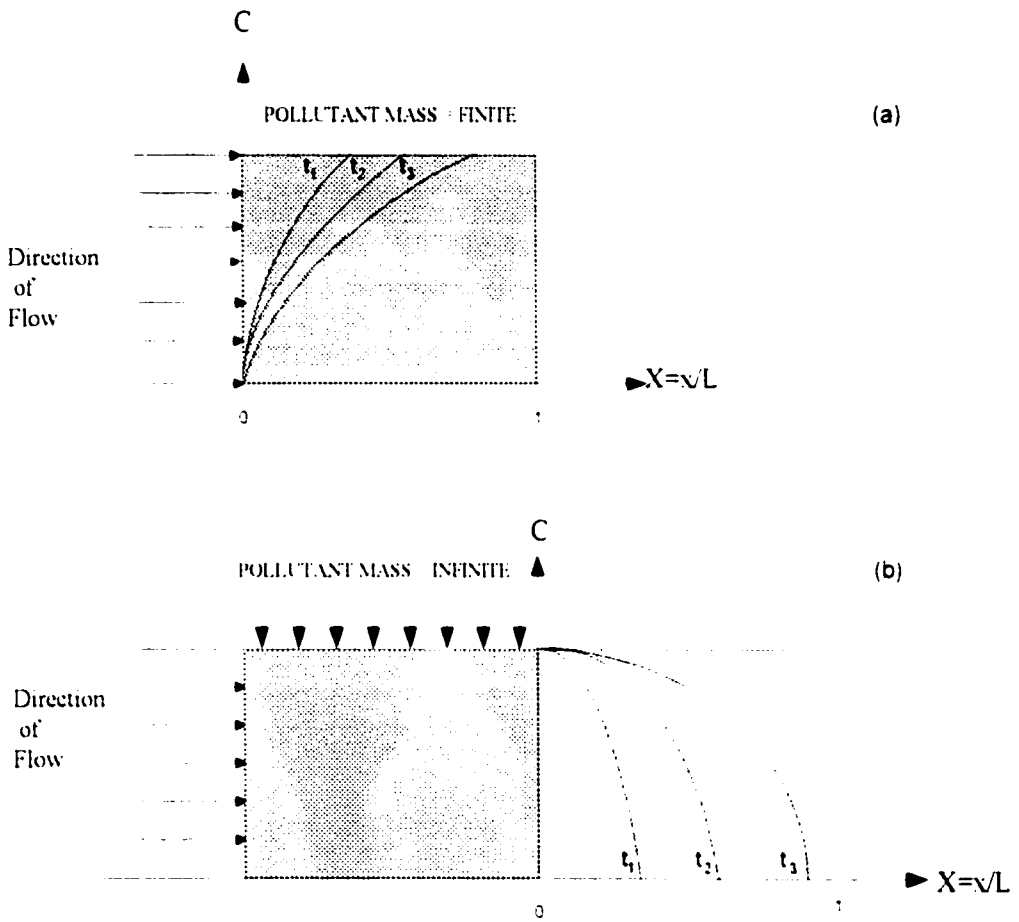

Figure 5-20: Sensitivity analysis for (a) contaminant remediation case, and (b) contaminant transport case.

Table 5-8. Range for flow parameters for saturated fine-grained soils, and specified values for sensitivity analysis for coupled flows.

Range for flow parameters for saturated fine-grained soils (1)					**Sensitivity Analysis (2)**		
Parameter	Symbol	Units	Minimum	Maximum	Chemical Osmosis	Electro Osmosis	Thermal Osmosis
Hydraulic conductivity	K_{hh}	m / s	1E-11	1E-6	**1E-11** **1E-10** **1E-9**	**1E-11** **1E-10** **1E-9**	**1E-11** **1E-10** **1E-9**
Effective diffusion coefficient	D_j^*	m^2 / s	2E-10 1E-10 (4)	2E-9 1.8E-9 (4)	1E-10	1E-10	1E-10
Electrical conductivity	σ_{ee}	S/m	0.01	1.0	N.A.	0.1	N.A.
Thermal conductivity	λ_{tt}	$Wm^{-1}K^{-1}$	0.25	2.5	N.A.	N.A.	1.0
Electric-osmotic conductivity	K_{he}	m^2 / V – s	1E-9	1E-8	N.A	**0** **5E-9** **1E-8**	N.A.
Osmotic efficiency coefficient	ω	dimensionless	0.0	1.0	**0.0, 0.5, 1.0**	N.A.	N.A.
Thermal osmosis coefficient	K_{ht}	$m^2K^{-1}s^{-1}$	1E-10 (3)	1E-9 (3)	N.A.	N.A.	**0** **1E-10** **1E-9**

(1) After Mitchell (1993), and Hsu (1997). (2) Used in simulation. (3) Dirksen (1969). (4) Shackelfold (1991).

Table 5-9. The input data used in simulation for sensitivity analysis cases 2.1 to 2.8.

Case number	Boundary conditions and Initial condition	Other parameters for governing equations
2.1	$h(0, t) = 1$ m $h(L, t) = 0$ m $h(x, 0) = 0$ m $C(0, t) = 100$ mg/l $\frac{C(L, t)}{\partial x} = 0$ mg/l/m $C(x, 0) = 0$ mg/l	$K_{hh} = 1E\text{-}10$ (m/s); $\omega = 0$ or 1; $S_s = 0$ (m^{-1}); $D^*_{cho} = 0$; $D^* = 1E\text{-}10$ or 0 (m^2s^{-1}); $n = 0.5$ $t = 100$, 1000, or 10,000 days $L = 1$ m
2.2	$h(0, t) = 1$ m $h(L, t) = 0$ m $h(x, 0) = 0$ m $C(0, t) = 100$ mg/l $\frac{C(L, t)}{\partial x} = 0$ mg/l/m $C(x, 0) = 0$ mg/l	$K_{hh} = 1E\text{-}11$, 5E-11, or 1E-10 (m/s); $\omega = 0$ or 1; $S_s = 0$ (m^{-1}); $D^*_{cho} = 0$; $D^* = 1E\text{-}10$ or 0 (m^2s^{-1}); $n = 0.5$ $t = 10{,}000$ days $L = 1$ m
2.3	$h(0, t) = 1$ m $h(L, t) = 0$ m $h(x, 0) = 0$ m $C(0, t) = 100$ mg/l $\frac{C(L, t)}{\partial x} = 0$ mg/l/m $C(x, 0) = 0$ mg/l	$K_{hh} = 1E\text{-}10$ (m/s); $\omega = 0$, 0.5, or 1, $S_s = 0$ (m^{-1}); $D^*_{cho} = 0$; $D^* = 1E\text{-}10$ (m^2s^{-1}); $n = 0.5$; $t = 100$, 1000, or 10,000 days; $L = 1$ m.

Table 5-9. The input data used in simulation for sensitivity analysis cases 2.1 to 2.8 (continue).

Case number	Boundary conditions and Initial condition	Other parameters for governing equations
2.4	h(0, t) = 1 m h(L, t) = 0 m h(x, 0) = 0 m C(0, t) = 100 mg/l $\frac{C(L, t)}{\partial x} = 0$ mg/l/m C(x, 0) = 0 mg/l	K_{hh} = 1E-11, 5E-11, or 1E-10 (m/s); ω = 0, 0.5, or 1; S_s = 0 (m^{-1}); D^*_{cho} = 0; D^* = 1E-10 ($m^2 s^{-1}$); n = 0.5; t = 10, 000 days.

2.5	h(0, t) = 1 m
	h(L, t) = 0 m
	h(x, 0) = 0 m
	C(0, t) = 100 mg/l
	$\frac{C(L, t)}{\partial x} = 0$ mg/l/m
	C(x, 0) = 0 mg/l
	E(0, t) = 1 volt
	E(L, t) = 0 volt
	E(x, 0) = 0 volt
		K_{hh} = 1E-10 (m/s); K_{hco} = 0;
		K_{he} = 0, 1E-9, or 1E-8 (m^2 sec^{-1} $volt^{-1}$); S_s = 0 (m^{-1});
		D^*_{cho} = 0; D^* = 1E-10 ($m^2 s^{-1}$); D^*_{eto} = 0;
		σ_{cho} = 0; σ_{eco} = 0;
		σ_{ee} = 0.1(C m^{-1} sec^{-1} $volt^{-1}$); σ_{eto} = 0;
		n = 0.5;
		t = 10, 100, or 1000 days;
		L = 1 m.

2.6	h(0, t) = 1 m
	h(L, t) = 0 m
	h(x, 0) = 0 m
	C(0, t) = 100 mg/l
	$\frac{C(L, t)}{\partial x} = 0$ mg/l/m
	C(x, 0) = 0 mg/l
	E(0, t) = 1 volt
	E(L, t) = 0 volt
	E(x, 0) = 0 volt
		K_{hh} = 1E-11, 1E-10 or 1E-9 (m/s);
		K_{hco} = 0;
		K_{he} = 0, 1E-9, or 1E-8 (m^2 sec^{-1} $volt^{-1}$);
		S_s = 0 (m^{-1}); D^*_{cho} = 0;
		D^* = 1E-10 ($m^2 s^{-1}$); D^*_{eto} = 0;
		σ_{cho} = 0; σ_{eco} = 0;
		σ_{ee} = 0.1(C m^{-1} sec^{-1} $volt^{-1}$); σ_{eto} = 0;
		n = 0.5;
		t = 1000 days;
		L = 1 m.

Table 5-9. The input data used in simulation for sensitivity analysis cases 2.1 to 2.8 (continue).

Case number	Boundary conditions and Initial condition	Other parameters for governing equations
2.7	h(0, t) = 1 m h(L, t) = 0 m h(x, 0) = 0 m C(0, t) = 100 mg/l $\frac{C(L, t)}{\partial x} = 0$ mg/l/m C(x, 0) = 0 mg/l T(0, t) = 25 °C T(L, t) = 20 °C T(x, 0) = 0 °C	K_{hh} = 1E-11(m/s); K_{hco} = 0; K_{ht} = 0, 1E-10, or 1E-9 ($m^2 sec^{-1} K^{-1}$); S_s = 0 (m^{-1}); D^*_{cho} = 0; D^* = 1E-10 ($m^2 s^{-1}$); D^*_{cto} = 0; C_{TP} = 0; λ_{th} = 0; λ_{tco} = 0; $\lambda_{tt} = 1\left(Wm^{-1}K^{-1}\right)$; n = 0.5; t = 100, 1000, or 10,000 days; L = 1 m.
2.8	h(0, t) = 1 m h(L, t) = 0 m h(x, 0) = 0 m C(0, t) = 100 mg/l $\frac{C(L, t)}{\partial x} = 0$ mg/l/m C(x, 0) = 0 mg/l T(0, t) = 25 °C T(L, t) = 20 °C T(x, 0) = 0 °C	K_{hh} = 1E-11, 1E-10 or 1E-9 (m/s); K_{hco} = 0; K_{ht} = 0, 1E-10, or 1E-9 ($m^2 sec^{-1} K^{-1}$); S_s = 0 (m^{-1}); D^*_{cho} = 0; D^* = 1E-10 ($m^2 s^{-1}$); D^*_{cto} = 0; C_{TP} = 0; λ_{th} = 0; λ_{tco} = 0; $\lambda_{tt} = 1\left(Wm^{-1}K^{-1}\right)$; n = 0.5; t = 10,000 days; L = 1 m.

Notes: See symbols' notation in Chapter III.

Case 2.1: Effective diffusion coefficient for different solute transport time at hydraulic conductivity of 1E-10 m/s (L=1m; C_0=100 mg/l).

When considering only the hydraulic and chemico-osmotic driving forces, the governing equation 4-5 can be reduced to equation 5-30.

$$\begin{bmatrix} K_{hh} & K_{hco} \\ 0 & nD_j^* + C_j K_{hco} \end{bmatrix} \begin{bmatrix} h \\ C_j \end{bmatrix} + \begin{bmatrix} 0 & 0 \\ 0 & +K_{hh}\nabla h + K_{hco}\nabla C_j \end{bmatrix} \begin{bmatrix} h \\ C_j \end{bmatrix} = \frac{\partial}{\partial t} \begin{bmatrix} S_s h \\ nC_j \end{bmatrix} \qquad [5\text{-}30]$$

Expressing equation 5-30 in steady state condition, we have

$$K_{hh}\frac{\partial h}{\partial x} + K_{hco}\frac{\partial C_j}{\partial x} = J_w \qquad [5\text{-}31a]$$

$$\left(nD_j^* + C_j K_{hco}\right)\frac{\partial^2 C_j}{\partial x^2} + \left(K_{hh}\frac{\partial h}{\partial x} + K_{hco}\frac{\partial C_j}{\partial x}\right)\frac{\partial C_j}{\partial x} = n\frac{\partial C}{\partial t} \qquad [5\text{-}31b]$$

Equation 5-31a, and equation 5-31b may be derived from fundamentals of soil behavior like equations 5-32a and 5-32b (Mitchell, 1993).

$$K_{hh}\frac{\partial h}{\partial x} + (-\omega)K_{hh}\frac{\partial h}{\partial x} = J_w \qquad [5\text{-}32a]$$

$$\left(nD_0\tau_0 - \frac{\omega C_j K_{hh} RT}{\gamma_w}\right)\frac{\partial^2 C_j}{\partial x^2} + \left(K_{hh}\frac{\partial h}{\partial x} - \omega\frac{K_{hh}RT}{\gamma_w}\right)\frac{\partial C_j}{\partial x} = n\frac{\partial C_j}{\partial t} \qquad [5\text{-}32b]$$

The details of the derivation are presented in Appendix D. The chemico-osmosis coefficient, K_{hco} in equations 5-31a and 5-31b, turns into chemico-osmotic efficiency, ω in equations 5-32a and 5-32b. The effective coefficient, D_j^*, is equal

to $D_0\tau_0$. Figure 5-21 shows the relationship between effective diffusion coefficient, D_j^* and chemico-osmotic efficiency, ω. When testing solute transport, it is necessary to correctly select the effective diffusion coefficient, D_j^*.

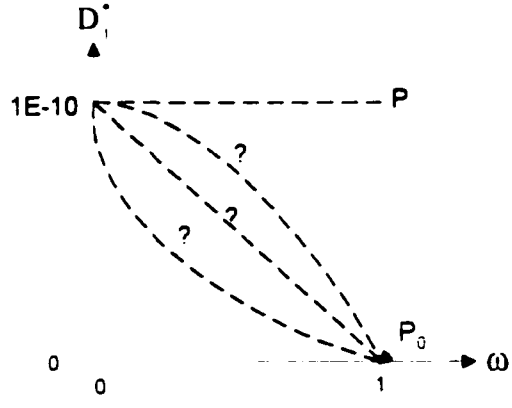

Figure 5-21: Conceptual drawing of the relationship between effective diffusion coefficient, D_j^* versus chemico-osmotic efficiency, ω

In modeling, we should not fix D_j^* as ω changes. At point P (D_j^* = 1E – 10 m^2/s), the effective diffusion coefficient is not changed as the chemico-osmotic efficiency, ω changes to one. At point P_0 (D_j^* = 0 m^2/s), the effective diffusion coefficient is changed as the chemico-osmotic efficiency, ω changes to one. Figure 5-22 shows two effective diffusion coefficients, D_j^* = 1E – 10 m^2/s versus D_j^* = 0 m^2/s, for different solute transport time at hydraulic conductivity of 1E-10 m/s (L=1m; C_0=100 mg/l). In reality, as osmosis efficiency, $\omega \rightarrow 1$, tortuosity, $\tau_{ij} \rightarrow 0$, then $D_j^* \rightarrow 0$ because it is a perfect membrane. The case, in Figure 5-22, indicates D_j^* = 0 m^2/s is necessary for

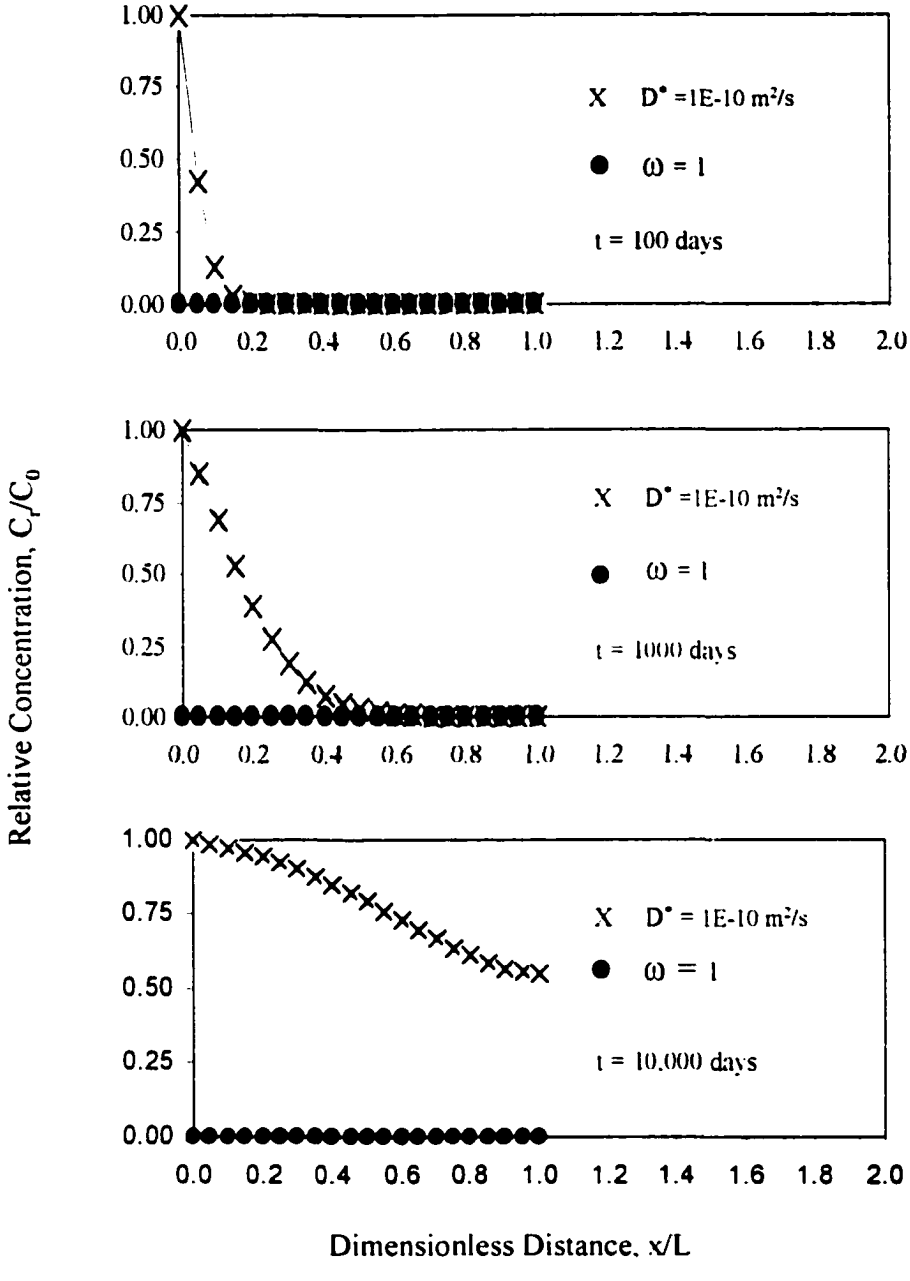

Figure 5-22: Effective diffusion coefficient for different solute transport time at hydraulic conductivity of 1E-10 m/s (L=1m; C_0=100 mg/l).

the chemico-osmotic efficiency, ω changes to one and has no flux pass through the study domain of interest.

Case 2.2: Effective diffusion coefficient for different hydraulic conductivities at fixed solute transport time 10,000 days (L=1m; C_0=100mg/l).

Figure 5-23 shows two effective diffusion coefficients, $D_j^* = 1E-10\ m^2/s$ versus $D_j^* = 0\ m^2/s$, for different hydraulic conductivities at fixed solute transport time 10,000 days (L=1m; C_0=100mg/l). $D_j^* = 1E-10\ m^2/s$ indicates there is some solute transport in the study domain. In contrast, there is no solute transport for $D_j^* = 0\ m^2/s$. Again, Figure 5-23 indicates the effective diffusion coefficient, D_i^* needs to be zero as the chemico-osmotic efficiency, ω changes to one to represent a membrane without solute pass through.

Case 2.3: Sensitivity analysis of the coupled chemico-osmotic efficiency for different solute transport time at hydraulic conductivity of 1E-10 m/s (L=1m; C_0=100 mg/l).

In practice, the range for the chemico-osmotic efficiency is from zero to one (Mitchell, 1993). The values used for this dimensionless chemico-osmotic efficiency in this study are 0, 0.5, and 1. The HCET model simulation of solute transport is used to show the effect of coupling the chemico-osmosis driving force with the hydraulic driving force.

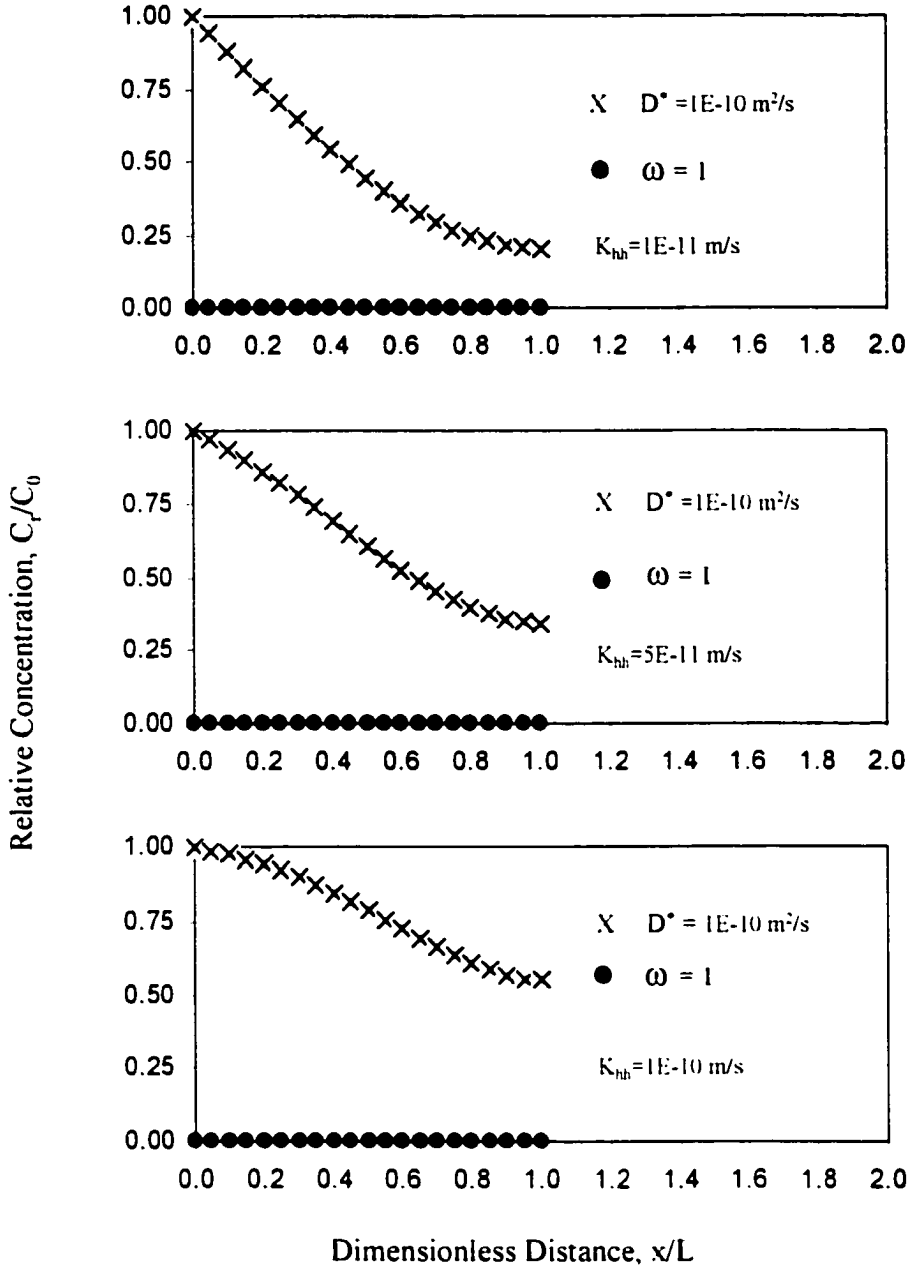

Figure 5-23: Effective diffusion coefficient for different hydraulic conductivities at fixed solute transport time 10,000 days (L=1m; C_0=100mg/l).

Figure 5-24 illustrates sensitivity of the coupled chemico-osmotic efficiency, ω, impacting the solute transport at varied transport time and at fixed hydraulic conductivity, K_{hh}=1.0 E-10 m/s. For $\omega = 0$, the contaminant transport is a function of hydraulic conductivity only. When $\omega = 0.5$, the transport of the contaminant is less than that by hydraulic conductivity alone. At $\omega = 1$, solute transport stops since the "membrane" has no solute flux through the system. Changing ω =0.0 to ω =0.5 in Figure 5-24, chemico-osmosis does no contribution much to solute transport at the time of 100 days, 1000 days, and 10,000 days. That is, for fixed hydraulic conductivity at level of 1.0 E-10 m/s, chemico-osmotic efficiency has very little impact on solute transport. When ω =1.0, the solute transport is stopped and no flux can penetrate the impermeable barrier. By considering the chemico-osmotic efficiency coupling to hydraulic conductivity on solute transport, it is not an important factor. In other words, chemico-osmotic efficiency is not a sensitive factor.

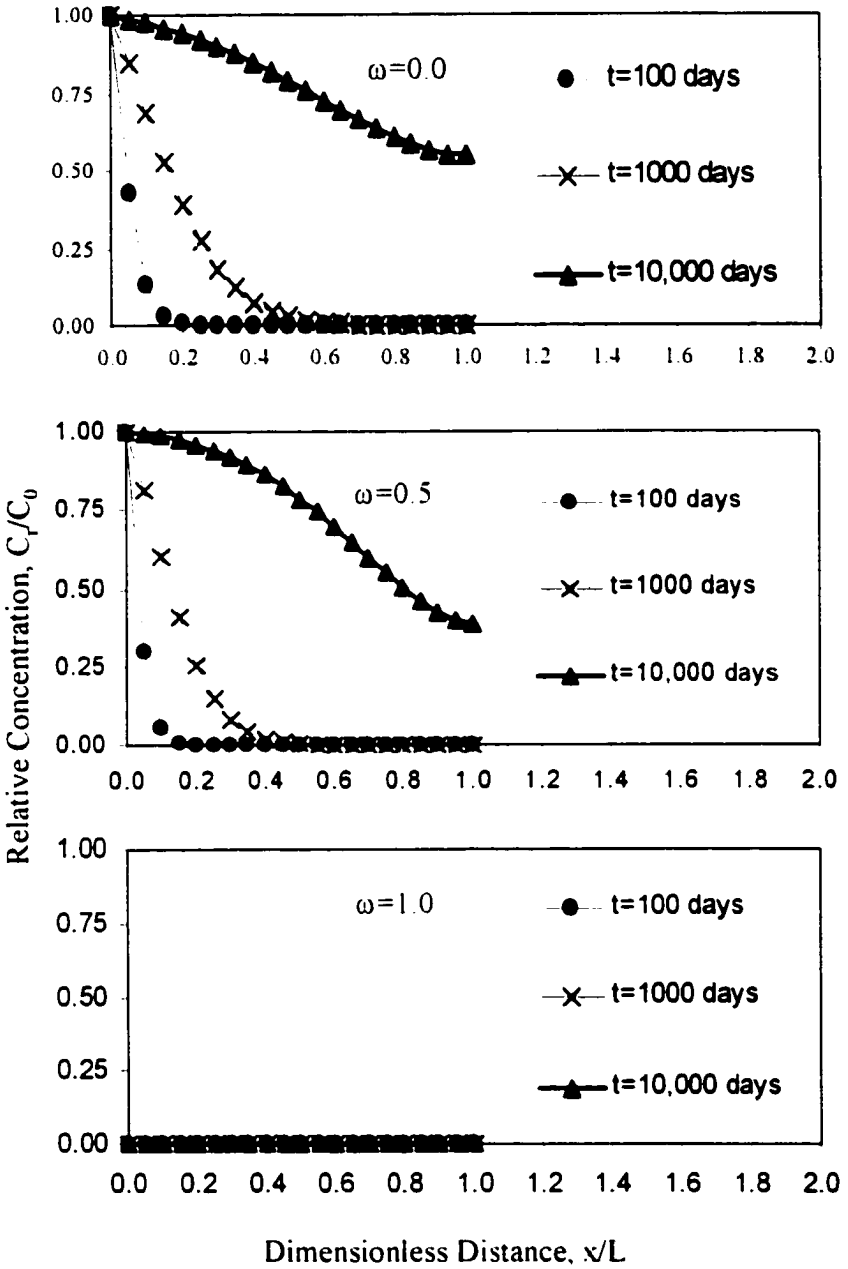

Figure 5-24: Sensitivity analysis of the coupled chemico-osmotic efficiency for different solute transport time at hydraulic conductivity of 1E-10 m/s (L=1m; C_0=100 mg/l).

Case 2.4: Sensitivity analysis of the coupled chemico-osmotic efficiency for different hydraulic conductivities at fixed solute transport time 10,000 days (L=1m; C_0=100mg/l).

Figure 5-25 illustrates sensitivity analysis of the coupled chemico-osmotic efficiency for different hydraulic conductivities at fixed solute transport time 10,000 days (L=1m; C0=100mg/l). For 10,000 days and changing ω =0.0 toω =0.5 in Figure 5-25, chemico-osmosis has no impact on solute transport at different levels of hydraulic conductivities 1E-10 m/s, and 5E-11 m/s, but has some impact on solute transport when hydraulic conductivity is 1E-11 m/s. Overall, chemico-osmotic efficiency is not a sensitive factor.

In conclusion, solute transport by the chemico-osmosis is not sensitive for clayey barriers. It is within the same order of hydraulic flow. Mitchell (1993) indicates hydraulic conductivity for clayey soil is less than 1E-10 m/sec. Since the hydraulic conductivity is low for most clayey barriers, the sensitivity of chemico-osmotic efficiency impacting on solute transport is minor.

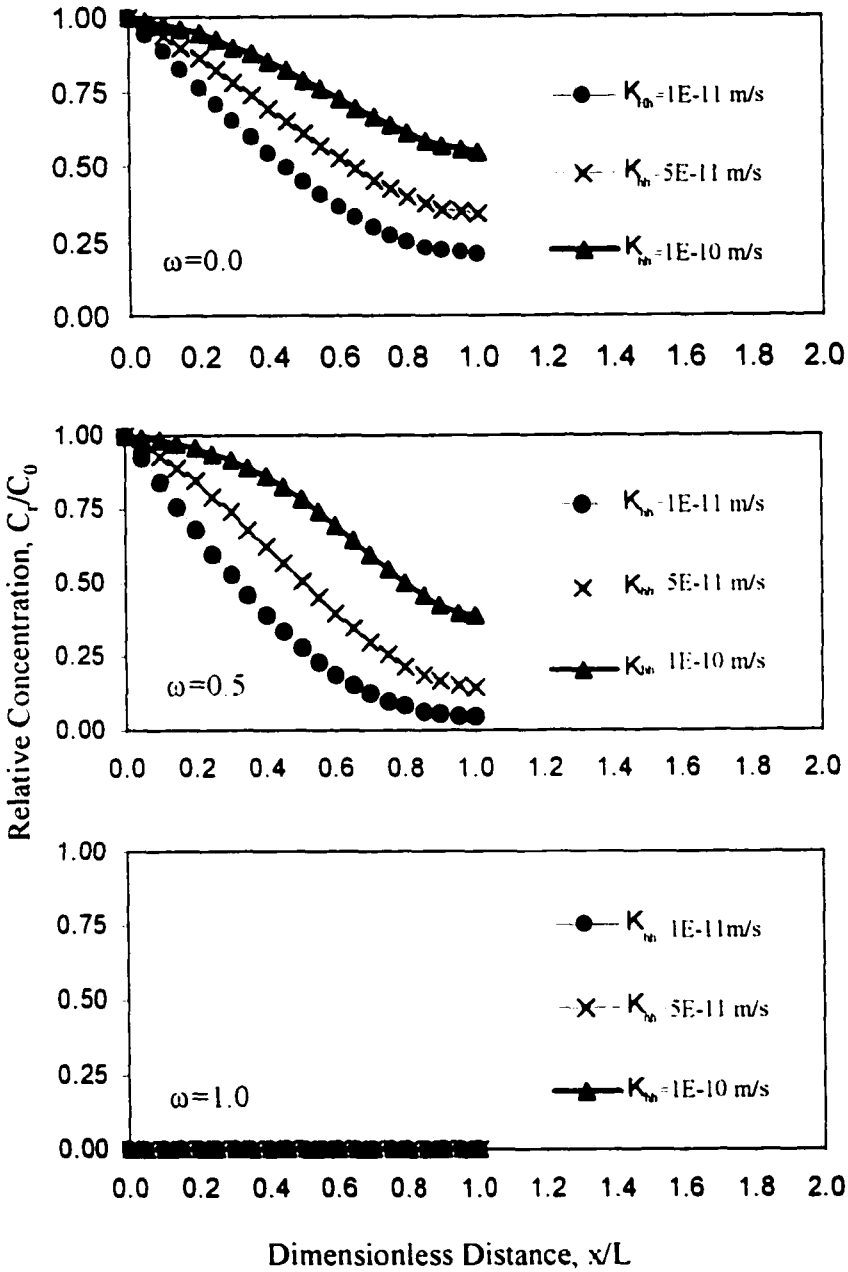

Figure 5-25: Sensitivity analysis of the coupled chemico-osmotic efficiency for different hydraulic conductivities at fixed solute transport time 10,000 days (L=1m; C_0=100mg/l).

Case 2.5: Coupled electro-osmotic conductivity for different solute remediation time at hydraulic conductivity of 1E-10 m/s (L=1m; C_0=100 mg/l).

Traditional solute transport is controlled by advection and diffusion. In this example, we examine the effect of coupling electro-osmosis flow and hydraulic driving forces on solute remediation. For this case, the governing equation 4-5 of the HCET model can be reduced to equation 5-33

$$\begin{bmatrix} K_{hh} & 0 & K_{he} \\ 0 & nD_l^* & 0 \\ 0 & 0 & \sigma_{ee} \end{bmatrix} \begin{bmatrix} h \\ C_l \\ E \end{bmatrix} + \begin{bmatrix} 0 & 0 & 0 \\ 0 & -K_{hh}\nabla h + -K_{he}\nabla E + & 0 \\ 0 & 0 & \nabla\sigma_{ee} \end{bmatrix} \begin{bmatrix} h \\ C_l \\ E \end{bmatrix} = \frac{\partial}{\partial t} \begin{bmatrix} S_s h \\ nC_l \\ C_{IP} E \end{bmatrix} \qquad [5\text{-}33]$$

Expanding equation 5-33, we have

$$K_{hh}\frac{\partial^2 h}{\partial x^2} + K_{he}\frac{\partial^2 E}{\partial x^2} = S_s\frac{\partial h}{\partial t} \qquad [5\text{-}34a]$$

$$D_l^*\frac{\partial^2 C_l}{\partial x^2} - (v - \frac{K_{he}}{n}\nabla E)\frac{\partial C_l}{\partial x} = \frac{\partial C_l}{\partial t} \qquad [5\text{-}34b]$$

$$\sigma_{ee}\frac{\partial^2 E}{\partial x^2} + \nabla\sigma_{ee} = C_{IP}\frac{\partial E}{\partial t} \qquad [5\text{-}34c]$$

We will illustrate the coupled hydraulic flow and electro-osmosis effects by HCET model simulation on solute remediation. In another point of view, we like to test sensitivity of electro-osmosis, $K_{he}\nabla E$ in equation 5-34b. Typical values used for

parameters used in modeling electro-osmotic effects on solute remediation are collected in previous Table 5-8 The practical range for electro-osmotic conductivity is from 1E-9 to 1E-8 m^2/V-s (Mitchell, 1993).

Figure 5-26 illustrates sensitivity analysis of the coupled electro-osmotic conductivity for different solute remediation time at hydraulic conductivity of 1E-10 m/s (L=1m; C_0=100 mg/l) in contaminant remediation. Changing electro-osmosis conductivities, K_{he}, electro-osmosis (with electro-osmotic conductivity K_{he}= 1E-9 $m^2V^{-1}s^{-1}$) has impact on solute remediation for time >100 days. With electro-osmotic conductivity, K_{he}= 1E-8 $m^2V^{-1}s^{-1}$, electro-osmosis has impact on solute remediation at any time level ≥ 10 days. By considering the electro-osmotic conductivity, K_{he}, coupling to hydraulic conductivity, K_{hh}, on solute remediation, electro-osmotic conductivity, K_{he} is an important factor Overall, it is a sensitive factor

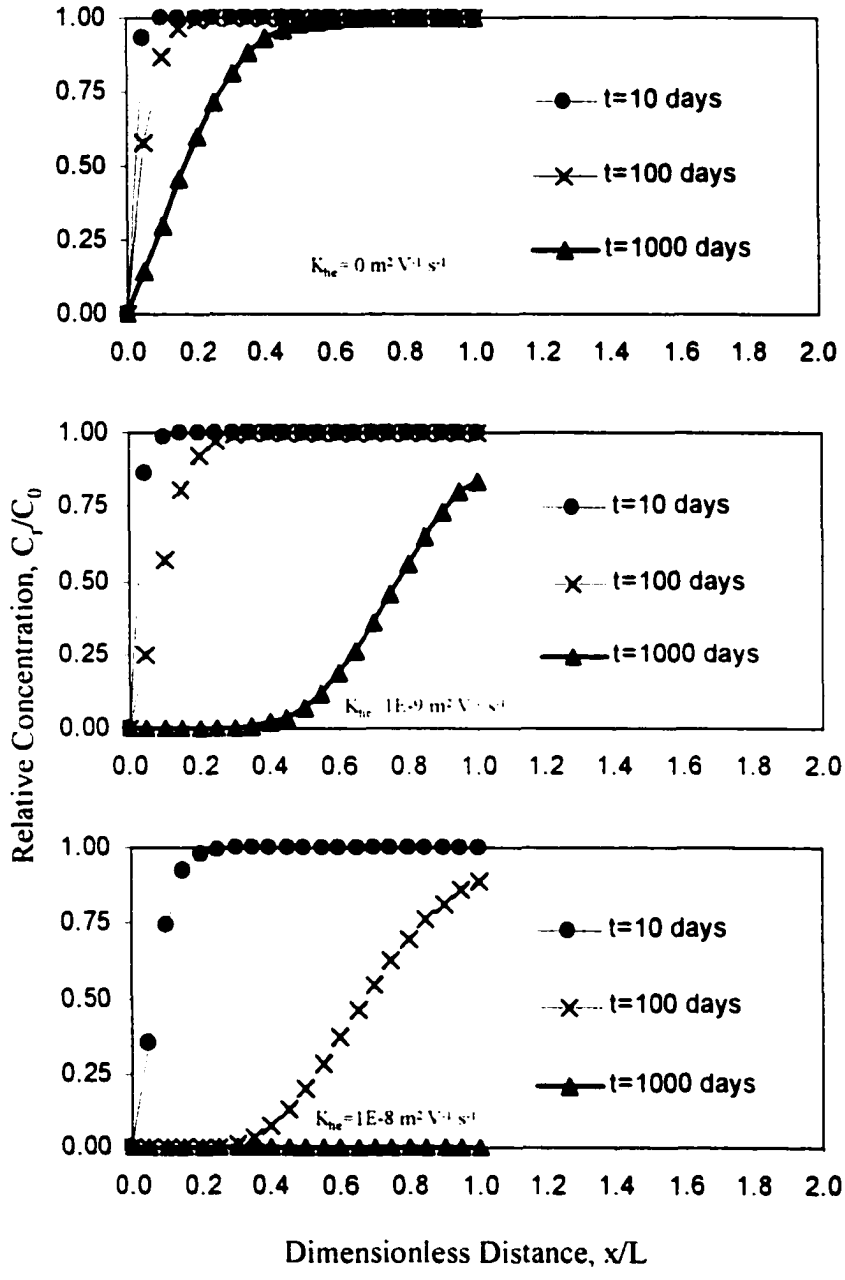

Figure 5-26: Sensitivity analysis of the coupled electro-osmotic conductivity for different solute remediation time at hydraulic conductivity of 1E-10 m/s (L=1m; C_0=100 mg/l).

Case 2.6: Coupled electro-osmotic conductivity for different hydraulic conductivities at fixed solute remediation time 1000 days (L=1m; C_0=100 mg/l).

Figure 5-27 illustrates sensitivity analysis of the coupled electro-osmotic conductivity for different hydraulic conductivities at fixed solute remediation time 1000 days (L=1m; C_0=100 mg/l). Changing electro-osmotic conductivity, K_{he} from 0.0 to 1E-9 $m^2V^{-1}s^{-1}$ in Figure 5-27, electro-osmosis does make a greater contribution on solute remediation at fixed time of 1000 days. For electro-osmotic conductivity, K_{he}= 1E-8 $m^2V^{-1}s^{-1}$, electro-osmosis flushes out all the pollutants with any hydraulic conductivities from 1E-11m/s to 1E-9 m/s. In conclusion, electro-osmotic conductivity, K_{he}, is a sensitive factor coupling to hydraulic conductivity on solute remediation at a time level of 1000 days.

Case 2.7: Coupled thermo-osmosis coefficient for different solute transport time at hydraulic conductivity of 1E-11 m/s (L=1m; C_0=1000 mg/l).

In this example, coupled effects on solute transport by thermo-osmosis and hydraulic flow will be examined. For this case, the governing equation 4-5 of the HCET model can be reduced to equation 5-35

$$\begin{bmatrix} K_{hh} & 0 & K_{ht} \\ 0 & nD_j^* & 0 \\ 0 & 0 & \lambda_{tt} \end{bmatrix} \begin{bmatrix} h \\ C_j \\ T \end{bmatrix} + \begin{bmatrix} 0 & 0 & 0 \\ 0 & +K_{hh}\nabla h \\ & +K_{ht}\nabla T & 0 \\ & & +K_{hh}\nabla h \\ 0 & 0 & +K_{ht}\nabla T \end{bmatrix} \begin{bmatrix} h \\ C_j \\ T \end{bmatrix} = \frac{\partial}{\partial t} \begin{bmatrix} S_s h \\ nC_j \\ C_{TP} T \end{bmatrix} \qquad [5\text{-}35]$$

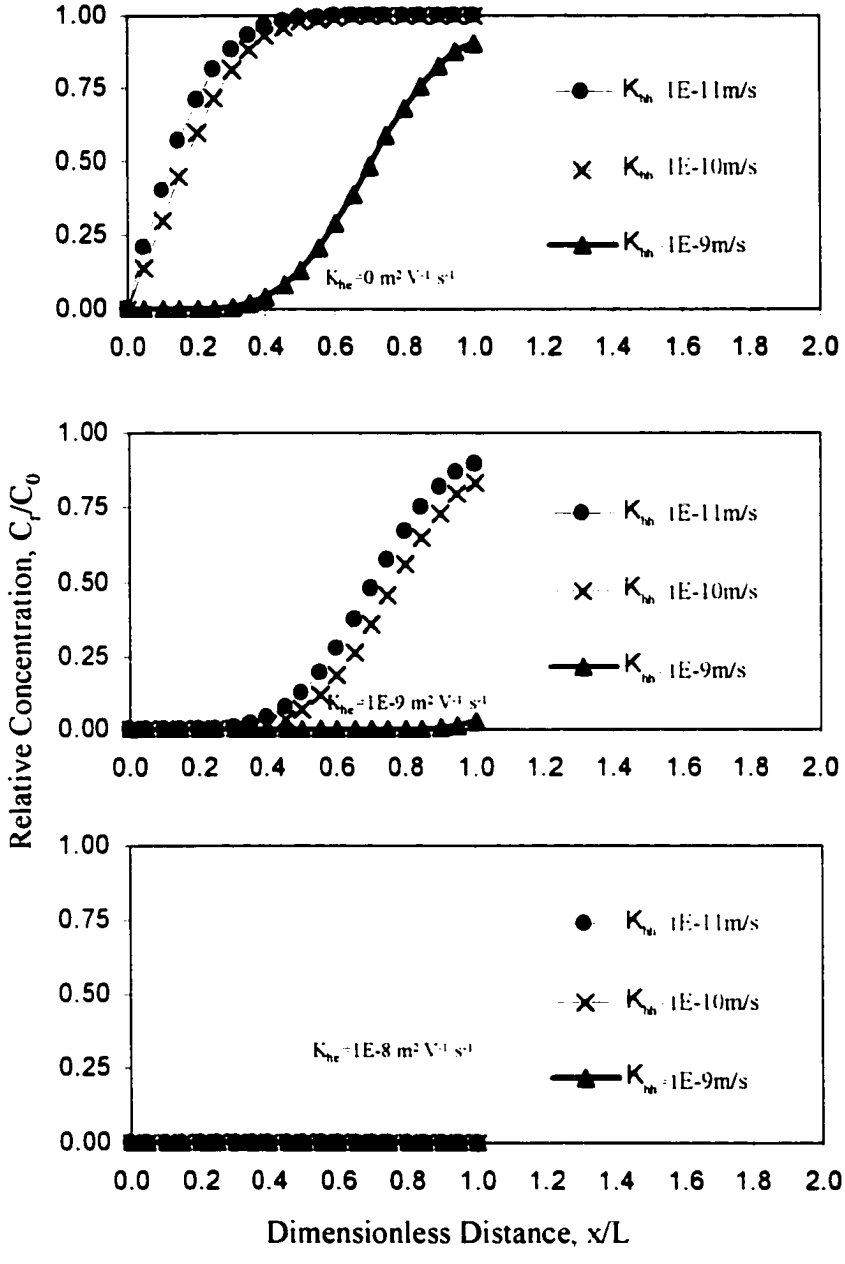

Figure 5-27: Sensitivity analysis of the coupled electro-osmotic conductivity for different hydraulic conductivities at fixed solute remediation time 1000 days (L=1m; C_0=100 mg/l).

Expanding equation 5-35, we have

$$K_{hh}\frac{\partial^2 h}{\partial x^2} + K_{ht}\frac{\partial^2 T}{\partial x^2} = S_s\frac{\partial h}{\partial t} \quad [5\text{-}36a]$$

$$D_l^*\frac{\partial^2 C_l}{\partial x^2} - (v - \frac{K_{ht}}{n}\nabla T)\frac{\partial C_l}{\partial x} = \frac{\partial C_l}{\partial t} \quad [5\text{-}36b]$$

$$\lambda_{tt}\frac{\partial^2 T}{\partial x^2} + K_{hh}\frac{\partial h}{\partial x}\frac{\partial T}{\partial x} + K_{ht}\frac{\partial T}{\partial x}\frac{\partial T}{\partial x} = C_{TP}\frac{\partial T}{\partial t} \quad [5\text{-}36c]$$

That is, we choose to test sensitivity of thermo-osmotic coefficient, K_{ht} in equation 5-35.

Column VIII in previous Table 5-8 summarizes the parameters used in modeling solute transport by coupling hydraulic flow and thermo-osmosis effects. Range of parameters for thermal conductivity, λ_{tt}, is from 0.25 to 2.5 $Wm^{-1}\,{}^{o}K^{-1}$ (Mitchell, 1993). The value used in simulation is set at 1.0 $Wm^{-1}\,{}^{o}K^{-1}$. Range of parameters for thermo-osmosis coefficient, K_{ht}, is from 1E-10 to 1E-9 $m^2K^{-1}s^{-1}$ (Dirksen, 1969). The value used in simulation is set at 0, 1E-10, or 1E-9, respectively. The source of pollutant concentration is 1000 mg/l

Figure 5-28 illustrates sensitivity analysis of the coupled thermo-osmosis coefficient for different solute transport time at hydraulic conductivity of 1E-11 m/s (L=1m; C_0=1000 mg/l). In Figure 5-28, thermo-osmosis coefficient, K_{ht}= 1E-10 $m^2K^{-1}s^{-1}$, has little impact on solute transport for time <1000 days, but has some impact for time = 10,000 days. In contrast, thermo-osmosis coefficient, K_{ht}= 1E-9 $m^2K^{-1}s^{-1}$, has strong impact on solute transport for any time level > 100 days. By

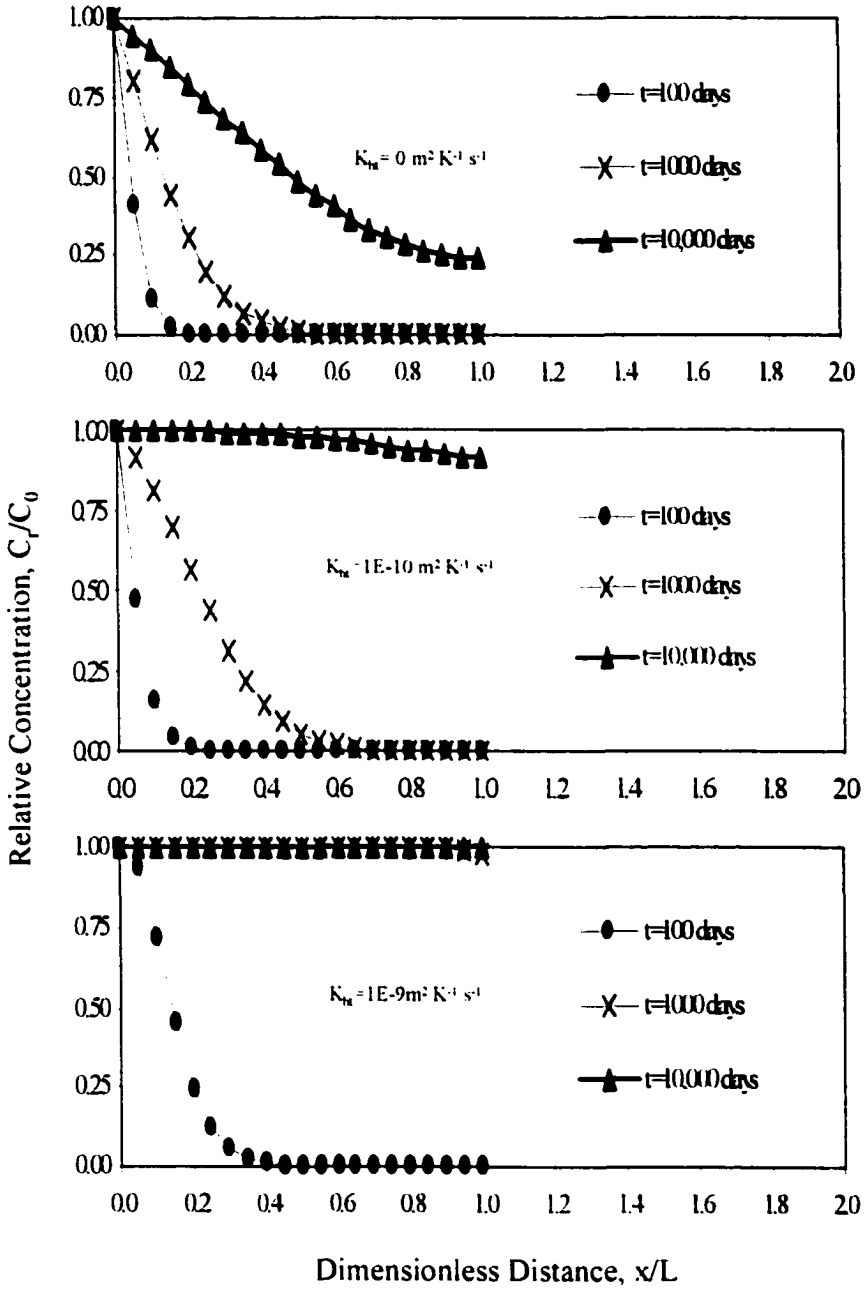

Figure 5-28: Sensitivity analysis of the coupled thermo-osmosis coefficient for different solute transport time at hydraulic conductivity of 1E-11 m/s (L=1m; C_0=1000 mg/l).

considering the thermo-osmosis coupling to hydraulic flow in solute transport, thermo-osmosis coefficient, K_{ht} is an important factor. Overall, it is a sensitive factor.

Case 2.8: Coupled thermo-osmosis coefficient for different hydraulic conductivities at fixed solute transport time 10,000 days (L=1m; C_0=1000 mg/l).

Figure 5-29 illustrates sensitivity analysis of the coupled thermo-osmosis coefficient for different hydraulic conductivities at fixed solute transport time of 10,000 days (L=1m; C_0=1000 mg/l). Changing thermo-osmosis coefficient, K_{ht} from 0.0 to 1E-9 $m^2K^{-1}s^{-1}$ in Figure 5-29, thermo-osmosis does make a greater contribution on solute transport at fixed time of 10,000 days for given ranges of hydraulic conductivities, K_{hh}, form 1E-11 m/s to 1E-9 m/s. In other words, coupled thermo-osmosis flushes out all the pollutants with any hydraulic conductivities from 1E-11m/s to 1E-9 m/s. In conclusion, thermo-osmotic coefficient, K_{ht}, is a sensitive factor coupling to hydraulic conductivity on solute transport at a time level of 10,000days.

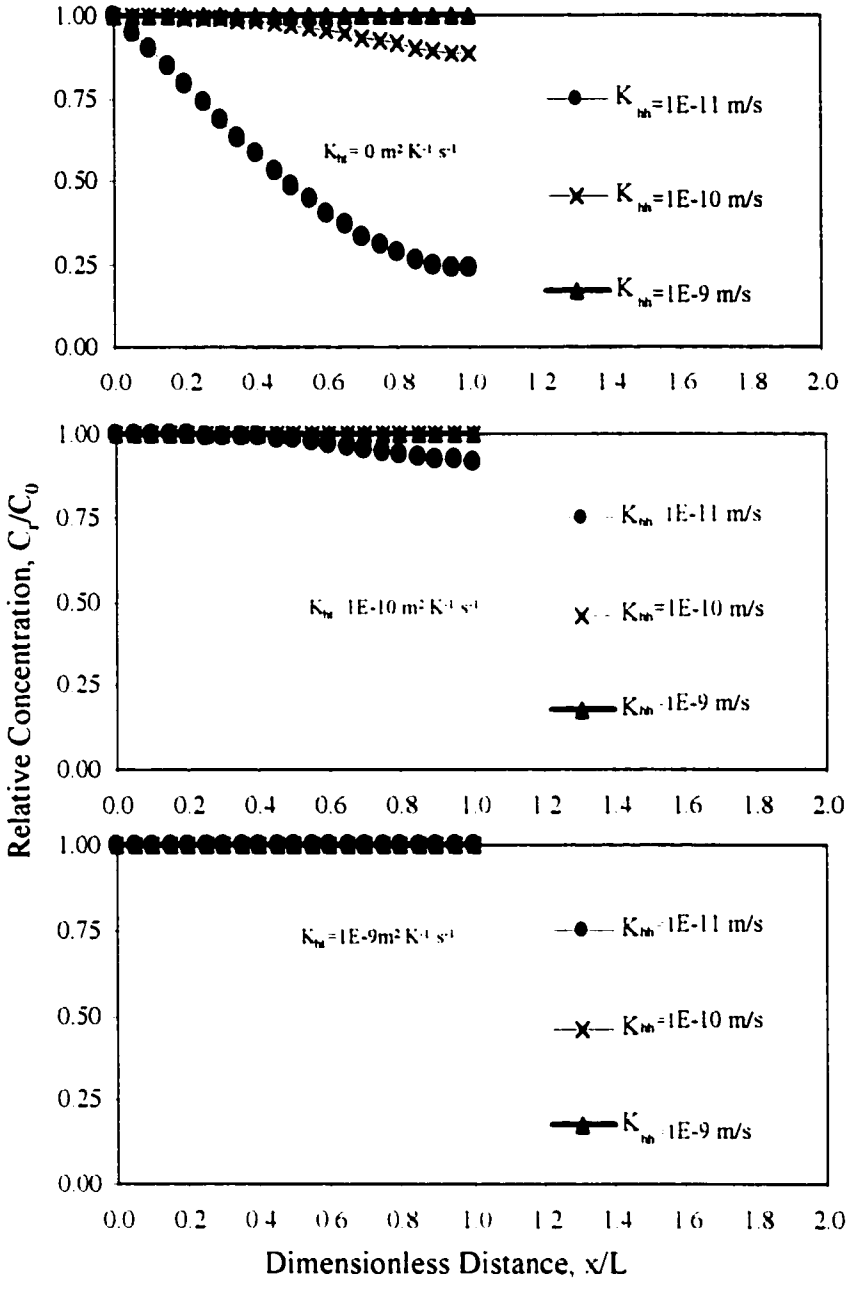

Figure 5-29: Sensitivity analysis of the coupled thermo-osmosis coefficient for different hydraulic conductivities at fixed solute transport time 10,000 days (L=1m; C_0=1000 mg/l).

Case 2.9: Contaminant transport from a nuclear waste repository.

In this example, we show the capability of the HCET model to simulate the relative importance of advection, diffusion, and thermo-osmosis for solute transport from a nuclear waste repository. Table 5-10 lists the material properties used in the simulation. Material properties used for a nuclear waste repository are not necessary the same as they are for clay liners and covers in practice. In nuclear waste repository, we are looking for material with lower values of effective diffusion coefficient and hydraulic conductivity.

Figure 5-30 illustrates the results for advection only (A), advection plus diffusion (A+D), and advection plus diffusion plus thermo-osmosis (A+D+T) for 100, 500, and 1000 years simulations (L=20 m, hydraulic conductivity, K_{hh}=1E-12 m/s, effective diffusion coefficient, D^* = 1E-11m^2/s, and thermo-osmosis coefficient, K_{ht} = 2E-10 $m^2K^{-1}s^{-1}$). For advection alone, the solute does not move far because of low hydraulic conductivity. However, after coupling diffusion and thermo-osmosis, solute transport is much greater than for advection alone.

Figure 5-31 is similar to Figure 5-30 except for changing the hydraulic conductivity, K_{hh} from 1E-12 m/s to 1E-11 m/s. Even this factor of ten change, the solute transport by advection is minimal, but is relative important by diffusion and thermo-osmosis.

Table 5-10. Material properties for contaminant transport from a nuclear waste repository.

Parameter	Symbol	Units	Reported values	Used values	References
Hydraulic conductivity	K_{hh}	m / s	<1E-11	1E-11/1E-12	Soler (1999)
Effective diffusion coefficient	D_i^*	m^2 / s	1E-12 -1E-11 2.8E-14 - 1.4 E-12	1E-11	Li and Gregory (1974); Sato et. al. (1997)
Thermal conductivity	λ_{tt}	$Wm^{-1}K^{-1}$	0.25 - 2.5	1.0	Mitchell (1993)
Osmotic efficiency coefficient	ω	dimensionless	0.0 - 1.0	0.0	Mitchell (1993)
Thermal osmosis coefficient	K_{ht}	$m^2K^{-1}s^{-1}$	2E-10 for Kaolinite	2E-10	Srivastava and Avasthi (1975)
Porosity	n	dimensionless	0.1-0.7	0.5	Mitchell (1993)

Notes: $h(0, t) = 1m$; $h(L, t) = 0$ m; $h(x, 0) = 0$ m; $C(0, t) = 1000$ mg/l; $\frac{C(L, t)}{\partial x} = 0$; $C(x, 0) = 0$; $T(0, t) = 25\ ^0C$; $T(L, t) = 20\ ^0C$; $T(x, 0) = 0\ ^0C$; $D^*_{cho} = 0$; $D^*_{cto} = \lambda_{ct} = 0$; $\lambda_{th} = 0$; $\lambda_{cto} = 0$; $C_{TP} = 0$; $S_s = 0$.

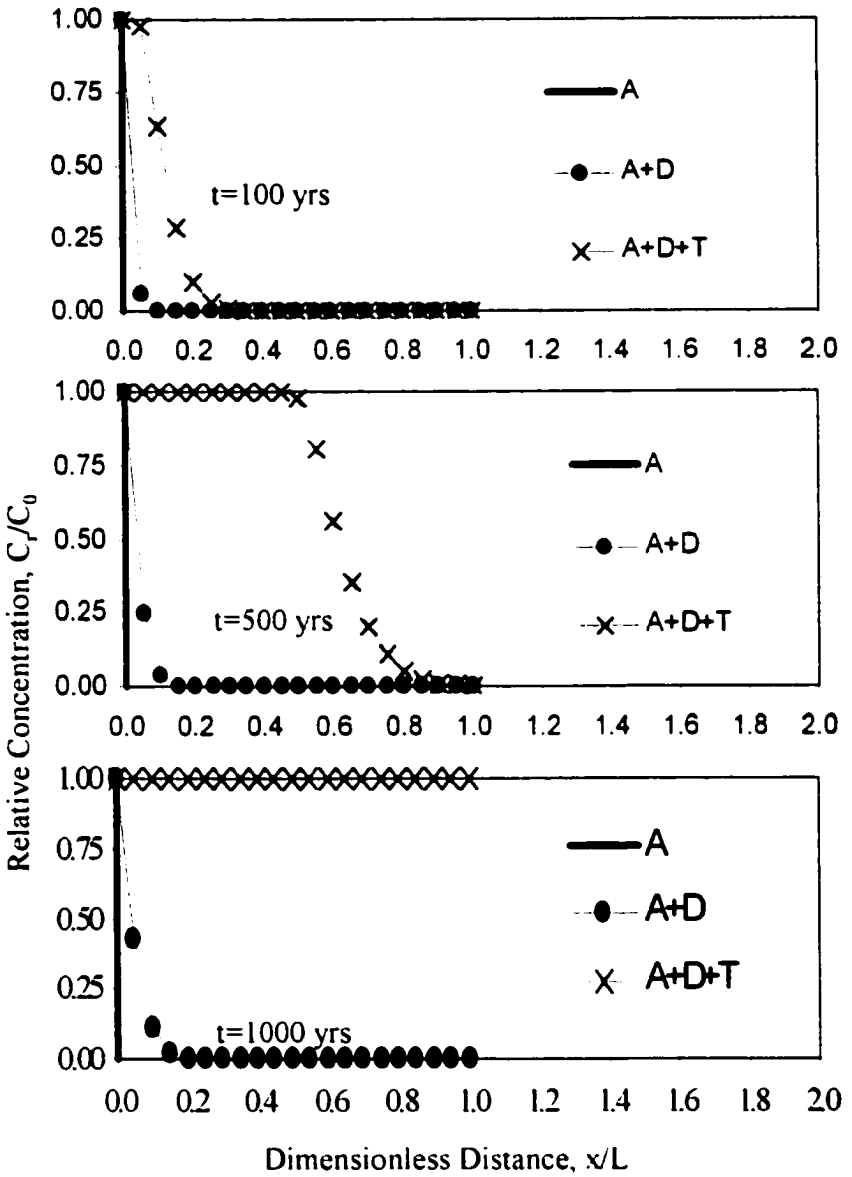

Figure 5-30: The results for advection only (A), advection plus diffusion (A+D), and advection plus diffusion plus thermal osmosis (A+D+T) for 100, 500, and 1000 years simulations (L=20 m, hydraulic conductivity, K_{hh}=1E-12 m/s, effective diffusion coefficient, D* = 1E-11m^2/s, and thermal osmosis coefficient, K_{ht} = 2E-10 $m^2K^{-1}s^{-1}$).

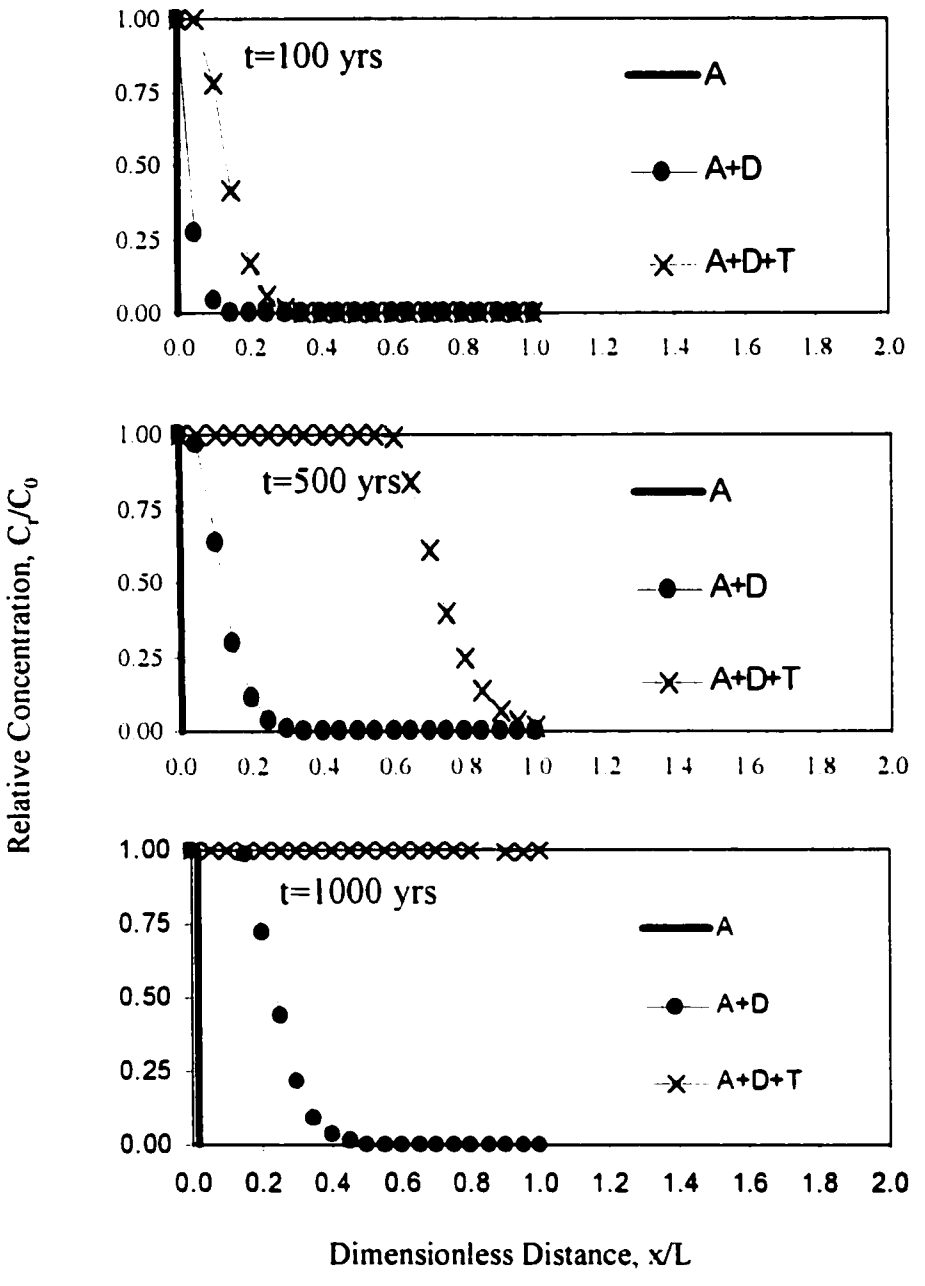

Figure 5-31: The results for advection only (A), advection plus diffusion (A+D), and advection plus diffusion plus thermal osmosis (A+D+T) for 100, 500, and 1000 years simulations (L=20 m, hydraulic conductivity, K_{hh}=1E-11 m/s, effective diffusion coefficient, D* = 1E-11m^2/s, and thermal osmosis coefficient, K_{ht} = 2E-10 $m^2K^{-1}s^{-1}$).

CHAPTER 6

SUMMARY, CONCLUSIONS, AND FUTURE STUDIES

6.1 SUMMARY

A finite element (HCET) model for coupled transport processes has been developed and validated using previous published analytical model and experimental results. The development of the model represents the first attempt to model general forms of coupling transport processes. The HCET model can be used as a tool for the evaluation and decision-making on environmental studies.

Chapter two of this study includes a literature review on dynamic irreversible thermodynamics coupling of flow processes. A new interpretation of irreversible thermodynamics applied to fine-gained soil barriers and clay-liner designs for applications in the field of environmental engineering also is presented.

Chapter three presents a mathematical development of the governing equations in general matrix form to deal with coupling transport processes. The adequacy of the model is demonstrated in terms of liquid flow, solute transport, electric migration, and heat transport. The model also accounts for coupling effects that have frequently been ignored in the past in fine-gained soil designs and applications, such as chemico-osmosis, electro-osmosis, and thermo-osmosis.

Chapter four in this research presents the finite element formulation. The space discrete, time discrete, and boundary and initial conditions to program the governing equations for general form of coupling transport processes are described.

Chapter five presents an evaluation of the HCET model. Simulations using the HCET model are compared with several examples of analytical solutions, other numerical solutions, and available experimental data. The comparisons showed that the HECT model is in well agreement with cases studied. The HCET model also showed sensitivity study on several coupled transport processes cases.

Appendixes A, B, and C of this study are the program structure (main program and subroutines), the user's guide, and the HCET model source code. The readers should be able to run the program following the explanation in these appendixes. Each subroutine is in a modular design such that it is easy to adopt the program for general use and for future improvement without too much modification.

6.2 CONCLUSIONS

There are advantages of the HCET model such as:

- The model is capable of handling transport cases from single variable to four-variable driving forces. It is also demonstrated that the program is able to fit previously collected experimental data. It is not limited to the specific cases presented; it can explore coupled chemo-osmosis, electro-osmosis, and thermo-osmosis analyses not considered by previous workers.
- Model offers opportunities to treat nonlinear properties of soils. The nonlinearity is difficult to handle in the field of electrokinetic remediation and has been

neglected by previous workers. The nonlinear approach is to impose a Pica iteration. Nonlinear solutions by the Pica method are not found in previous electrokinetic numerical modeling.

- Matrix form for the model allows simultaneously solutions for multiple variables of the coupled transport processes. The algorithm has benefits such as 1) ability to save iteration times required to reach a final solution for a specific case, and 2) ability to include thermal effects in electrokinetic phenomena, which most workers would like to do, but have not done so in previous studies.
- Model provides economic and efficient means for evaluation and decision-making for fined-grained soil barrier applications in geoenvironmental engineering.

In addition to the assumptions described in Chapter I, the HCET model has limitations:

- The flow rate under investigation is limited to Peclet number in the range $1 \leq P_L \leq 20$, which is applied to fined-grained soils with diffusion is the dominant transport relative to advection transport and numerical dispersion by high flow rate advection can be neglected for solute transport. Beyond a Peclet value of 20, contaminant transport will be dominated by advection and numerical dispersion or instability may occur.
- Boundary conditions, initial condition, and parameters used in numerical simulation are focused on fine-grained soil applications, which may not be applied directly to other situations without further study.
- When coupled with hydraulic flow for solute transport, the chemico-osmosis is not an important factor for the cases studied, but the electro-osmosis and thermo-

osmosis are important factors. The conclusions drawn from this research are based upon the specific simulations studied and may not be applied to other situations without further study.

The model is a basic working tool that may be used by the regulation agencies, mining companies, industrial waste project consultants, electrokinetic's remediation, and others concerned with groundwater restoration. Especially, it is able to study the main effects and their co-effects of coupled transport processes. It opens a new point of view to the study of irreversible thermodynamics coupled processes in a more general form in the field of clay barrier/liner applications.

6.3 FUTURE STUDIES

Several topics explored during the research are presented herein for future studies:

- **Interdependency of on site parameter measurements.**

The parameters used in this model are picked up from literature reviews. Real parameters are also site sensitive. There are limit field data available for discussion since the coupling transport processes are complicated and measurements of parameters are too much time consumed in the field of fine-grained soil application. Two ways to get further study of these on site parameters measurements of coupled transport processes are by experimental design, and by basic fluid and soil properties calculations. The experimental design is recommended for the measurement of phenomenological parameters. For example, a fractional factorial experimental design to decide the phenomenological coefficients is well developed in the field of

statistics. Interested readers may start with statistical point of view to construct an experimental design to measure the on site parameters. The other way starts with basic fluid and soil properties to select the transport parameters/coefficients.

- **Nonlinearity studies.**

Some reports have indicated that the thermodynamic coefficients for the clay barriers are not constant during experimental measurements (Hueckel etc., 1987, and Hsu, 1996). These may be the thermal changes in the water-solid interaction that affects clay behavior. The HCET model does construct the non-linear algorithm by Pica iteration. Interested readers may count the non-linearity properties providing an empirical formula and modifying the subroutines of the HCET model to run output comparison with test results. Material non-linear properties may be temperature dependent. It requires further studies.

- **Reactive chemical transport.**

The HCET model is focused on solving the coupled transport processes and is not on reactive chemical system. Since most chemical transport involves multi-components, the need exists to incorporate reactive chemical transport accounting all significant chemical interactions and processes. To enhance the HCET model capacity in accounting reactive chemical transport, a pre-screen on candidate reaction models has been reviewed, but is not present in this research. These are MINTEQ, HYDROGEOCHEM, and GEOCHEM models. The MINTEQ model is a reactive chemical model. It is well document and extensively used by the Environmental Protection Agency on the general evaluation of most groundwater transport (Leopper etc., 1995). Yeh and Tripathi (1990) wrote the HYDROGEOCHEM model. It is a

coupled model of hydrologic transport and geochemical equlibria in reactive multi-component mentioned in the most numerical groundwater modeling (Nelson etc., 1998). Afifi developed the GEOCHEM model in 1994. It is a short, simple version of HYDROGEOCHEM model. GEOCHEM program is available at the computer lab provided by the Groundwater Engineering, Civil Engineering Department at the Colorado Sate University. The interested users may save some time on developing reactive capability by including one of these reactive chemical models to enhance the HCET model in the near future.

- **A friendly interface.**

Although the HCET model is capable of testing the coupled transport processes, much can still be done to enhance the capabilities of this model. Two suggestions to improve this model's friendly interface are: 1) more efforts to provide a two dimensional, or three-dimensional algorithm to have a visual view of the point of interested studies, and 2) a post processor for the model to visualize graphically the output files.

APPENDIX A

PROGRAM STRUCTURE

The HCET code is written in Fortran 90 in a modular form. It contains a main program and 14 subroutines. Each subroutine can be complied separately. This facilitates reading the program and allows the user to make changes or replace entire modules (Press, etc., 1992).

A.1 MAIN PROGRAM

A flow chart of the main program for the HCET model is illustrated in Figure A-1. The main program specifies the sizes of all arrays, reads input data, assembles matrices, calls each subroutine to execute its specified function, and solve the governing equations. The program includes 4 loops to complete the numerical calculation. The outer loop is a time step to perform dynamic computation. The second loop is the pica iteration to judge the criteria for nonlinear convergence. The third loop is written to obtain global matrix by computing each finite element assembling. The fourth is a variable specified loop to enable the program to handle a simple variable flow process to a more complicated four-variable coupled flow problem. The function of each subroutine is described below.

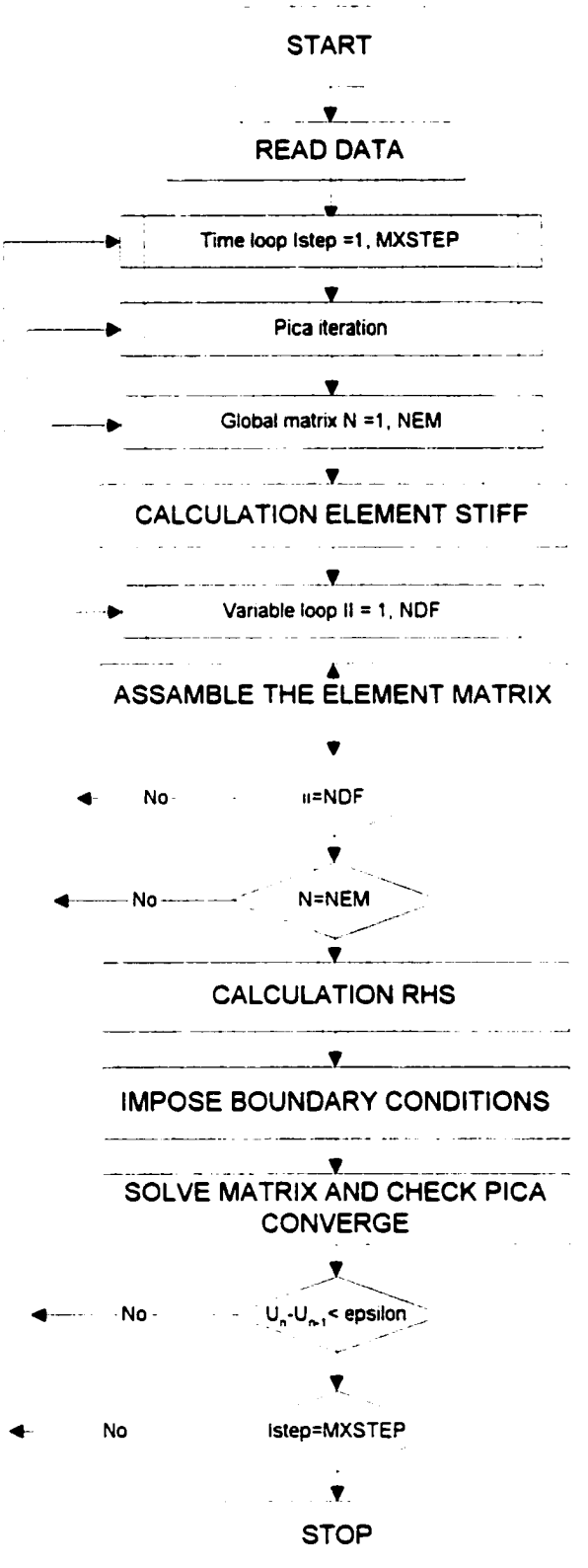

Figure A-1: Flow chart for the main program.

A.2 SUBROUTINES

A.2.1 Subroutine NODES

The subroutine NODES inputs the node numbers and coordinates for each node in finite element mesh. It will generalize missing node numbers and coordinates for given domain and returns to the main program for use by other subroutines. It can be used to simplify data input. Node numbers for missing nodes are generated by adding the node number increment to the node number for the proceeding node. Coordinates for missing nodes are computed by the subroutine using linear interpolation. To terminate input, place a -1 in all fields of the input file.

Called from: MIAN PROGRAM

Subroutine called: none

A.2.2 Subroutine ELEMENT

The purpose of subroutine element is to generate node connectivity for assembly of finite elements. It reads number of element and node per element, and then the node connectivity is generated. It passes the node array back to the main program for the usage by other subroutines. . To terminate input, place a -1 in all fields of the input file.

Called from: MAIN PROGRAM

Subroutine called: none

A.2.3 Subroutine MATERL

Subroutine MATERL is used to input element material set numbers and material properties for each material set. The input data are from the user-defined file called kctest.dat, and output file to kctest.out. Data are read in sequentially (one element number, and material set number per line). To terminate input, place a -1 in all fields of

the input file. Material set numbers for missing elements are auto-generated by assigning the material set number of the proceeding element to each missing element. The program then reads the number of material set properties in each material set, and calls the subroutine COEF to recalculate the coefficient matrix for later usage by the main program.

Called from: MAIN PROGRAM

Subroutine called: COEF

A.2.4 Subroutine COEF

Subroutine COEF recalculates the coefficient matrix. It coverts the input thermodynamic properties to the form of calculation used by the HCET model. The initial guessed value of temperature and concentration of governing equations is set herein. It is suggested that thermodynamic properties be calculated in this subroutine if they are not read from the input file or if they are to be generated by certain function.

Called from: MATERL

Subroutine called: none

A.2.5 Subroutine COEIR

Subroutine COEIR recalculates the coefficient matrix during pica iteration.

Called from: MAIN PROGRAM

Subroutine called: none

A.2.6 Subroutine INITIAL

Subroutine INITIAL inputs control parameters and initial conditions needed to solve transient coupling transport processes problems. All data are read from the user-supplied file as KCTEST.dat. The relaxation factor ALPHA, and converge criteria EPS

are read first. Second, a list of time steps and time intervals are read. Third, a list of times and values of the time function for each time are read. Finally, the initial values of the field variables for each node are read. Read data are terminated by placing a -1 in all fields of these records at the end. Output data are assigned to the file as KCTEST.out.

Called from: MAIN PROGRAM

Subroutine called: none

A.2.7 Subroutine ELKBAR2

The purpose of the subroutine ELKBAR2 is to compute the element conductance matrix for a one-dimensional, linear bar element.

Called from: MAIN PROGRAM

Subroutine called: none

A.2.8 Subroutine CBAR2

The purpose of the subroutine CBAR2 is to compute the element capacitance matrix for a one-dimensional, linear bar element. The mass lumped formulation is used to compute the capacitance of two-node elements.

Called from: MAIN PROGRAM

Subroutine called: none

A.2.9 Subroutine ADVV

The purpose of the subroutine ADVV is to compute the element advective matrix for the coupling equation 4-1 defined in Chapter IV.

Called from: MAIN PROGRAM

Subroutine called: none

A.2.10 Subroutine CNVEC

The purpose of the subroutine CNVEC is to reoder the element nodes for the multivariable problems for the advection terms of the coupling transport processes. This will reduce the half-bandwith of the assembled coefficient matrix (Reddy, 1993).

Called from: MAIN PROGRAM

Subroutine called: none

A.2.11 Subroutine RHSIDE

Subroutine RHSIDE assembles the right hand side vector for coupled transport processes problems. For each time step, the right hand side vector is computed using the values of variables for the previous time step, the assembled global conduction and capacitance matrix, relation factor, and the time interval for that time step which are compute at the main program. Then, it adds the given flux if specified.

Called from: MAIN PROGRAM

Subroutine called: none

A.2.12 Subroutine BOUNDC

Subroutine BOUNDC input three kinds of boundary conditions for the coupled transport processes problems. They are specified fixed values of field variables (Dirichlet type), flux kind of variables (Neumann type), and mixed boundary conditions (Cauchy conditions). If any type of boundary condition is not zero, the subroutine will impose them onto the governing equations.

Called from: MAIN PROGRAM

Subroutine called: none

A.2.13 Subroutine LUDCMP and Subroutine LUBKSB

Subroutine LUDCMP is used in combination with LUBKSB to solve governing equations. The LUDCMP subroutine decomposes a given matrix, and the LUBSK subroutine backward substitutes the unknown variables and store the solution vector. They are taken from the book of numerical recipes (Press etc., 1992).

Called from: MAIN PROGRAM

Subroutine called: none

APPENDIX B

USER'S GUIDE

B.1 RUNNING THE PROGRAM

The HCET model code is written in Fortran language. The program was developed and debugged on Pentium I PC's using Fortran 90 compiler developed by Microsoft PowerStation Professional Development System 4.0. Before running the program, users should define the work project to include all subroutines and provide the input data file named as KCTEST.dat.

B.2 INPUT DATA (KCTEST.DAT) AND OUTPUT DATA (KCTEST.OUT)

The input data listed here is the example to simulate the one-dimensional transient flow equation. Table B-1 is the input data file. Table B-2 describes the input file in more details. Table B-3 is the output data file. To run the example using the HCET model, the readers may follow each record description from these Tables. These input files must be placed in the same directory as main program. The program permits all data to be provided in free format.

Table B-1. Input data file for one-dimensional transient flow equation.

```
1        1        0
1        1        100
21       2        0
0        100
1
1
20
1
-1
1        6        0.1
1.0      0.001
100   1
-1
0.0      1.0
1.0      1.0
100.0    1.0
-1       -1
0.0
0.0
0.0
0.0
0.0
0.0
0.0
0.0
0.0
0.0
0.0
0.0
0.0
0.0
0.0
0.0
0.0
0.0
0.0
0.0
0.0
```

```
PARAMETER (NEM=20,NNM=21,NEQ=21,NSIZE=2,NDF=1,
     *        MXEBC=8,MXNBC=8,MNDT=200)
```

Table B-2. Description of input file for one-dimensional transient flow equation.

Record	Type	Symbol	Description
1	Int	NSPDF	Number of specified primary degree of freedom
1	Int	NSSDF	Number of specified secondary degree of freedom
1	Int	NNBC	Number of Newton mixed boundary conditions
2	Int	ISPDF (I,1)	= global node of the Ith boundary condition
2	Int	ISPDF (I,2)	= degree of freedom specified at the global node.
2	Real	VSPDF	Value of specified primary degree of freedom
3			Continue as record row 2
4	Real	X_o	Element coordination at inlet
4	Real	X_L	Element coordination at outlet
5	Int	ELM	Element number
6	Int	MATSET	Material set number
7-8			Continue as record row 5, and 6
9	Int	-1	End of reading data
10	Int	SETNUM	Sub-material set number
10	Real	PROP (1,1,1)	K_{hh} = the coefficient of hydraulic conductivity (m sec^{-1})
10	Real	PROP(1.1.2)	S_s = the specific storage of the porous medium (m^{-1})

11	Real	ALPHA	Relaxation factor
11	Real	EPS	Prescribed tolerance
12	Real	DTSTEP	Number of time steps
12	Real	DELTAT	Size of time step
13		-1	End of reading data
14	Real	TIME	Specified time
14	Real	GT	Value of time function at time t
15-16			Continue as record row 14
17		-1, -1	End of reading data
18	Real	AINI	(I,1) = Initial condition of hydraulic head
19-38			Continue as row 18

Table B-3. Sample of output data.

```
          1           1           1           0

  ELEMENT
    NO.          MATERIAL SET NUMBER
  -------        -------------------
     1                    1
     2                    1
     3                    1
     4                    1
     5                    1
     6                    1
     7                    1
     8                    1
     9                    1
    10                    1
    11                    1
    12                    1
    13                    1
    14                    1
    15                    1
    16                    1
    17                    1
    18                    1
    19                    1
    20                    1
  MATERIAL
   SET NO.              MATERIAL PROPERTIES
  ---------             -------------------
      1               6.000000        .100000
CoeF                  6.000000        .100000
CoeF                  6.000000        .100000
CoeF                  6.000000        .100000
CoeF                  6.000000        .100000
CoeF                  6.000000        .100000
CoeF                  6.000000        .100000
CoeF                  6.000000        .100000
CoeF                  6.000000        .100000
CoeF                  6.000000        .100000
CoeF                  6.000000        .100000
CoeF                  6.000000        .100000
CoeF                  6.000000        .100000
CoeF                  6.000000        .100000
CoeF                  6.000000        .100000
CoeF                  6.000000        .100000
CoeF                  6.000000        .100000
CoeF                  6.000000        .100000
CoeF                  6.000000        .100000
CoeF                  6.000000        .100000

  ALPHA =   1.0000   EPS=   .0010
  START         END           DELTA T
  -----        -----         -----------
     1          100            1.0000
```

```
          TOTAL TIME =       100.0000

        TIME T            G(T)
       --------          ------
         1.0000          1.0000
       100.0000          1.0000
      100.000000
ISTEP=           1MXSTEP=        100

   1.2000 -1.2000
  -1.2000  1.2000
   .250  .000
   .000  .250
   .000  .000
   .000  .000
   1.2000 -1.2000
  -1.2000  1.2000
   .250  .000
   .000  .250
   .000  .000
   .000  .000

 TSUM=       1.000000  Iter=1 if call rhs          1
 emorU(I)B(I)        1    7.629395E-06    100.000000    100.000000
 emorU(I)B(I)        2       53.004920  0.000000E+00     53.004920
 emorU(I)B(I)        3       53.004920  0.000000E+00     28.095210
 emorU(I)B(I)        4       53.004920  0.000000E+00     14.891840
 emorU(I)B(I)        5       53.004920  0.000000E+00      7.893408
 emorU(I)B(I)        6       53.004920  0.000000E+00      4.183894
 emorU(I)B(I)        7       53.004920  0.000000E+00      2.217669
 emorU(I)B(I)        8       53.004920  0.000000E+00      1.175474
 emorU(I)B(I)        9       53.004920  0.000000E+00  6.230590E-01
 emorU(I)B(I)       10       53.004920  0.000000E+00  3.302521E-01
 emorU(I)B(I)       11       53.004920  0.000000E+00  1.750502E-01
 emorU(I)B(I)       12       53.004920  0.000000E+00  9.278595E-02
 emorU(I)B(I)       13       53.004920  0.000000E+00  4.918249E-02
 emorU(I)B(I)       14       53.004920  0.000000E+00  2.607173E-02
 emorU(I)B(I)       15       53.004920  0.000000E+00  1.382419E-02
 emorU(I)B(I)       16       53.004920  0.000000E+00  7.336716E-03
 emorU(I)B(I)       17       53.004920  0.000000E+00  3.906212E-03
 emorU(I)B(I)       18       53.004920  0.000000E+00  2.103296E-03
 emorU(I)B(I)       19       53.004920  0.000000E+00  1.176753E-03
 emorU(I)B(I)       20       53.004920  0.000000E+00  7.405246E-04
 emorU(I)B(I)       21       53.004920  0.000000E+00  6.128480E-04

 emor B-old Bnew          1    0.000000E+00       100.000000
100.000000
 emor B-old Bnew          2    0.000000E+00        97.701590
97.701590
 emor B-old Bnew          3    0.000000E+00        95.417340
95.417340
 emor B-old Bnew          4    0.000000E+00        93.161350
93.161350
 emor B-old Bnew          5    0.000000E+00        90.947540
90.947540
```

```
 emor B-old Bnew          6     0.000000E+00       88.789540
88.789540
 emor B-old Bnew          7     0.000000E+00       86.700650
86.700650
 emor B-old Bnew          8     0.000000E+00       84.693770
84.693770
 emor B-old Bnew          9     0.000000E+00       82.781270
82.781270
 emor B-old Bnew         10     0.000000E+00       80.974930
80.974930
 emor B-old Bnew         11     0.000000E+00       79.285900
79.285900
 emor B-old Bnew         12     0.000000E+00       77.724590
77.724590
 emor B-old Bnew         13     0.000000E+00       76.300610
76.300610
 emor B-old Bnew         14     0.000000E+00       75.022750
75.022750
 emor B-old Bnew         15     0.000000E+00       73.898900
73.898900
 emor B-old Bnew         16     0.000000E+00       72.935960
72.935960
 emor B-old Bnew         17     0.000000E+00       72.139870
72.139870
 emor B-old Bnew         18     0.000000E+00       71.515540
71.515540
 emor B-old Bnew         19     0.000000E+00       71.066820
71.066820
 emor B-old Bnew         20     0.000000E+00       70.796470
70.796470
 emor B-old Bnew         21     0.000000E+00       70.706170
70.706170
 converge now goto new time step
 TSUM before converge=     100.000000converge at Iter=          2

      100.000000
       97.701590
       95.417340
       93.161350
       90.947540
       88.789540
       86.700650
       84.693770
       82.781270
       80.974930
       79.285900
       77.724590
       76.300610
       75.022750
       73.898900
       72.935960
       72.139870
       71.515540
       71.066820
       70.796470
       70.706170
```

APPENDIX C

PROGRAM SOURCE CODE--HCET MODEL

References from:

Istok, J. D. (1989), Groundwater Modeling by the Finite Element Method, American Geophysical Union, Washington, D.C. 495pp.

Press, W. H., etc. (1992), Numerical Recipes in FORTRAN, Cambridge University Press, 963pp.

Huyakorn, P. S, and Pinder, G. F. (1983), Computational Methods in Subsurface flow, Academic Press, Inc., London, 473pp.

Wang, H. (1982), Introduction to Groundwater Modeling--Finite Difference and Finite Element Methods, W. H. Freeman Company, 237pp.

Reddy, J. N. (1993), An Introduction to the Finite Element Method, 2nd Ed., McGraw-Hill, Inc., New York, 684pp.

```
C       MAIN PROGRAM
        INCLUDE       'SAME.F90'
        PARAMETER (NEM=10,NNM=11,NEQ=11,NSIZE=2,NDF=1,
     *   MXEBC=4,MXNBC=4,MNN=20,MNDT=60)
        INTEGER DTSTEP(MNDT)
        DIMENSION DELTAT(MNDT),TIME(MNDT),TAV(NEM),CAV(NEM)
        DIMENSION ELK(NSIZE,NSIZE),CE(NSIZE,NSIZE),FLX(NSIZE,NSIZE),
     *   PROP(NEM,NDF,NDF+1),PROPI(NEM,NDF,NDF+1),ELX(2),
     *   Coc(NEM,NDF,NDF+1),ADV(NEM,NDF,NDF)
        DIMENSION GSTIF(NEQ,NEQ),AINI(NNM,4),
     *   NOD(100,2),GLF(NEQ),X(NEQ),MATSET(100)
        DIMENSION ISPDF(MXEBC,2),VSPDF(8),ISSDF(MXNBC,2),VSSDF(8),
     *  INBC(MXNBC,2),VNBC(MXNBC),UREF(MXNBC)
        dimension GB(NEQ,NEQ),U(NEQ),UNEW(NEQ),DIF(NEQ),B(NEQ),b_1(NEQ),
     *   BTEMP(NEQ),BW(NNM,NDF),GUO(NEQ) integer index(NEQ)
        OPEN(8,FILE='KCTEST.DAT',STATUS='OLD')
        OPEN(9,FILE='KCTEST.OUT',STATUS='unknown')
        OPEN(10,FILE='check.OUT',STATUS='unknown')
        OPEN(11,FILE='ADVH.OUT',STATUS='unknown')
        OPEN(12,FILE='H.OUT',STATUS='unknown')
        OPEN(13,FILE='C.OUT',STATUS='unknown')
        OPEN(14,FILE='E.OUT',STATUS='unknown')
        OPEN(15,FILE='T.OUT',STATUS='unknown')
        IDT=0
        NPE=2
CC      NNM=(NEM*(NPE-1))+1

        READ(8,*)NSPDF,NSSDF,NNBC
        WRITE(9,*)NDF,NSPDF,NSSDF,NNBC
C
C       ALL B.C. FIRST KIND
C
        IF (NSPDF .NE. 0)THEN
                DO 10 NB=1, NSPDF
                  READ (8,*) (ISPDF(NB,J),J=1,2),VSPDF(NB)
  10            CONTINUE
        ENDIF
C           WRITE(9,*)(VSPDF(I),I=1,NSIZE)
C
C       ALL B.C. SECOND KIND
C
        IF (NSSDF .NE. 0)THEN
                DO 20 NF=1, NSSDF
                  READ (8,*) (ISSDF(NF,J),J=1,2),VSSDF(NF)
  20            CONTINUE
        ENDIF
C
C           WRITE(9,*)(VSSDF(I),I=1,NSIZE)
C
C
C       ALL MIXED B.C.
C
        IF (NNBC .NE. 0)THEN
                DO 30 I=1, NNBC
                  READ (8,*) (INBC(I,J),J=1,2),VNBC(I),UREF(I)
```

```
 30              CONTINUE
        ENDIF
C
C  1. INPUT NODE COORDINATES
C
    CALL NODES (X,NNM)
C
C  2. INPUT ELEMENT (NUMBERS, TYPES, AND) NODE CONNECTIVE
C
    CALL ELEMENT (NEM,NPE,NOD)
C
C  3. INPUT MATERIAL PROPERTIES FOR EACH ELEMENT
C    READ & CALCULATE COEFFICIENT OF Coc(4,5)
C
        CALL MATERL(NEM,MATSET,NDF,PROP,Coc,PROPI)
C
C  4. IMPOSE INITIAL CONDITIONS
C
        CALL INITIAL(U,NEQ,NDF,DTSTEP,ALPHA,ALPHAA,DELTAT,EPS,
    *              PROS,MXSTEP,TIME,NNM,AINI,GUO)
C
C  5. INITIALIZE COUNTERS
C
    IDT = 0 TSUM = 0.

C
C  6. FOR EACH TIME STEP
C
        DO 320 ISTEP = 1, MXSTEP
        WRITE(9,*)"ISTEP=",ISTEP,"MXSTEP=",MXSTEP

C
C  7.    BEGIN PICARD ITERATION
C
         MAXIT=10
         DO 240 ITER = 1, MAXIT
         WRITE(9,*)"ITER", ITER,"adding"
C
C     IF SIZE OF TIME STEP CHANGES REASSEMBLE GLOBAL MATRICES
C
    IF((ISTEP.EQ.1).AND.(ITER .EQ.1).OR.(ISTEP .GT. DTSTEP(IDT)))THEN
          IDT = IDT + 1
    ENDIF
C
C    INITIALIZE THE MATRICES
C
    DO 40 I=1,NEQ
    GLF(I)=0.0
    DO 40 J=1,NEQ
    GB(I,J)=0.0
 40 GSTIF(I,J)=0.0
C
C 8. FORM THE GLOBAL STIFFNESS--(K+C) MATRIX
C
    DO 200 N=1,NEM
C
```

```
C 9. CALCULATE THE GLOBAL COORDINATES OF EACH NODE
C
    DO 60 I=1,NPE
      ELX(I)=X(NOD(N,I))
 60 CONTINUE
     CALL ELKBAR2(NEM,ELX,NSIZE,NDF,N,NDF,NDF,4,Coe,ELK)
          CALL CBAR2(NEM,ELX,NSIZE,NDF,N,NDF,NDF,4,Coe,CE)
          CALL ADVV(ELX,N,NEM,NNM,NDF,PROS,AINI,Coe,ADV)
          CALL CNVEC(NEM,ELX,NSIZE,NDF,N,NDF,NDF,4,adv,flx)
    DO 61 I = 1,NSIZE
      write(9,900)(ELK(I,J),J=1,NSIZE)
 61 continue
900 format(1x,8F8.4)
          do 62 II = 1,NSIZE write(9,901)(CE(II,J),J=1,NSIZE)
 62 continue
901 format(1x,8f6.3)
         do 63 II = 1,NSIZE write(11,903)(flx(II,J),J=1,NSIZE)
 63 continue
903 format(1x,8f6.3)
C
C 10. ASSEMBLE THE ELEMENT MATRICES (K,C)
C
    DO 150 I=1,NPE
    NR=(NOD(N,I)-1)*NDF
    DO 150 II=1,NDF
    NR=NR+1
    L=(I-1)*NDF+II
CC     write(9, *) I,L
    DO 150 J=1,NPE
    NC=(NOD(N,J)-1)*NDF
    DO 150 JJ=1,NDF
    NC=NC+1
cc     print *, NR,NC
    M=(J-1)*NDF+JJ

    GSTIF(NR,NC)=GSTIF(NR,NC)+DELTAT(IDT)*ALPHA*(ELK(L,M)+FLX(l,m))
*                    +CE(L,M)
    GB(NR,NC)=GB(NR,NC)-DELTAT(IDT)*ALPHAA*(ELK(L,M)+FLX(l,m))+CE(L,M)
 150 CONTINUE
 200 CONTINUE
C
C 12. CALCULATE THE RIGHT HAND SIDE VECTOR FOR THIS TIME STEP
C
      IF(ITER.EQ.1)THEN
             do I=1,NEQ
                WRITE (10,*)"U before call RHS", U(I)
             ENDDO
             CALL RHSIDE (GLF,NEQ,U,GB,B)
             TSUM = TSUM + DELTAT(IDT)
             write(9,*)"TSUM=",TSUM," Iter=1 if call rhs",ITER
           DO I=1,NEQ
              BTEMP(I)=B(I)
              WRITE (9,*)"ITER=1 BTEMP(I)=B(I)",B(I)
           ENDDO
       ELSEIF(ITER.GT.1) THEN
           DO I=1,NEQ
```

```
            B(I)= BTEMP(I)
            WRITE (9,*)"ITER >1 B(I)= BTEMP(I)",B(I)
          ENDDO
        ENDIF
C
C  11. IMPOSE BCs
C
        CALL BOUNDC(ALPHA,NDF,NEQ,GSTIF,GUO,
     *              B,NSPDF,ISPDF,VSPDF,IDT,NNBC,
     *              DELTAT,MXEBC,MXNBC,NSSDF,ISSDF,VSSDF,INBC,VNBC,UREF)
C
C  13. Solve the MATRIX
C
      call ludcmp(GSTIF,NEQ,NEQ,index,d)
      call lubksb(GSTIF,NEQ,NEQ,index,B)
C
C  14. CHECK THE PICA CONVERGE
C
        emor=0.0
        IF (ITER.EQ.1)THEN
          DO I=1,NEQ
            DIF(I)=ABS(U(I)-B(I))
            EMOR=MAX(EMOR,DIF(I)) write (9,*) "emorU(I)B(I)",I, emor,U(I),B(I)
          ENDDO
        ELSEIF(ITER.GT.1)THEN
          do i=1,neq
            dif(i)=abs(b_1(i)-b(i))
            EMOR=MAX(EMOR,DIF(I))
            write (9,*) "emor B-old Bnew",I, emor,b_1(i),B(I)
          ENDDO
        ENDIF
      do i=1,neq
          b_1(i)=b(i)
      enddo
     IF (EMOR .LE. EPS) THEN
          DO K=1,NEQ
              U(K)=B(K)
          ENDDO

        DO I=1,NNM
            DO J=1,NDF
              BW(I,J)=B((I-1)*NDF+J)
            ENDDO
            WRITE       (12,*)BW(I,1)
            WRITE       (13,*)BW(I,2)
            WRITE       (14,*)BW(I,3)
            WRITE       (15,*)BW(I,4)
        ENDDO
            GOTO 50
      ELSE IF (EMOR .GT. EPS .AND. ITER .LT. MAXIT) THEN
          DO N=1,NEQ
              UNEW(N)=(0.6*U(N)+0.4*B(N))
          ENDDO
          DO L=1,NNM
            DO J=1,NDF
              AINI(L,J)=UNEW((L-1)*NDF+J)
```

```
            ENDDO
          ENDDO
          DO I=1,NEM
C              NEED TO BE MORE GENERAL
           IF (NDF.GE.2) CAV(I)=(0.5*AINI(I,2)+0.5*AINI(I+1,2))
            IF (NDF.EQ.4) TAV(I)=(0.5*AINI(I,4)+0.5*AINI(I+1,4))
                CALL COEIR(I,NEM,NDF,TAV,CAV,PROPI,Coe)

          ENDDO
       ELSE IF (emor.gt.eps .and. iter.ge.maxit) THEN
          WRITE(*,*)'***EXCEED MAX ITERATIONS***'
          PAUSE
          stop
       ENDIF
          write (9,*) emor,eps
 240     CONTINUE
 50      write(9,*)"converge now goto new time step"
         write(9,*)"TSUM before converge=",TSUM," convergeatIter=",ITER
 320    CONTINUE

       STOP
       END
```

COMMON /CONST/ ALPHA.ALPHAA.MXSTEP.TSUM.IDT

```
      SUBROUTINE NODES (X,NNM)
          DIMENSION X(400)
      READ(8,*) X0, RL
      DX=RL/(NNM-1)
      DO 30 I=1,NNM
   30 X(I)=DX*(I-1)+X0
        RETURN
        END
```

```
      SUBROUTINE ELEMENT (NEM,NPE,NOD)
C*********************************************************************
C
C  PURPOSE:
C        TO GENERATE NODE CONNECTIVITY
C
C*********************************************************************
      INCLUDE 'SAME.F90'
      DIMENSION NOD(100,2)
C     READ: NUMBER OF ELEMENT, AND NODE PER ELEMENT
      DO 20 I=1,NPE
   20 NOD(1,I)=I
      DO 25 N=2,NEM
      DO 25 I=1,NPE
   25 NOD(N,I)=NOD(N-1,I)+NPE-1
      RETURN
      END
```

```
SUBROUTINE MATERL(NEM,MATSET,NDF,PROP,Coc,PROPI)
C*********************************************************************
C
C  PURPOSE:
C       TO INPUT ELEMENT MATERIAL SET NUMBERS AND MATERIAL
C       PROPERTIES FOR EACH MATERIAL SET
C
C*********************************************************************
      INCLUDE 'SAME.F90'
       INTEGER OLDNEM,ELM,SETNUM
      DIMENSION MATSET(100),PROP(NEM,NDF,NDF+1),Coc(NEM,NDF,NDF+1),
*                 PROPI(NEM,NDF,NDF+1)
       OLDNEM = 200
       NUMMAT = 0
C      READ FROM INPUT FILE: ELEMENT NUMBER, AND MATERIAL SET NUMBER
  10   READ(8,*) ELM, MATSET(ELM)
       IF (ELM .EQ. -1) GOTO 30
C      DETERMINE THE NUMBER OF MATERIAL SETS
       IF (MATSET(ELM) .GT. NUMMAT) NUMMAT = MATSET(ELM)
C       GENERATE THE MATERIAL SET NUMBER FOR EACH "MISSING" ELEMENT
       IF (ELM .GT. OLDNEM + 1) THEN
          DO 20 I = OLDNEM + 1, ELM - 1
          MATSET (I) = MATSET (I-1)
  20      CONTINUE
       ENDIF
       OLDNEM = ELM
       GOTO 10
C       WRITE THE MATERIAL SET NUMBER FOR EACH ELEMENT TO OUTPUT FILE
C  30       READ (8,*) NEM
   30  IF (NEM .GT. 0) THEN
       WRITE (9,40)
   40   FORMAT (//2X,'ELEMENT'/4X,'NO.'9X,'MATERIAL SET NUMBER'/
     1         2X,'-------',7X,'--------------------')
        DO 60 I = 1, NEM
          WRITE (9, 50) I,MATSET (I)
   50     FORMAT (I6,I20)
   60   CONTINUE
C       READ FROM INPUT FILE: THE NUMBER OF PROPERTIES IN EACH
C       MATERIAL SET
        WRITE(9,70)
   70   FORMAT(//2X,'MATERIAL'/3X,'SET NO.',13X,
     1      'MATERIAL PROPERTIES'/2X,'---------',13X,
     2      '--------------------')
C       WRITE MATERIAL PROPERTIES INFORMATION TO OUTPUT FILE
       DO I=1,NUMMAT
CCCC      write (9,*) I
            DO II =1, NDF
              READ(8,*) SETNUM,(PROP(SETNUM,II,J),J=1,NDF+1)
             WRITE(9,80) SETNUM,(PROP(SETNUM,II,J),J=1,NDF+1)
   80         FORMAT(I7,7X,5(F15.6))
            ENDDO
       ENDDO
C
C          RECALCULATE COEF
C
```

```
          DO N=1,NEM
           DO I=1,NDF
            DO J=1,NDF+1
             PROPI(N,I,J)=PROP(MATSET(N),I,J)
            ENDDO
            write (10,9999)(PROP(MATSET(N),I,J),J=1,NDF+1)
9999                    format(4x,5f5.2)
           ENDDO
           CALL COEF(N,NEM,NDF,PROPI,Coc)
          ENDDO
     ELSE
        WRITE(9,100)
 100    FORMAT('NO ELEMENT MATERIAL PROPERTY DATA READ.')
     ENDIF
    RETURN
    END
```

```
SUBROUTINE COEF(SETNUM,NEM,NDF,PROP,Coe)
      INCLUDE 'SAME.F90'
      DIMENSION PROP(NEM,NDF,NDF+1),Coe(NEM,NDF,NDF+1)
      INTEGER SETNUM
C     ADD Coe with nonlinear variable
C     Need to calculate omega of Chemical osmosis
C
    T=30.0
       Conc=100.0
    Do i=1,NDF
       Do j=1,NDF
        If (i.EQ.2) Then
       Coe(SETNUM,i,j)=PROP(SETNUM,i,j)+Conc*PROP(SETNUM,1,j)
        ElseIf(i.EQ.4) Then
       Coe(SETNUM,i,j)=PROP(SETNUM,i,j)+T*PROP(SETNUM,1,j)
        Else
       Coe(SETNUM,i,j)=PROP(SETNUM,i,j)
        EndIf
       End Do
         Coe(SETNUM,i,NDF+1)=PROP(SETNUM,i,NDF+1)
         WRITE(9,110)(Coe(SETNUM,i,j),j=1,NDF+1)
110      FORMAT('CoeF',10X,5(F15.6))
    End Do

    Return
    End
```

```
      SUBROUTINE   COEIR(SETNUM,NEM,NDF,TAV,CAV,PROP,Coe)
      INCLUDE 'SAME.F90'
      DIMENSION PROP(NEM,NDF,NDF+1),
     *              TAV(NEM),CAV(NEM),Coe(NEM,NDF,NDF+1)
      INTEGER SETNUM
C     ADD Coe with nonlinear variable
C     Need to calculate omega of Chemical osmosis
C
    Do i=1,NDF
      Do j=1,NDF
        If (i.EQ.2) Then
          Coe(SETNUM,i,j)=PROP(SETNUM,i,j)+CAV(SETNUM)*PROP(SETNUM,1,j)
        ElseIf(i.EQ.4) Then
          Coe(SETNUM,i,j)=PROP(SETNUM,i,j)+TAV(SETNUM)*PROP(SETNUM,1,j)
        Else
          Coe(SETNUM,i,j)=PROP(SETNUM,i,j)
        EndIf
      End Do
          Coe(SETNUM,i,NDF+1)=PROP(SETNUM,i,NDF+1)
          WRITE(9,110)(Coe(SETNUM,i,j),j=1,NDF+1)
110       FORMAT('CoeIR',11X,5(F15.6))
    End Do
    Return
    End
```

```
      SUBROUTINE INITIAL(U,NEQ,NDF,DTSTEP,ALPHA,ALPHAA,DELTAT,
     *                   MXSTEP,TIME,NNM,AINI,GUO)
C*********************************************************************
C
C PURPOSE:
C       SUBROUTINE INITIAL INPUTS CONTROL PARAMETERS AND INITIAl
C       CONDITIONS NEEDED TO SOLVE TRANSIENT COUPLING TRANSPORT
C       PROCESSES PROBLEM.
C
C*********************************************************************
            INCLUDE 'SAME.F90'
           PARAMETER (MNDT=20)
           INTEGER DTSTEP(MNDT)
           DIMENSION DELTAT(MNDT),TIME(MNDT),GT(MNDT)
           DIMENSION AINI(NNM,NDF),U(NEQ),GUO(NEQ)
C     INPUT ALPHA AND EPS FROM INPUT FILE
      READ(8,*) ALPHA,EPS,PROS
      WRITE(9,10) ALPHA,EPS,PROS
   10 FORMAT(//2X,'ALPHA = ',F8.4,'  EPS=',F8.4, '  PROS=',F8.4)
      ALPHAA = 1. - ALPHA
C     INPUT LIST OF TIME STEPS AND TIME STEP INTERVALS FROM INPUT FILE
      IT = 1
      MXSTEP = 0
   20 READ(8,*) DTSTEP(IT),DELTAT(IT)
      IF (DTSTEP(IT) .LE. 0) GOTO 30
      IF (DTSTEP(IT) .GT. MXSTEP) MXSTEP = DTSTEP(IT)
      IT = IT + 1
      GOTO 20
   30 IT = IT - 1
      WRITE(9,40)
   40 FORMAT(//2X,'START',8X,' END ',10X,'DELTA T'/
     1       2X,5('-'),8X,5('-'),8X,11('-'))
     ISTART = 1
     TOTALT = 0.
     DO 60 I = 1, IT
         WRITE(9,50) ISTART,DTSTEP(I),DELTAT(I)
   50    FORMAT(2X,I4,9X,I4,3X,F15.4)
         TOTALT = TOTALT + (DTSTEP(I) - ISTART + 1) * DELTAT(I)
         ISTART = DTSTEP(I) + 1
   60 CONTINUE
      WRITE(9,70) TOTALT
   70 FORMAT(/10X,'TOTAL TIME =',F15.4)
C     INPUT LIST OF TIME STEPS AND VALUES OF TIME FUNCTION
      IT = 1
   80 READ(8,*) TIME(IT),GT(IT)
      IF (TIME(IT) .LT. 0.) GOTO 90
      IT = IT + 1
      GOTO 80
   90 IT = IT - 1
       IF (TIME(IT) .LT. TOTALT) TIME(IT) = TOTALT
      WRITE(9,100)
  100 FORMAT(//8X,'TIME T',11X,'G(T)'/7X,8('-'),9X,6('-'))
      DO 120 I = 1, IT
         WRITE(9,110) TIME(I),GT(I)
  110    FORMAT(2F15.4)
  120 CONTINUE
```

```
C     INPUT INITIAL VALUES OF FIELD VARIABLE FROM INPUT FILE
      ISTART = 1
C       ========================================
      DO I=1,NNM
         READ (8,*)(AINI(I,J), J=1,NDF)
         WRITE (9,*)(AINI(I,J), J=1,NDF)
      ENDDO
         DO I=1,NNM
            DO J=1,NDF
              U((I-1)*NDF+J)=U((I-1)*NDF+J)+AINI(I,J)
              GUO((I-1)*NDF+J)=U((I-1)*NDF+J)+AINI(I,J)
            ENDDO
         ENDDO

      RETURN
      END
```

```
SUBROUTINE ELKBAR2(NEM,ELX,NSIZE,NDF,N,N1,N2,NE,Coc,ELK)
    INCLUDE   'SAME.F90'
   REAL TMP
   DIMENSION ELX(2),Coc(NEM,NDF,NDF+1),ELK(NSIZE,NSIZE)
        DO 121 I=1,NSIZE
           DO 122 J=1,NSIZE
               ELK (I,J)=0.0
122        CONTINUE
121    CONTINUE
               EL = ELX(2)-ELX(1)
        DO I=1,N1
           DO J=1,N2
              DO K=1,NE
                 TMP=COE(N,I,J)/EL
                 IF (K.EQ.1) THEN
                     ELK(I,J)=TMP
                 ELSE IF(K.EQ.2)THEN
                      KK2=J+N2
                      ELK(I,KK2)=-1.*TMP
                 ELSE IF(K.EQ.3)THEN
                     KK1=I+N1
                      ELK(KK1,J)=-1.*TMP
                 ELSE
                      KK1=I+N1
                      KK2=J+N2
                      ELK(KK1,KK2)=TMP
                 END IF
              END DO
           END DO
        END Do
        RETURN
        END
```

```
SUBROUTINE CBAR2(NEM,ELX,NSIZE,NDF,N,N1,N2,NE,Coc,CE)
C***********************************************************************
C
C  PURPOSE:
C    TO COMPUTE THE CONSISTENT FORM OF THE ELEMENT
C    CAPACITANCE MATRIX FOR A ONE-DIMENSIONAL, LINEAR
C    BAR ELEMENT
C
C  DEFINITIONS OF VARIABLES:
C         E   = ELEMENT NUMBER
C    CE(I,J) = ELEMENT CAPACITANCE MATRIX
C       SSE  = ELEMENT SPECIFIC STORAGE
C        LE  = ELEMENT LENGTH
C
C  REFERENCES:
C    ISTOK,J D. GROUNDWATER FLOW AND SOLUTE TRANSPORT
C    MODELING BY THE FINITE ELEMENT METHOD. FIGURE 4.5,
C    EQUATION 4.16a.
C
C***********************************************************************
    INCLUDE 'SAME.F90'
        REAL TMP
        DIMENSION ELX(2),Coc(NEM,NDF,NDF+1),CE(NSIZE,NSIZE)
        DO 100 I=1,NSIZE
            DO 101 J=1,NSIZE
                CE(I,J)=0.0
 101        CONTINUE
 100    CONTINUE
         EL = ELX(2) - ELX(1)
          Write(*,*)'yy',N
        DO I=1,N1
          DO J=1,N2
             DO K=1,NE
                TMP=Coc(N,I,NDF+1)*EL/2
                IF (K.EQ.1)THEN
                  CE(I,I)=TMP
                ELSE IF(K.EQ.2)THEN
                  KK2=I+N2
                  CE(I,KK2)=0.*TMP/2
                ELSE IF(K.EQ.3)THEN
                  KK1=I+N1
                  CE(KK1,I)=0.*TMP/2
                ELSE
                   KK1=I+N1
                   KK2=I+N2
                   CE(KK1,KK2)=TMP
                END IF
             END DO
          END DO
        END Do
        RETURN
        END
```

```
SUBROUTINE ADVV(ELX,N,NEM,NNM,NDF,PROS,AINI,Coc,ADV)
      INCLUDE       'SAME.F90'
      DIMENSION ELX(2),Coc(NEM,NDF,NDF+1),ADV(NEM,NDF,NDF)
      DIMENSION QT(NEM),QI(NEM,NDF),AINI(NNM,NDF)
        QT(N)=0.0
        EL = ELX(2)-ELX(1)
      DO J=1,NDF
       DHDX=(AINI(N+1,J)-AINI(N,J))/EL
       QI(N,J)=-Coc(N,1,J)*DHDX
       QT(N)=QT(N)+QI(N,J)
      END DO
      IF (NDF .EQ. 2 .OR. NDF .EQ. 3) ADV(N,2,2)=QT(N)/PROS
      IF (NDF .EQ. 4) ADV(N,4,4)=QT(N)/PROS
      do i=1,ndf
        WRITE (11,*) (adv(N,I,J),j=1,ndf)
      enddo
      RETURN
      END
```

```
SUBROUTINE CNVEC(NEM,ELX,NSIZE,NDF,N,N1,N2,NE,adv,flx)
C*********************************************************************
C
C  PURPOSE:
C      Reoder the element nodes for the multivariable problems for the advection terms
C      of the coupling  transport processes.
C
C*********************************************************************
    INCLUDE 'SAME.F90'
        REAL TMP
        DIMENSION ELX(2),adv(NEM,NDF,NDF),FLX(NSIZE,NSIZE)
        DO 100 I=1,NSIZE
           DO 101 J=1,NSIZE
              flx(I,J)=0.0
 101       CONTINUE
 100    CONTINUE
         EL = ELX(2) - ELX(1)
       DO I=1,N1
          DO J=1,N2
             DO K=1,NE
                TMP=adv(N,I,J)
                IF (K.EQ.1)THEN
                   flx(I,I)=-TMP/2.
                ELSE IF(K.EQ.2)THEN
                   KK2=I+N2
                   flx(I,KK2)=TMP/2
                ELSE IF(K.EQ.3)THEN
                   KK1=I+N1
                    flx(KK1,I)=-TMP/2.
                ELSE
                    KK1=I+N1
                    KK2=I+N2
                    flx(KK1,KK2)=TMP/2.
                END IF
             END DO
          END DO
       END Do
       RETURN
       END
```

```
SUBROUTINE RHSIDE (GLF.NEQ.U.GB.B)
C*********************************************************************
C
C PURPOSE:
C       SUBROUTINE RHS ASSEMBLES THE RIGHT-HAND-SIDE VECTOR
C       FOR TRANSIENT COUPLING TRANSPORT PROCESSES
C       PROBLEMS.
C
C*********************************************************************
      DIMENSION B(NEQ).U(NEQ).GLF(NEQ)
      DIMENSION GB(NEQ.NEQ)
C     WHEN FLUX IS TIME'S FUNCTION. CHANGE HERE WITH FC & GLF
       I = 0
          DO 10 J = 1. NEQ
              I = I + 1
              B(I) = GLF(J)
   10     CONTINUE

            DO 15 I=1.NEQ
                  DO 20 J=1.NEQ

                  B(I)=B(I)+GB(I.J)*U(J)

   20             CONTINUE
                   print *. B(I)
   15         CONTINUE


         RETURN
         END
```

```
      SUBROUTINE BOUNDC(ALPHA,NDF,NEQ,GSTIF,GUO,B,NSPDF,ISPDF,VSPDF,
     *                  IDT,NNBC,
     *                   DELTAT,MXEBC,MXNBC,NSSDF,ISSDF,VSSDF,INBC,VNBC,UREF)

      DIMENSION ISPDF(MXEBC,2),VSPDF(MXEBC),B(NEQ)
      DIMENSION ISSDF(MXNBC,2),VSSDF(MXNBC),UREF(MXNBC)
      DIMENSION INBC(MXNBC,2),VNBC(MXNBC)
      DIMENSION GSTIF(NEQ,NEQ),DELTAT(100)
C
C 1st BC IMPOSE
C
        IF (NSPDF.NE.0) THEN
          DO 30 NB =1, NSPDF
           NQ=(ISPDF(NB,1)-1)*NDF+ISPDF(NB,2) GSTIF(NQ,NQ)=GSTIF(NQ,NQ)*1.0E+20
           B(NQ)=GSTIF(NQ,NQ)*VSPDF(NB)
30        CONTINUE
        ENDIF
C
C 2nd BC IMPOSE
C

        IF (NSSDF.NE.0) THEN
              DO 40 NF =1, NSSDF
              NG=(ISSDF(NF,1)-1)*NDF+ISSDF(NF,2)
              B(NG)=B(NG)+VSSDF(NF)*DELTAT(IDT)
40            CONTINUE
        ENDIF
C
C Mixed BC IMPOSE
C
        IF(NNBC.NE.0) THEN
              DO 50 IC =1, NNBC
              NC=(INBC(IC,1)-1)*NDF+INBC(IC,2)
         GSTIF(NC,NC)=GSTIF(NC,NC)+ALPHA*DELTAT(IDT)*VNBC(IC)
              B(NC)=B(NC)+VNBC(IC)*DELTAT(IDT)*(UREF(IC)
     *                -(1-ALPHA)*GUO(NC))
50            CONTINUE
        ENDIF

      RETURN
      END
```

```
      SUBROUTINE ludcmp(a,n,np,indx,d)
          INTEGER n,np,indx(n),NMAX
          REAL d,a(np,np),TINY
          PARAMETER (NMAX=500,TINY=1.0e-20)
          INTEGER i,imax,j,k
          REAL aamax,dum,sum,vv(NMAX)
          d=1.
          do 12 i=1,n
             aamax=0.
             do 11 j=1,n
                if (abs(a(i,j)).gt.aamax) aamax=abs(a(i,j))
      11     continue
             if (aamax.eq.0.) pause 'singular matrix in ludcmp'
             vv(i)=1./aamax
      12  continue
          do 19 j=1,n
            do 14 i=1,j-1
               sum=a(i,j)
               do 13 k=1,i-1
                  sum=sum-a(i,k)*a(k,j)
      13       continue
               a(i,j)=sum
      14     continue
             aamax=0.
            do 16 i=j,n
               sum=a(i,j)
               do 15 k=1,j-1
                  sum=sum-a(i,k)*a(k,j)
      15       continue
               a(i,j)=sum
               dum=vv(i)*abs(sum)
               if (dum.ge.aamax) then
                  imax=i
                  aamax=dum
               endif
      16     continue
             if (j.ne.imax)then
               do 17 k=1,n
                  dum=a(imax,k)
                  a(imax,k)=a(j,k)
                  a(j,k)=dum
      17        continue
                d=-d
                vv(imax)=vv(j)
             endif
            indx(j)=imax
            if(a(j,j).eq.0.)a(j,j)=TINY
            if(j.ne.n)then
              dum=1./a(j,j)
              do 18 i=j+1,n
                 a(i,j)=a(i,j)*dum
      18       continue
            endif
      19    continue
          return
          END
```

```
C  (C) Copr. 1986-92 Numerical Recipes Software .V.
      SUBROUTINE lubksb(a,n,np,indx,b)
      INTEGER n,np,indx(n)
      REAL a(np,np),b(n)
      INTEGER i,ii,j,ll
      REAL sum
      ii=0
      do 12 i=1,n
        ll=indx(i)
        sum=b(ll)
        b(ll)=b(i)
        if (ii.ne.0)then
          do 11 j=ii,i-1
            sum=sum-a(i,j)*b(j)
11        continue
        else if (sum.ne.0.) then
          ii=i
        endif
        b(i)=sum
12    continue
      do 14 i=n,1,-1
        sum=b(i)
        do 13 j=i+1,n
          sum=sum-a(i,j)*b(j)
13      continue
        b(i)=sum/a(i,i)
14    continue
      return
      END
C  (C) Copr. 1986-92 Numerical Recipes Software .V.
```

APPENDIX D

DERIVATION OF CHEMICO-OSMOSIS EQUATION

$$J_c = J_D + J_A \qquad [D\text{-}1]$$

For $i_e = 0$, no electric gradient, Mitchell (1993) indicated that

$$J_w = \left[\frac{K_{hh}}{n}\right] i_h + RT\left[-\frac{\omega K_{hh}}{\gamma_w n}\right] i_c = \left((1-\omega)\frac{K_{hh}}{n}\right) i_h \qquad [D\text{-}2]$$

$$J_c' = J_D' + J_A' = \left[D^* - \frac{\omega C_i K_{hh}}{\gamma_w n} RT\right] i_c + \left[(1-\omega)\frac{C_i K_{hh}}{n}\right] i_h \qquad [D\text{-}3]$$

Equations D-2 and D-3 are derived by Young (1993), and he used the actual area, A_v, which is not practical. We only measure the bulk area, $A = nA_v$, such that $J_A = nJ_A'$ and $J_c = nJ_c'$. Young's formula has three limitations: steady state flow, no net exchange of component, and inert material, such that the case will apply for $R_d = 1$

$$\frac{\partial m}{\partial t} = -\bar{\nabla} \bullet \bar{J}_c = -\frac{\partial J_c}{\partial x} \qquad [D\text{-}4]$$

$$J_c = \left[nD_0\tau_0 - \frac{\omega C_j K_{hh}}{\gamma_w} RT \right] i_c + \left[(1-\omega) C_j K_{hh} \right] i_h \qquad [D\text{-}5]$$

For steady flow condition and unit volume, the flux change is

$$-\frac{\partial J_c}{\partial x} = \frac{\partial \left[nD_0\tau_0 - \frac{\omega C_j K_{hh}}{\gamma_w} RT \right] \frac{\partial C_j}{\partial x}}{\partial x} + \left[(1-\omega) K_{hh} \frac{\partial C_j}{\partial x} \right] \frac{\partial h}{\partial x} \qquad [D\text{-}6]$$

If τ_0 and C_j are elementally constants, then

$$n\frac{\partial C_j}{\partial t} = \left[nD_0\tau_0 - \frac{\omega C_j K_{hh}}{\gamma_w} RT \right] \frac{\partial^2 C_j}{\partial x^2} + \left[(1-\omega) K_{hh} \frac{\partial h}{\partial x} \right] \frac{\partial C_j}{\partial x} \qquad [D\text{-}7]$$

Or,

$$\left(nD_0\tau_0 - \frac{\omega C_j K_{hh} RT}{\gamma_w} \right) \frac{\partial^2 C_j}{\partial x^2} + \left(K_{hh} \frac{\partial h}{\partial x} - \omega K_{hh} \frac{\partial h}{\partial x} \right) \frac{\partial C_j}{\partial x} = n \frac{\partial C_j}{\partial t} \qquad [D\text{-}8]$$

where $D^* = D_0\tau_0$

As $\omega \rightarrow 1, \tau_0 \rightarrow 0$, and $C_j = 0$ for a perfect membrane.

C_j can be represent by $C_j = \frac{C_{j+1} + C_{j-1}}{2}$ in general cases.

Therefore, $J_c = 0$ for a perfect membrane.

We establish the relationship between the ω and K_{hco} from fundamentals of soil behavior by Mitchell (1993, p. 258).

$$\omega \frac{K_{hh}}{\gamma_w n} RTi_c = \omega \frac{K_{hh}}{\gamma_w n} RT\Delta c / \Delta x \qquad [D\text{-}9]$$

This form is analogous to Darcy's law, with the quantity $RT\Delta c / \gamma_w$ being the head difference, Δh

The input parameters for the HCET model are:

$$\begin{bmatrix} K_{hh} & K_{hco} \\ D^*_{cho} + C_j K_{hh} & nD^*_j + C_j K_{hco} \end{bmatrix} \begin{bmatrix} h \\ C_j \end{bmatrix} + \begin{bmatrix} 0 & 0 \\ 0 & -K_{hh}\nabla h - K_{hco}\nabla C_j \end{bmatrix} \begin{bmatrix} h \\ C \end{bmatrix} = \frac{\partial}{\partial t} \begin{bmatrix} S_s h \\ nC_j \end{bmatrix} \qquad [D\text{-}10]$$

Expanding equation D-10 in steady state condition, we have

$$K_{hh} \frac{\partial h}{\partial x} + K_{hco} \frac{\partial C_j}{\partial x} = J_w \qquad [D\text{-}11a]$$

$$\left(nD^*_j + C_j K_{hco}\right) \frac{\partial^2 C_j}{\partial x^2} + \left(K_{hh} \frac{\partial h}{\partial x} + K_{hco} \frac{\partial C_j}{\partial x}\right) \frac{\partial C_j}{\partial x} = n \frac{\partial C_j}{\partial t} \qquad [D\text{-}11b]$$

By setting

$$K_{hco}\frac{\partial C_j}{\partial x} = -\omega K_{hh}\frac{\partial h}{\partial x}, \qquad \text{[D-12]}$$

we have

$$K_{hco} = -\omega K_{hh}\frac{\Delta h}{\Delta C_j} = -\omega K_{hh}\frac{RT}{\gamma_w} \qquad \text{[D-13]}$$

Substituting the chemico-osmosis coefficient into first term of solute transport equation D-11b, we have

$$\left(nD_j^* + C_j K_{hco}\right)\frac{\partial^2 C_j}{\partial x^2} = \left(nD_j^* - C_j \omega K_{hh}\frac{\Delta h}{\Delta C_j}\right)\frac{\partial^2 C_j}{\partial x^2}$$

$$= \left(nD_j^* - \frac{\omega C_j K_{hh}}{\gamma_w}RT\right)\frac{\partial^2 C_j}{\partial x^2} \qquad \text{[D-14]}$$

Therefore, equations D-11a and 11b become

$$K_{hh}\frac{\partial h}{\partial x} + \qquad (-\omega)K_{hh}\frac{\partial h}{\partial x} = J_w \qquad \text{[D-15a]}$$

$$\left(nD_0\tau_0 - \frac{\omega C_j K_{hh}}{\gamma_w}RT\right)\frac{\partial^2 C_j}{\partial x^2} + \left(K_{hh}\frac{\partial h}{\partial x} - \omega K_{hh}\frac{\partial h}{\partial x}\right)\frac{\partial C_j}{\partial x} = n\frac{\partial C_j}{\partial t} \qquad \text{[D-15b]}$$

REFERENCES

Acar, Y. B., and Alshawabkeh, A. N. (1996), "Electrokinetic Remediation. I: Pilot-Scale Tests with Lead-Spiked Kaolinite", *Journal of Geotechnical Engineering Division*, ASCE, Vol. 122(3), 173-185.

Acar, Y. B., Alshawabkeh, A. N., and Gale, R. (1993), "Fundamental of Extracting Species from Soils by Electrokinetics", *Waste Management*, Pregamon Press, London, Vol. 12(3), 141-151.

Acar, Y. B., Gale, R, J., Putnam, G., and Hamed, J. (1989), "Electrochemical Processing of Soils: Its Potential Use in Environmental Geotechnology and Significant of pH Gradients", *Proceeding 2nd International Sympsia Environmental Geotechnology*, Shanghi, Vol. 1, 25-38.

Acar, Y. B., Gale, R, J., Putnam, G., Hamed, J., and Wong, R. (1990), "Electrochemical Processing of Soils: Theory of pH Gradients Development by Diffusion, Migration and Linear Convection", *Journal of Environmental Science and Health*, A2(6), 687-714

Acar, Y. B., Hamed, J., Alshawabkeh, A. N., and Gale, R. (1994), "Removal of Cd(II) from Saturated Kaolinite by Application of Electrical Current", *Geotechnique*, Vol. 44(2), 239-254.

Acar, Y. B., Li, H., and Gale, R, J. (1992), "Phenol Removal from Kaolinite by Electrokinetics", *Journal of Geotechnical Engineering*, ASCE, Vol. 118(11), 1837-1852.

Afifi, S. M. (1994), "A Three-Dimensional Finite-Element Model for Reactive Multicomponent-Multispecies Subsurface Transport", Ph. D. Dissertation, Colorado State University, Fort Collins, CO, 178pp.

Allison, J. D. and Brown, D. S. (1995), "MINTEQA2/PRODEFA2-A Geochemical Speciation Model and Interactive Preprocessor", in Chemical Equilibrium and Reaction Models, SSSA Special Publication Number 42, SSSA, Madison, WI., 422pp.

Alshawabkeh, A. N., and Acar, Y. B. (1996), "Electrokinetic Remediation. II: Theoretical Model", *Journal of Geotechnical Engineering Division*, ASCE, Vol. 122(3), 186-196.

Alshawabkeh, A. N. (1994), "Theoretical and Experimental Modeling of Removing Contaminants from Soils by an Electric Field", Louisiana State University, Ph. D. Dissertation, 376pp.

Alshawabkeh, A. N. and Acar, Y. B. (1992), "Removal of Contaminants form Soil by Electrokinetics: A Theoretical Treatise", *Journal of Environmental Science and Health*, A27(7), 1835-1861.

Andrews, C. B., and Anderson, M. P. (1980), "Impact of Coal-Fired Power Plants on Local Groundwater Systems", Wisconsin Power Plant Impact Study, U.S. EPA, Duluth, Minnesota 55804, Report EPA 600/3-80-079.

Bear, J. (1972), Dynamics of Fluids in Porous Media, American Elsevier, New York, 764pp.

Bernard, R., Vauclin, M., and Vidal-Madjar, D. (1981), "Possible Use of Active Microwave Remote Sensing Data for Prediction of Regional Evapotranspiration by Numerical Simulation of Soil Water Movement in the Unsaturated Zone", *Water Resources Research*, Vol. 17(6), 1603-1610.

Bird, R. B., Stewart, W. E., and Lightfoot, E. N., Transport Phenomena, John Wiley and Sons Inc., New York, 780pp.

Cary, J. W. (1979), "Soil Heat Transducers and Water Vapor Flow", *Soil Science Society of America Journal*, Vol. 43, 835-839.

Casagrande, L. (1983), "Stabilization of Soils by Means of Electro-Osmosis--State-of-Art", *Journal of Boston Society Civil Engineering*, ACSE, Vol. 69(2), 255-302.

Cleary, R.W., and Adrian, D. D. (1973), "Analytical Solution of the Convective-Dispersive Equation for Cation Adsorption in soils", *Soil Science Society Of America Journal*, Vol. 37, 197-199.

De Groot, S. R. (1952), Thermodynamics of Irreversible Processes, Interscience Publishers, Inc., New York, 243pp.

Dirksen, C. (1969), "Thermo-osmosis through Compacted Saturated Clay Membranes", *Soil Science Society Of America Proceeding*, Vol. 33, 821-826.

Entwistle, K. M. (1999), Basic Principles of the Finite Element Method, IOM Communications, London, 183pp.

Eu, B. C. (1992), Kinetic Theory and Irreversible Thermodynamics, John Wiley and Sons, Inc., 732pp.

Fletcher, C. A. J. (1991), Computational Techniques for Fluid Dynamics Volume I, Springer-Verlag New York, Berlin, Heidelberg, 401pp.

Freeze, R. A. and Cherry, J. A. (1979), Groundwater, Englewood Cliffs: Prentice-Hall, 604pp.

Gillham, R. W, Sudicky, E. A., Cherry, J. A., and Frind, E. O. (1984), "An Advection-Diffusion Concept for Solute Transport in Heterogeneous Unconsolidated Geological Deposits", *Water Resources Research*, Vol. 20(3), 369-378.

Gupta, S. K., Cole, C. R., Kincaid, C. T., and Monti, A. M. (1987), "Coupled Fluid, Energy, and Solute Transport (CFEST) Model: Formulation and User's Manual", Battelle Memorial Institute, Columbus, OH, 466pp.

Hamed, J., Acar, Y. B., and Gale, R. J. (1991), "Pb(II) Removal from Kaolinite by Electro-kinetics", *Journal of Geotechnical Engineering Division*, ASCE, Vol. 117(2), 241-271.

Huyakorn, P. S., and Gelhar, L. W. (1981), "Derivation and Application of Computer Model for Simulation of Geothermal Systems", New Mexico Energy and Minerals Department, Report No. EMD 2-66-2314.

Huyakorn, P. S, and Pinder, G. F. (1983), Computational Methods in Subsurface flow, Academic Press, Inc., London, 473pp.

Huyakorn, P. S., White, H. O. Jr., Guvanasen, V. M., and Lester, B. H. (1986), "TRAFRAP: A Two-Dimensional Finite Element Code for Simulating Fluid Flow and Transport of Radionuclides in Fractured Porous Media", FOS-33, International Ground Water Modeling Center, Colorado School of Mines, Colorado.

Istok, J. D. (1989), Groundwater Modeling by the Finite Element Method, American Geophysical Union, Washington, D C. 495pp.

Kipp, Jr., K. L.(1987), "HST3D: A Computer Code for Simulation of Heat and Solute Transport in Three-Dimensional Groundwater Flow Systems", *Water Resources Investigations* Report 86-4095, U. S. Geological Survey, Denver, CO, 517pp.

Lageman, R.(1993), "Electro-Reclamation", *Environmental Science and Technology*, Vol. 27(13), 2648-2650.

Lageman, R., Wieberen, P., and Seffinga, G. (1989), "Electro-Reclamation: Theory and Practice", *Chemistry Industry London*, Vol. 9, 585-590.

Lasaga, A. C. (1998), Kinetic Theory in the Earth Sciences, Princeton University Press, Princeton, New Jersey, 811pp.

Li, Y. H., and Gregory, S. (1974), "Diffusion of Ions in Sea Water and in Deep-sea Sediments", *Geochimica Et Cosmochimica Acta*, Vol. 38, 703-714.

Lindeburg, M., R. (1990), Engineer-IN-Training Reference Manual 7th Ed., Professional Publications, Inc., Belmont, California.

Liu D. H. F., Lipták, B. G., and Bouis, P. A. (2000) Groundwater and Surface Water Pollution, Lewis Publishers, Boca Raton, Florida, 150pp.

Manassero, M., and Shackelford, C. D. (1994), "The Role of Diffusion in Contaminant Migration through Soil Barries ", *Italian Geotechnical Journal*, Vol. 28, No.1, 5-31.

Mangold, D. C., and Tsang, C. (1991), "A Summary of Subsurface Hydrological and Hydrochemical Models", *Reviews of Geophysics*, Vol. 29(2), 51-79.

McWhorter, D. B., and Sunada D. K. (1977), Ground-water Hydrology and Hydraulics, Water Resources Publications, CO, 290pp.

Milly, P. C. D. (1982), "Moisture and Heat Transport in Hysteretic, Inhomogeneous Porous Media: A Matric Head-Based Formulation and Numerical Model", *Water Resources Research*, Vol.18(3), 489-498.

Mitchell, J. K. (1993), Fundamentals of Soil Behavior, 1st Ed., John Wiley and Sons Inc., New York, 422pp.

Mitchell, J. K. (1993), Fundamentals of Soil Behavior, 2nd Ed., John Wiley and Sons Inc., New York, 437pp.

Mitchell, J. K., and Yeung, A. T. (1991), "Electro-Kinetic Flow Barriers in Compacted Clay", *Geotechnical Engineering*, Transportation Research Record No. 1288, 1-10.

Pamukcu, S. Khan, L., and Fang, H. (1990), "Zinc Detoxification of Soils by Electro-Osmosis", *Geotechnical Engineering*, Transportation Research Record No. 1288, 41-46.

Press, W. H., etc. (1992), Numerical Recipes in FORTRAN, Cambridge University Press, 963pp.

Reed, J. E. (1985), "Digital Model for Simulating Stead-State Ground Water and Heat Flow", *Water Resources Investigations* Report 05-4248, U. S. Geological Survey, Denver, CO, 134pp.

Reddy, J. N. (1993), An Introduction to the Finite Element Method, 2nd Ed., McGraw-Hill, Inc., New York, 684pp.

Runnels, D. D., and Larson, J. L. (1986), "A Laboratory Study of Electromigration as a Possible Field Technique for the Removal of Contaminants from Ground Water", *Ground Water Monitoring Review*, VOL. 6(4), 81-91.

Runnels, D. D., and Wahli, C. (1993), "In Situ Electromigration as a Method for Removing Sulfate, Metals, and Other Contaminants from Groundwater", *Ground Water Monitoring Review*, VOL. 13(1), 121-129.

Sato, H., Shibutani, T., and Yui, M. (1997), "Experimental and Modeling Studies on Diffusion of Cs, Ni, and Sm in Granodiorite, Basalt and Mudstone", *Journal of Contaminant Hydrology*, Elsevier Science Publishers B. V., Amsterdam, Vol. 26, 119-133.

Shackelford, C. D. (1995), "Analytical Models For Cumulative Mass Column Testing", Geoenvironment 2000, *Proceedings of a Specialty Conference Sponsored by the Geotechnical Engineering Divisions ASCE*, Hold February 24-26, 1995, New Orleans, Louisiana, 355-372.

Shackelford, C. D. (1994), "Critical Concepts for Column Testing", *Journal of Geotechnical Engineering*, ASCE, Vol. 120, No.10, 1804-1828.

Shackelford, C. D. (1991), "Laboratory Diffusion Testing for Waste Disposal- a Review", *Journal of Contaminant Hydrology*, Elsevier Science Publishers B. V., Amsterdam, Vol. 7, 177-217.

Shackelford, C. D. (1989), "Transit-time Design of Earthen Barriers", *Engineering Geology*, Elsevier Science Publishers B. V , Amsterdam, Vol. 29, 79-94.

Shapiro, A. P., and Probestein, R. F. (1993), "Removal of Contaminants from Saturated Clay by Electroosmosis", *Environmental Science and Technology*, Vol. 27(2), 283-291.

Shapiro, A. P., Renauld, P., and Probestein, R. (1989), "Preliminary Studies on Removal of Chemical Species from Saturated Porous Media by Electro-osmosis", *Physicochemical Hydrodynamics*, Vol. 11, No 5/6, 785-802.

Soler, J. M. (1999), "Coupled Transport Phenomena in the Opalinus Clay Implications for Radionuclide Transport", Paul Scherrer Institut Report No. 99-07, Villigen, Switzerland.

Srivastava, R. C., and Avasthi, P. K. (1975), "Non-equilibrium Thermodynamics of Thermo-osmosis of Water through Kaolinite", *Journal of Hydrology*, North-Holland Publishing Company, Amsterdam, Vol. 24, 111-120.

Stumm, W., and Morgan, J. (1981), Aquatic Chemistry, John Wiley and Sons, New York, 2nd. Ed. , 780pp.

Thompson, E. (1995), The Finite Element Class Notes CE665, Colorado State University, Fort Collins, CO, 250pp.

Tsang, C. F. (1987), Coupled Processes Associated with Nuclear Waste Repositories, Academic Press, Inc., New York, 801pp.

van der Heijde, P.K.M. (1993), Compilation of Ground-Water Models, EPA/600/R-93/118, U.S. EPA, R. S. Kerr Environmental Res. Lab., Ada, OK, 29-44.

van Genuchten, M. T., and Alves, W. J. (1982), "Analytical Solution for the one-dimensional Convective-Dispersive Solute Transport Equation", Technical Bulletin No. 1661, U.S. Department of Agriculture, Washington, D.C.

van Genuchten, M. T., and Paker, J. C. (1984), "Boundary Conditions for Displacement Experiments through Short Laboratory Soil Columns", *Journal, Soil Science Society Of America*, Vol. 48, 703-708.

Voss, C. I. (1984), "SUTRA: A Finite Element Simulation Model for Saturated-Unsaturated Fluid Density-Dependent Ground Water Flow with Energy Transport or Chemically Reactive Style Species Solute Transport", *Water Resources Investigations* Report 84-4369, U. S. Geological Survey, Denver, CO, 409pp.

Walker, W. R., Sabey, J. D., and Hampton, D. R. (1981), "Studies of Heat Transfer and Water Migration in Soils", Report of the Solar Energy Laboratory, Colorado State University, Fort Collins, CO, 1-34.

Wang, H. (1982), Introduction to Groundwater Modeling--Finite Difference and Finite Element Methods, W. H. Freeman Company, 237pp.

Yeh, G. T., and Tripathi, V. S.(1991), "A Model for Simulating Transport of Reactive Multispecies Components: Model Development and Demonstration", *Water Resources Research*, Vol. 27(12), 3075-3094.

Yeh, G. T., and Tripathi, V. S.(1989), "A Critical Evaluation of Recent Developments in Hydrogeochemical Transport Models of Reactive Multichemical Components", *Water Resources Research*, Vol. 25(1), 93-108.

Yeung, A. T., and Mitchell, J. K. (1993), "Coupled Fluid, Electrical and Chemical Flows in Soils", *Geotechnique* Vol. 43(1), 121-134.

Zaslavsky, D., and Ravlina, I. (1965), "Review and Some Studies of Electrokinetic Phenomena", *Moisture Equilibria and Moisture Changes in Soils Beneath Covered Areas*, Butterworths, 55-69